OFFICIAL JOURNAL OF THE SCIENTIFIC SOCIETY OF ANATOMISTS, HISTOLOGISTS, EMBRYOLOGISTS AND TOPOGRAPHIC ANATOMISTS OF UKRAINE

DOI: 10.31393
ISSN 1818-1295
eISSN 2616-6194

ВІСНИК МОРФОЛОГІЇ
REPORTS OF MORPHOLOGY

Vol. 25, №3, 2019

Scientific peer-reviewed journal in the fields of normal and pathological anatomy, histology, cytology and embryology, topographical anatomy and operative surgery, biomedical anthropology, ecology, molecular biology, biology of development

Published since 1993
Periodicity: 4 times a year

Vinnytsya • 2019

ВІСНИК МОРФОЛОГІЇ - REPORTS OF MORPHOLOGY

Founded by the "Scientific Society of Anatomists, Histologists, Embryologists, and Topographic Anatomists of Ukraine" and National Pyrogov Memorial Medical University, Vinnytsya in 1993

Certificate of state registration КВ №9310 from 02.11.2004

Professional scientific publication of Ukraine in the field of medical sciences (approved by the order of the Ministry of Education and Science of Ukraine No. 528 dated 12.05.2015, annex 10); professional scientific publication of Ukraine in the field of biological sciences by specialty groups 14.01.00-14.03.00 (approved by the order of the Ministry of Education and Science of Ukraine No. 747 dated 13.07.2015, annex 17)

Approved by the Academic Council of National Pyrogov Memorial Medical University, Vinnytsya, protocol №1 from 29.08.2019

Indexation: CrossRef, elibrary.ru, Google Schoolar Metrics, National Library of Ukraine Vernadsky

Address editors and publisher:
Pyrogov Str. 56,
Vinnytsya, Ukraine - 21018
Tel.: +38 (0432) 553959
E-mail: nila@vnmu.edu.ua

Computer page-proofs - Klopotovska L.O.
Translator - Gunas V.I.
Technical support - Levenchuk S.S., Parashuk O.I.
Scientific editing - editorship

The site of the magazine - https://morphology-journal.com

CONTENT

DOI: 10.31393/morphology-journal-2019-25(3)-01 Reports of Morphology, Vol. 25, №3, Pages 5-9

ISSN 1818-1295 eISSN 2616-6194

REPORTS OF MORPHOLOGY

Official Journal of the Scientific Society of Anatomists, Histologists, Embryologists and Topographic Anatomists of Ukraine

journal homepage: https://morphology-journal.com

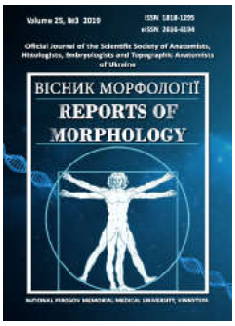

Features of microscopic changes in lung structure of young rats under conditions of hyperhomocysteinemia

Samborska I.A.
National Pirogov Memorial Medical University, Vinnytsya, Ukraine

ARTICLE INFO
Received: 31 May, 2019
Accepted: 23 June, 2019

UDC: 616.24:577.112.386:599.323.45

CORRESPONDING AUTHOR
e-mail: samborska1990@gmail.com
Samborska I.A.

Hyperhomocysteinemia is a risk factor for many diseases, including pathologies of the respiratory system. The pathogenesis of lung tissue damage is complex and multifactorial, however, it has now been found that homocysteine has a toxic effect on the vascular system and parenchyma of the organ. The purpose of the study is to identify the features of microscopic changes in the structure of the lungs of young rats under conditions of hyperhomocysteinemia. The experimental study was performed on 22 white non-linear young (1-2 months) male rats. During the experiment, the animals were divided into two groups - control and experimental. Simulation of persistent hyperhomocysteinemia was achieved by administering to rats of the experimental group thiolactone homocysteine at a dose of 200 mg/kg body weight intragastrically for 60 days. Histological specimens were examined using an SEO SCAN light microscope and photo-documented using a Vision CCD Camera with the system output images of histological preparations. It was found that the introduction of thiolactone homocysteine to young rats at a dose of 200 mg/kg led to the development of destructive changes in blood vessels, bronchi, components of the respiratory department with signs of atelectasis. Hemodynamic disorders and increased vascular permeability led to perivascular, peribronchial, interstitial, intra-alveolar edema, histo-leukocyte infiltration. The detected changes are reversible and have a compensatory nature.

Keywords: *hyperhomocysteinemia, lungs, aerohematic barrier, macrophages, neutrophils.*

Introduction

Homocysteine (HC) is a non-proteinogenic amino acid that is formed in the body under normal conditions during methionine metabolism. A considerable amount of it is involved in methionine resynthesis by transsulfuration [7]. Also, recycling of HC is carried out through remethylation and desulfurization reactions. Vitamins B6, B9 and B12 have been found to be extremely important for its metabolism, since they are involved in the synthesis of coenzymes, without which the metabolism of this amino acid is impossible [20]. According to most researchers, the normal level of HC in the blood is 5-15 μmol/L [22]. However, due to impaired synthesis and recycling processes, its level may increase, leading to the development of a health-threatening condition of hyperhomocysteinemia. To date, many causes for the development of hyperhomocysteinemia have been proven. These include: hereditary defects of enzymes methylenetetrahydrofolate reductase, cystathionine-β-synthase, methionine synthase; taking certain medicines (oral contraceptives, barbiturates, etc.), a diet high in methionine, kidney disease, drinking lots of coffee, smoking, alcoholism, a sedentary lifestyle [11, 13, 21]. Careful analysis of the sources of scientific literature has established that hyperhomocysteinemia is an independent risk factor for the development of coronary heart disease, strokes, obliterating atherosclerosis of the lower extremities, arterial and venous thrombosis, chronic heart failure [3, 4]. Numerous studies have also demonstrated its relationship to Alzheimer's disease, autism, vascular dementia, pregnancy miscarriage, non-alcoholic fatty liver disease, osteoporosis, cancer [9, 16].

In recent years, studies have focused on the relationship between blood plasma HC and the onset and progression of lung disease. Patients with chronic obstructive pulmonary disease record a state of hyperhomocysteinemia, which, according to the researchers, is evidence of severe disease [15]. Hypotheses regarding the role of HC in lung and pleural cancer development are also available [5].

HC has a direct toxic effect on the endothelial layer of the vascular wall, so in the pathogenesis of lung lesions in hyperhomocysteinemia attach great importance to the vascular system of the organ. In particular, it has been proved that HC causes a violation of the reactivity of the pulmonary artery wall due to the development of oxidative stress [18]. In addition, the HC is able to exert a direct damaging effect on the lung parenchyma and extracellular matrix [17].

Thus, studying the peculiarities of morphological changes in the structure of the lungs is an extremely important task, since the data obtained will contribute to a better understanding of the key links in the pathogenesis of hyperhomocysteinemia, to improve the diagnosis and treatment of respiratory diseases.

The purpose of the study is to identify the features of microscopic changes in the structure of the lungs of young rats under conditions of hyperhomocysteinemia.

Materials and methods

The experiments were performed on 22 white nonlinear young (1-2 months) male rats. During the experiment, the animals were divided into two groups - control and experimental. Simulation of persistent hyperhomocysteinemia was achieved by administering rats of the thiolactone HC to rats of test group at a dose of 200 mg/kg body weight intragastrically for 60 days. Animals were immobilized by decapitation under thiopental anesthesia. For microscopic examination, pieces of lung were collected from pre-weighed animals of all groups. The pieces were fixed in 10% formalin solution, the duration of the exposure did not exceed 1-2 days. The fixing solution used prevents the autolysis process and stabilizes the cells and tissues for their further processing and use in staining procedures. Next, the dehydration of the pieces in alcohols of increasing concentration and poured into paraffin blocks. The sections, 4-5 μm thick, were stained with hematoxylin and eosin and methylene blue [6]. Histological specimens were examined using an SEO SCAN light microscope and photo-documented using a Vision CCD Camera with the system of output of the image from histological preparations.

Results

Histological studies of the lungs of young rats under conditions of hyperhomocysteinemia caused by the introduction of thiolactone HC at a dose of 200 mg/kg, revealed impaired pulmonary hemodynamics, edema of the structural components of the respiratory compartment, vessel walls and bronchi.

Large, medium and especially small bronchial tubes and bronchioles are characterized by swelling and thickening of the wall, its deformation. Destruction of the fibro-cartilage sheath and muscle plate resulted in a reduction of the mucous folds. In the lumen of the bronchi revealed serous mucous contents with desquamated epitheliocytes. Adventitia infiltrated with leukocytes,

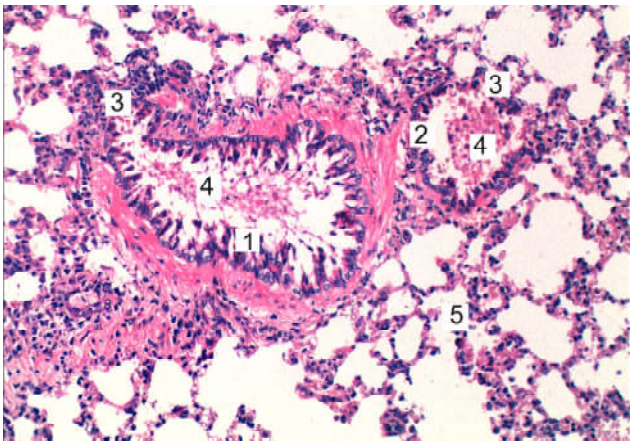

Fig. 1. Microscopic changes in the lungs of young rats under conditions of hyperhomocysteinemia. Large (1) and medium diameter (2) bronchus, deformation of the wall (3), serous-mucous contents in the lumen (4), respiratory department (5). Staining with hematoxylin and eosin. x100.

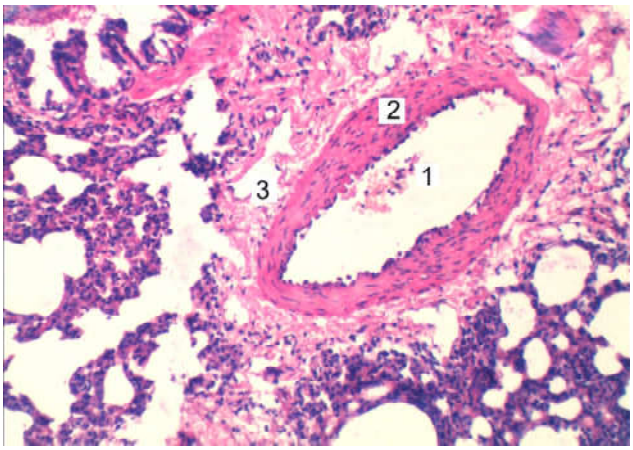

Fig. 2. Histological changes in the lungs of young rats under conditions of hyperhomocysteinemia. Large-diameter artery lumen (1), edema, media (2) and adventitia (3) destruction. Staining with hematoxylin and eosin. x100.

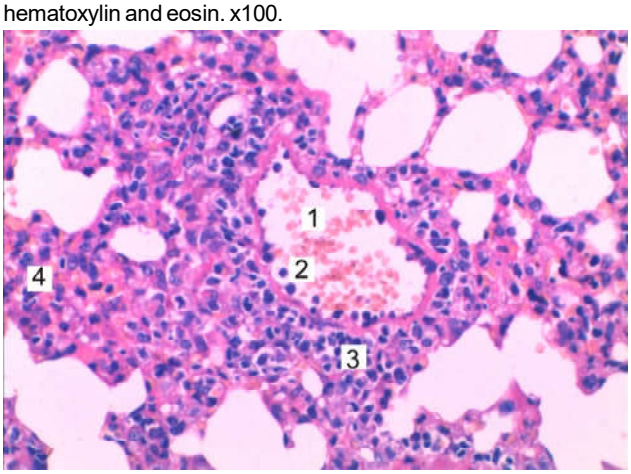

Fig. 3. Microscopic changes in the lungs of young rats under conditions of hyperhomocysteinemia. Small-diameter vein lumen (1), marginal lymphocyte standing near endothelium (2), leukocyte accumulation in adventitia (3), swelling and infiltration of respiratory compartment (4). Staining with hematoxylin and eosin. x200.

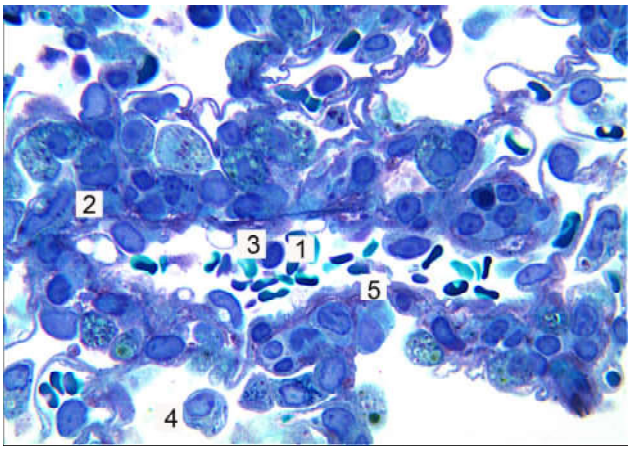

Fig. 4. Microscopic changes in the lungs of young rats under conditions of hyperhomocysteinemia. Venula lumen with blood cells (1), histo-leukocyte infiltration of the wall (2), destructively altered endothelial cells (3), alveolar macrophages in the lumen of the alveoli (4), basement membrane (5). Semi-thin section. Methylene blue. x400.

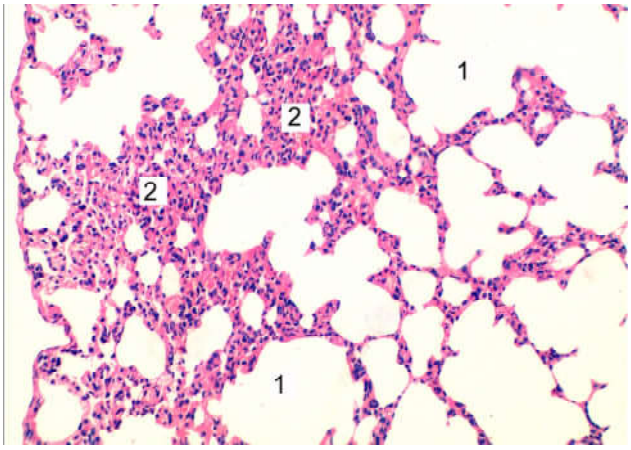

Fig. 5. Microscopic changes in the respiratory department of the lungs of young rats under conditions of hyperhomocysteinemia. Alveolar sacs (1), sites of atelectasis and histo-leukocyte infiltration (2). Staining with hematoxylin and eosin. x100.

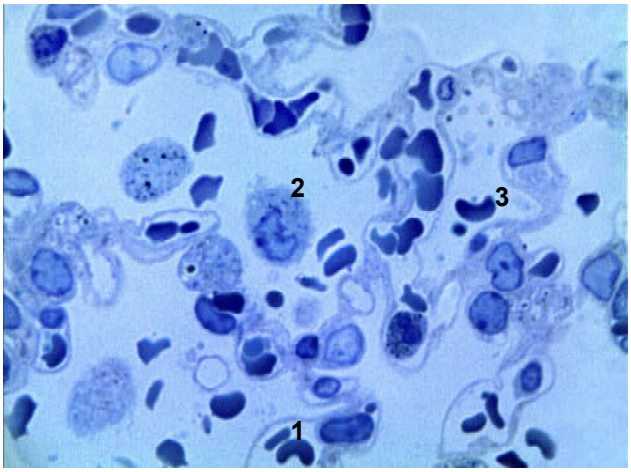

Fig. 6. Microscopic changes in the lungs of young rats of the respiratory department under conditions of hyperhomocysteinemia. Blood filled capillaries (1), alveolar macrophages (2), erythrocytes in the lumen of the alveoli (3). Semi-thin section. Methylene blue. x400.

macrophages (Fig. 1).

Reorganization of the vascular wall of large and medium diameter manifested expansion gaps and blood flow, edema and leukocyte infiltration, predominantly adventitia, also revealed blood vessels with narrowed lumen (Fig. 2, Fig. 3).

Microscopic changes in the vessels of the microcirculatory bed on semi-thin sections were characterized by heteromorphism. The venous blood flow was determined, with stasis, erythrocyte coagulation, platelet accumulation, neutrophils in the lumen, and leukocyte marginal standing near the endothelium. In the swollen endothelial cells, vacuoles were found, burning the nuclei into the lumen of the vessel. The basement membrane was also swollen, indistinct (Fig. 4). Microvessels with thickened wall, cramped by a narrow lumen were also detected. Dystonia of the vessel wall was also manifested by thinness, uneven thickening, narrow or collapsed lumen.

Manifestations of inflammatory character were determined in the migration of leukocytes mainly of lymphocytes into the intra alveolar septa with the formation of foci of inflammation.

In the respiratory department of the lungs, the intra alveolar septa were thickened due to the blood filling of the hemocapillaries and edema due to the increased permeability of the walls of the microvessels to the blood plasma. Histo-leukocyte infiltration of the parenchyma of the organ was also detected. The gaps of the alveoli showed an increase in the number of alveolar macrophages.

Among the unchanged histostructure of the lung tissue, small areas of dys- and atelectasis were also identified, with partially or completely absent luminal alveoli (Fig. 5). In the peripheral, subpleural areas, an emphysematous altered lung tissue was observed with sophisticated intra alveolar septa and significantly enlarged gups of the alveoli. The thinned sections of the aerohematic barrier were destroyed or ruptured, which led to the formation of elements and plasma in the lumen of the alveoli (Fig. 6).

Discussion

The data obtained from the experimental study confirm the already existing results, conducted with the aim of establishing the role of HC in lung injury. In particular, it was found that hyperhomocysteinemia, which develops as a result of cystathionine-β-synthase deficiency, leads to the development of pulmonary artery thrombosis, characterized by the presence of pulmonary tissue fibrosis and the destruction of the aerohematic barrier. The changes are accompanied by increased expression of collagen type I and transforming growth factor-β1 [8].

Severe chronic hyperhomocysteinemia causes activation of lipid peroxidation and inhibition of mechanisms of antioxidant protection of the lungs. The result of these changes is the development of oxidative stress, which

causes damage to lung tissue, increased production of macrophages and lymphocytes [2].

It has been established that in severe hyperhomocysteinemia, HC accumulates in the mitochondria of the lungs in rats, causing a direct toxic effect on them. Under these conditions, the metabolism of NO is impaired and its bioavailability is reduced, however, the production of reactive oxygen species is enhanced against the background of inhibition of the reserve-adaptive potential of lung mitochondria and, as a consequence, damage to the organ parenchyma [12].

To date, the role of hyperhomocysteinemia in the development of endothelial dysfunction has been confirmed. The latter is due to increased production of reactive oxygen species and reduced synthesis of nitric oxide. The decrease in the level of nitric oxide under conditions of hyperhomocysteinemia can also be caused by inhibition of the enzyme dimethylarginine dimethylaminohydrolase. Hyperhomocysteinemia-induced damage to mitochondrial DNA leads to dysfunction of these organelles and exacerbates bioenergetic processes in them, leading to the appearance of a closed circle and increased signs of oxidative stress. In addition, homocysteine activates the necrotic factor kappa β (NF-kβ) and the activation of the blood coagulation system, the production of adhesion molecules, cytokines and chemokines [14].

Experimental studies also revealed that hyperhomocysteinemia causes apoptosis of type II alveolocytes due to the development of oxidative stress in them [1, 10]. Hyperhomocysteinemia and folate deficiency are at risk of developing lung cancer due to impaired DNA synthesis and methylation [19].

Conclusions

The histological studies of the lungs of young rats under conditions of hyperhomocysteinemia revealed the initial destructive changes of the vessels, bronchi, components of the respiratory department. Hemodynamic disorders and increased vascular permeability led to perivascular, peribronchial, interstitial, intra-alveolar edema, histo-leukocyte infiltration. In the tissue of the respiratory department, small areas of dys- and atelectasis, emphysematous expansion, were found among the sites of unchanged organ structure. The detected changes are reversible and have a compensatory nature.

References

[1] Bai, Y., Fang, F., Jiang, J., & Xu, F. (2017). Extrinsic Calcitonin Gene-Related Peptide Inhibits Hyperoxia-Induced Alveolar Epithelial Type II Cells Apoptosis, Oxidative Stress, and Reactive Oxygen Species (ROS) Production by Enhancing Notch1 and Homocysteine-Induced Endoplasmic Reticulum Protein (HERP) Expression. *Med. Sci. Monit.*, 23, 5774-5782. doi: 10.12659/MSM.904549

[2] da Cuncha, A. A., Ferreira, A. G., da Cuncha, M. J., Pederzolli, C. D., Becker, D. L., Coelho, J. G. … Wyse, A. T. (2011). Chronic hyperhomocysteinemia induces oxidative damage in the rat lung. *Mol. Cell. Biochem.,* 358(1-2), 153-160. doi: 10.1007/s11010-011-0930-2

[3] Dayal, S., Blokhin, I., Erger, R. A., Jensen, M., Arging, E., Stevens, J. W. … Lentz, S. R. (2014). Protective Vascular and Cardiac Effects of Inducible Nitric Oxide Synthase in Mice with Hyperhomocysteinemia. *PLoS One,* 9(9): e107734. doi: 10.1371/journal.pone.0107734

[4] Dionisio, N., Jardin, I., Salido, G. M., & Rosado, J. A. (2010). Homocysteine, Intracellular Signaling and Thrombotic Disorders. *Curr. Med. Chem.,* 17(27), 3109-3119. doi: 10.2174/092986710791959783

[5] Durda, K, K?klewski, K, Gupta, S, Szydlowski, M, Baszuk, P, Jaworska-Bieniek, K. … Jakubowska, A. (2017). Serum folate concentration and the incidence of lung cancer. *PLoS One,* 12(5): e0177441. doi: 10.1371/journal.pone.0177441

[6] Goralskiy, L. P., Homich, V. T., & Kononskiy, O. I. (2011). *Fundamentals of histological technique and morphofunctional methods of research in normal and pathology.* Zhytomyr: Polissya.

[7] Grechanina, O. Ya. (2013). Methionine - an essential amino acid. *Clinical genetics and perinatal diagnostics*, 1(2), 19-35.

[8] Hamelet, J., Maurin, N., Fulchiron, R., Delabar, J. M., & Janel, N. (2007). Mice lacking cystathionine beta synthase have lung fibrosis and air space enlargement. *Exp. Mol. Pathol.,* 83(2), 249-253. doi: 10.1016/j.yexmp.2007.04.005

[9] Kaur, R., & Sekhon, B. S. (2013). Hyperhomocysteinemia: an overviews. *International journal of comprehensive pharmacy,* 5(1), 1-4.

[10] Liu, W. L., Liu, Z. W., Li, T. S., Wang, C., & Zhao, B. (2013). Hydrogen sulfide donor regulates alveolar epithelial cell apoptosis in rats with acute lung injury. *Clin. Med. J.*, 126(3), 494-499. PMID: 23422113

[11] Lutsyuk, M. B., Zaichko, N. V., Grigor'eva, G. S., Konahovich, M. A., Artemchuk, M. A., Pentyuk, N. O., & Postovitenko, K. P. (2013). Hyperhomocysteinemia syndrome: causes, methods of prevention and treatment. *Rational pharmacotherapy*, 29(4), 55-60.

[12] Medvedev, D. V., Zvyagina, V. I., Uryasev, O. M., Belskih, E. S., Bulatetskiy, S. V., & Ryabkov, A. N. (2017). Metabolic changes in lung mitochondria in experimental hyperhomocysteinemia in rats. *Biomedical Chemistry*, 63(3), 248-254. doi: 10.18097/PBMC20176303248

[13] Pentyuk, O. O., Lutsyuk, M. B., & Artemchuk, M. A. (2007). *Preclinical studies of hyperhomocysteinemic action of potential drugs.* K.: SPC MoH Ukraine.

[14] Pushpakunar, S., Kundu, S. & Sen, U. (2014). Endothelial Dysfunction: The Link Between Homocysteine and Hydrogen Sulfide. *Curr. Med. Chem.,* 21(32), 3662-3672. PMID: 25005183

[15] Prokofeva, T. V., Lipnitskaya, E. A., Kuzmichev, B. Yu., Polunina, O. S., Voronina, L. P., & Polunina, E. A. (2019). The effect of chronic obstructive pulmonary disease on the level of homocysteinemia and the condition of the coronary vessels in patients with myocardial infarction. *Tuberculosis and lung diseases,* 10(97), 12-18. doi: https://doi.org/10.21292/2075-1230-2019-97-10-12-18

[16] Skovierova, H., Vidomanova, E., Mahmood, S., Sopkova, J., Drgova, A., Cervenova, T. … Lehotsky, J. (2016). The molecular and cellular effect of homocysteine metabolism imbalance on human health. Intern. *J. of Molecular Scien.,* 17, 1-18. doi:

10.3390/ijms17101733
[17] Starcher, B., & Hill, C. H. (2005). Elastin defects in the lungs of avian and murine models of homocysteinemia. *Exp. Lung Res.,* 31(9-10), 873-885. doi: 10.1080/01902140600611629
[18] Tasatargil, A., Sadan, G., & Karasu, E. (2007). Homocysteine-induced changes in vascular reactivity of guinea-pig pulmonary arteries: role of the oxidative stress and poly (ADP-ribose) polymerase activation. *Pulm. Pharmacol. Ther.,* 20(3), 265-272. doi: 10.1016/j.pupt.2006.02.004
[19] Tastekin, D., Erturk, K., Bozbey, H. U., Olmuscelik, O., Kizitan, H., Tuna, S., & Tas, F. (2015). Plasma homocysteine, folate and vitamin B12 levels in patients with lung cancer. *Exp. Oncol.,* 37(3), 218-222. PMID: 26422108
[20] Wang, H., Sun, Q., Zhou, Y., Zhang, H., Luo, C., Xu, J. …Wang, W. (2017). Nitration-mediated deficiency of cystathione β-synthase activity accelerates the progression of hyperhomocysteinemia. *Free radical biology and medicine,* 113, 519-529. doi: https://doi.org/10.1016/j.freeradbiomed.2017.10.389
[21] Zaichko, N. V. (2010). Homocysteine, cysteine, and hydrogen sulfide levels in blood plasma of patients with deep vein thrombosis: association with C677T polymorphism in methylenetetrahydrofolate reductase gene. *Experimental and clinical physiology and biochemistry,* (4), 35-41.
[22] Zaichko, N. V., Lutsyuk, M. B., & Grigor'eva, G. O. (2012). Hyperhomocysteinemia: medico-social and pharmacological aspects. *Pharmaceutical courier,* (9), 30-35.

ОСОБЛИВОСТІ МІКРОСКОПІЧНИХ ЗМІН СТРУКТУРИ ЛЕГЕНЬ МОЛОДИХ ЩУРІВ ЗА УМОВ ГІПЕРГОМОЦИСТЕЇНЕМІЇ

Самборська І.А.

Гіпергомоцистеїнемія є фактором ризику розвитку багатьох захворювань, в тому числі і патології органів дихальної системи. Патогенез ураження тканини легень є складним та багатофакторним, однак на сьогоднішній день встановлено, що гомоцистеїн чинить токсичний вплив на судинну систему та паренхіму органу. Метою дослідження є виявлення особливостей мікроскопічних змін структури легень молодих щурів за умов гіпергомоцистеїнемії. Експериментальне дослідження проведено на 22 білих нелінійних молодих (1-2 місяці) щурах-самцях. У ході експерименту тварин було розподілено на 2 групи - контрольну і дослідну. Моделювання стану стійкої гіпергомоцистеїнемії досягали шляхом введення щурам дослідної групи тіолактону гомоцистеїну у дозі 200 мг/кг маси тіла інтрагастрально протягом 60 днів. Гістологічні препарати вивчали за допомогою світлового мікроскопа SEO SCAN та фотодокументували за допомогою відеокамери Vision CCD Camera з системою виводу зображення з гістологічних препаратів. Було встановлено, що введення тіолактону гомоцистеїну молодим щурам в дозі 200 мг/кг призвело до розвитку деструктивних змін судин, бронхів, компонентів респіраторного відділу з ознаками ателектазів. Гемодинамічні розлади і посилення судинної проникності призвели до периваскулярного, перибронхіального, інтерстиційного, внутрішньоальвеолярного набряку, гістолейкоцитарної інфільтрації. Виявлені зміни зворотні та мають пристосувально-компенсаторний характер.

Ключові слова: *гіпергомоцистеїнемія, легені, аерогематичний бар'єр, макрофаги, нейтрофіли.*

ОСОБЕННОСТИ МИКРОСКОПИЧЕСКИХ ИЗМЕНЕНИЙ СТРУКТУРЫ ЛЕГКИХ МОЛОДЫХ КРЫС В УСЛОВИЯХ ГИПЕРГОМОЦИСТЕИНЕМИИ

Самборская И.А.

Гипергомоцистеинемия является фактором риска развития многих заболеваний, в том числе и патологии органов дыхательной системы. Патогенез поражения ткани легких является сложным и многофакторным, однако, на сегодняшний день установлено, что гомоцистеин оказывает токсическое воздействие на сосудистую систему и паренхиму органа. Целью исследования является выявление особенностей микроскопических изменений структуры легких молодых крыс в условиях гипергомоцистеинемии. Экспериментальное исследование проведено на 22 белых нелинейных молодых (1-2 месяца) крысах-самцах. В ходе эксперимента животных разделили на две группы - контрольную и опытную. Моделирование состояния устойчивой гипергомоцистеинемии достигали путем введения крысам опытной группы тиолактона гомоцистеина в дозе 200 мг/кг массы тела интрагастрально в течении 60 дней. Гистологические препараты изучали с помощью светового микроскопа SEO SCAN и фотодокументировали с помощью видеокамеры Vision CCD Camera с системой вывода изображения с гистологических препаратов. Было установлено, что введение тиолактона гомоцистеина молодым крысам в дозе 200 мг/кг привело к развитию деструктивных изменений сосудов, бронхов, компонентов респираторного отдела с признаками ателектазов. Гемодинамические расстройства и усиление сосудистой проницаемости привели к периваскулярному, перибронхиальному, интерстициальному, внутриальвеолярному отеку, гистолейкоцитарной инфильтрации. Выявленные изменения обратимы и имеют приспособительно-компенсаторный характер.

Ключевые слова: *гипергомоцистеинемия, легкие, аэрогематический барьер, макрофаги, нейтрофилы.*

DOI: 10.31393/morphology-journal-2019-25(3)-02 Reports of Morphology, Vol. 25, №3, Pages 10-15

ISSN 1818-1295 eISSN 2616-6194

REPORTS OF MORPHOLOGY

Official Journal of the Scientific Society of Anatomists, Histologists, Embryologists and Topographic Anatomists of Ukraine

journal homepage: https://morphology-journal.com

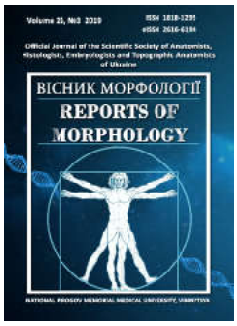

Structural changes of lymph nodes under high calorie diet and melatonin correction

Harapko T.V.[1], Mateshuk-Vatseba L.R.[2], Holovatskyi A.S.[1]

[1]Department of Human Anatomy and Histology, Uzhhorod National University, Medical Faculty, Uzhhorod, Ukraine
[2]Department of Normal Anatomy, Lviv National Medical University named after Danylo Halytskyi, Lviv, Ukraine

ARTICLE INFO
Received: 11 June, 2019
Accepted: 15 July, 2019

UDC: 616-056.257:611.018.53:611.428

CORRESPONDING AUTHOR
e-mail: garapkotv@gmail.com
Harapko T.V.

The article presents and analyzes data from an experimental study conducted on white rats in females and males of reproductive age. The purpose of the study to study the morphometric and histological changes in the parenchyma of the lymph nodes of rats under the high-calorie diet (HCD) and with the correction of melatonin. The study was performed on 80 white rats of reproductive age. Microanatomy of the structural components of lymph nodes of white rats under physiological norms was examined in 10 intact animals. Experimental animals are divided into 5 groups. Statistical processing of digital data was performed using "Excel" software and "STATISTICA 6.0" using the parametric method. Eight weeks after HCD, there was a significant decrease in the relative area of the cortical substance in the parenchyma of lymph nodes of white rats of males and females by 10.3 % and 8.3 %, respectively, and an increase in the relative area of the medullary substance by 16.1 % and 13.2 %, respectively, greater than the intact animal group parameter. Corticomedullary index (CMI) decreased by 22.9 % and 19.0 %. After six weeks of HCD and the next six weeks of standard vivarium diet and melatonin administration, the relative area of cortical substance in the parenchyma of lymph nodes of white rats in males and females was 2.0 % and 2.9 %, respectively, greater than the parameters of the intact group of animals. Accordingly, the relative area of the medullary substance is 3.1 % and 4.6 % less than the parameters of the intact group of animals. CMI in both male and male rats was 5.1 % and 7.6 %, respectively, greater than the intact animal group parameter. Under the conditions of melatonin correction, it was found that on the histological preparations of lymph nodes the vein and artery were full-blooded. Empty hemocapillaries with thickened wall are observed. In the paracortical region, the number of high endothelial capillary venules decreases. Thus, long-term administration of melatonin improves the morphometric parameters of the parenchyma of the lymph nodes of rats, restores the morphological structure of the organ.

Keywords: *experiment, lymph node, sodium glutamate, melatonin, correction.*

Introduction

Obesity is a risk factor for human health. This is a complex medico-social problem of today, as most overweight people do not see this condition as a real threat to health [9, 11, 22]. The current issue is the study of the effect of obesity on organs and tissues, as well as the possibility of correction of these changes [1, 14, 15]. Of particular interest are the organs of the immune system, in particular lymph nodes, which provide protection of the body against genetically foreign cells and substances coming exo- or endo-pathways [6, 7, 13, 18, 20]. They are also called biological "filters".

In most cases, a high-calorie diet is used to develop experimental obesity. We choose sodium glutamate as a dietary supplement to the standard vivarium diet. The monosodium salt of glutamic acid (glutamate sodium), known as the "flavor enhancer", is used in most groceries.

Melatonin, a pineal hormone, was selected for correction. It is an important regulator of sleep and circadian rhythms [4, 16, 19, 24]. Melatonin (N-acetyl-5methoxytryptamine) is a hormone synthesized by pinealocytes of the epiphysis under the control of the suprachiasmatic nucleus of the hypothalamus (the principal driver of circadian rhythms) [5, 12, 17]. It can also be formed in the heart, kidneys, digestive canal, genitals and other cells [2]. Interest in the healing properties of melatonin increased when it was noted that it

was not only found in humans but also identified in many foods - olive oil, tomatoes, fish, wine and others [8].

Aim of the study: to study the morphometric and histological changes of the parenchyma of the lymph nodes of rats under high-calorie diet and with melatonin correction.

Materials and methods

The study was conducted on 80 white rats females and males of reproductive age (2.5-6.5 months) weighing 120-280 g.

The structure of lymph nodes of white rats under normal conditions was examined in ten intact animals. All experimental animals were divided into 5 groups: the first group (10 animals), which were fed HCD for 8 weeks; the second group (10 animals), which were fed a HCD for 8 weeks and then transferred to a standard vivarium diet (for 8 weeks); a third group (10 animals) fed a HCD for 6 weeks, then transferred to a standard vivarium diet and administered melatonin for 2 weeks; the fourth group (10 animals) and the fifth group (10 animals) are similar to the previous one, but melatonin was administered for 4 and 6 weeks, respectively. Each group consisted of 5 male rats and 5 female rats. HCD was achieved by adding 0.07 g/kg of rat body weight to food glutamate. The dose of melatonin was 10 mg/kg of body weight of the rat. The drug was administered orally daily in the afternoon at the same time. The control was served by 20 white rats who received a standard vivarium diet instead of the high-calorie diet.

All the test animals were in the vivarium of Danylo Halytsky Lviv National Medical University. The studies were carried out in accordance with the provisions of the "European Convention for the Protection of Vertebrate Animals Used for Experimental and Other Scientific Purposes" (Strasbourg, 1986), Council of Europe Directive 86/609/EEC (1986), Law of Ukraine No. 3447-IV "On the protection of animals from ill-treatment", general ethical principles of animal experiments approved by the First National Congress of Ukraine on Bioethics (2001).

Morphometric studies were performed on histological specimens stained with hematoxylin and eosin, as well as with Heidenhain's azan using Videotest-5.0, KAAPA Image Base, Stepanizer and Microsoft Exel on a personal computer.

Statistical processing of digital data was performed using "Excel" and "STATISTICA 6.0" software using parametric methods. The numerical values of the parameters are represented by sample averages (M), standard deviation (σ), standard error of the mean (m), Student's t test (t). The results of the calculations were presented in graphical form in histograms using Microsoft Office, indicating confidence intervals at 95 % confidence level (p=0.95).

Results

The structure of mesenteric lymph nodes in rats of intact and control groups corresponded to the species norm, as evidenced by the results of histological examinations. Lymph nodes are surrounded externally by the connective tissue capsule, from which go deep into the parenchyma numerous cortex and medulla trabeculae. On the cramped part of the node there is hilum. The parenchyma of the lymph node consists of located on the periphery cortex, and closer to the hilum - medulla. Under the capsule contains the marginal sinus. The primary and secondary lymph nodes are located in the cortex. Secondary nodes contain an illumination center - a germinal center or breeding center. A darker boundary zone is located around such a center. The medulla consists of medullar cords and medullar sinuses (Fig. 1).

After 8 weeks of HCD, a significant decrease in the relative area of the cortex in the parenchyma of lymph nodes of white rats of males and females was found, by 10.3 % and 8.3 %, respectively, compared to the intact group of animals (Tables 1, 2). The relative area of the medulla increases and exceeds the parameters of the intact group of animals by 16.1 % and 13.2 %, respectively (see Tables 1, 2). CMI decreases in both male and female rats by 22.9 % and 19.0%, respectively.

In both male rats and female rats, cortical, medullar, and marginal lymphatic sinuses were dilated and deformed after 8 weeks of experiment. In their lumen, the proportion of reticular connective tissue increased, which was accompanied by a decrease in the proportion of lymphocytes (Fig. 2). Dense B-lymphocytes, plasmocytes, and macrophages were observed in the medullar cord. Empty hemocapillaries with thickened walls were often noticeable. The number of capillary venules increased, especially in the paracortical region of the lymph nodes. The process of migration of lymphocytes from the bloodstream to the parenchyma of the lymph node was pronounced, as evidenced by the large number of them in the lumen of the vessels and the wall. This confirms the

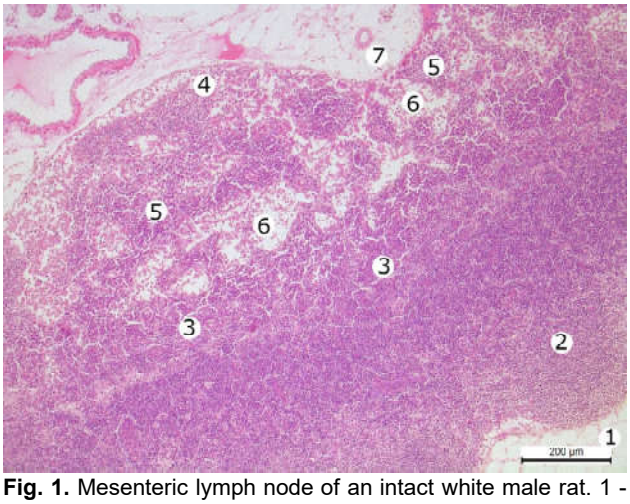

Fig. 1. Mesenteric lymph node of an intact white male rat. 1 - capsule of the lymph node; 2 - cortex; 3 - paracortical region; 4 - medulla; 5 - medullary cord; 6 - medullary sinus; 7 - hilum of the lymph node. Hematoxylin-eosin. Objective x10, eyepiece x10.

Table 1. Dynamics of changes in the relative area of cortex and medulla and corticomedullary index (CMI) of lymph nodes of white male rats in control and experimental groups (M±m).

Group of animals	S_{cortex},%	$S_{medulla}$,%	CMI
Intact animals	61.08±1.56	38.92±0.78	1.569±0.112
Group 1 (8 weeks of HCD)	54.80±1.61*	45.20±0.87*	1.212±0.211*
Group 2 (8 weeks of HCD, 8 weeks of cancellation)	53.67±1.45*	46.33±0.81*	1.158±0.179*
Group 3 (6 weeks of HCD, 2 weeks of melatonin)	55.05±1.21*	44.95±0.76*	1.225±0.119*
Group 4 (6 weeks of HCD, 4 weeks of melatonin)	58.94±1.19*	41.06±0.83*	1.435±0.113*
Group 5 (6 weeks of HCD, 6 weeks of melatonin)	62.29±1.34	37.71±0.71	1.652±0.171

Notes: here and in the future, * - values that are statistically significantly different from those of the intact group of animals ($p<0.05$).

Table 2. Dynamics of changes in the relative area of cortex and medulla and corticomedullary index (CMI) of lymph nodes of white female rats in control and experimental groups (M±m).

Group of animals	S_{cortex},%	$S_{medulla}$,%	CMI
Intact animals	61.23±1.70	38.77±0.76	1.579±0.109
Group 1 (8 weeks of HCD)	56.12±1,65*	43.88±0.78*	1.279±0.123*
Group 2 (8 weeks of HCD, 8 weeks of cancellation)	55.46±1.55*	44.54±0.67*	1.245±0.157*
Group 3 (6 weeks of HCD, 2 weeks of melatonin)	57.75±1.45*	42.25±0.71*	1.367±0.147*
Group 4 (6 weeks of HCD, 4 weeks of melatonin)	59.05±1.54	40.95±0.75*	1.442±0.211*
Group 5 (6 weeks of HCD, 6 weeks of melatonin)	63.01±1.45	36.99±0.81	1.703±0.185*

common belief among morphologists that obesity is a chronic inflammatory process that leads to the continued activity of the immune protection units. The number of secondary lymph nodes in the cortex of lymph nodes of white rats increases, they contain extended centers of reproduction. The relative area of the paracortex decreases. The enlarged, full-blooded and deformed arteries and veins contain platelets and erythrocytes with signs of adhesion and aggregation in their lumen. Often, vessels of the hemomicrocirculatory bed with a damaged wall are found, which leads to bleeding in the parenchyma of the organ.

After 8 weeks of abrogation of HCD, the relative area of the cortex in the parenchyma of lymph nodes of white rats of males and females decreased by only 2.1 % and 1.2 %, which is 12.1 % and 9.4 % less than the parameters of the intact group of animals (see Tables 1, 2). Accordingly, the relative area of the medulla increases by 2.5 % and 1.5 %, which is 19.0 % and 14.9 % higher than the parameters of the intact group of animals (see Tables 1, 2). CMI decreases in both male and female rats by 26.1 % and 20.1 %, respectively. Histologically, both in male rats and female rats, the structure of the parenchyma of the lymph nodes differed little from the previous experimental group (Fig. 3). The fat content was significantly increased around the organ compared to the control group of animals. Trabeculae extending from the capsule are clearly expressed, thickened. Arteries with thickened wall, full-blooded, veins deformed, enlarged and full-blooded. The marginal sinus is unevenly expanded and deformed. The medullary sinus is enlarged, tortuous. The relative area of the paracortex decreases.

Morphometric indices in group 3 of animals (six weeks of HCD followed by 2 weeks of melatonin administration) indicate that the relative area of the cortex in the lymph nodes parenchyma of white rats of males and females decreased by 9.9 % compared to intact group of animals, by 9.9 % and 5.7 % (see Tables 1, 2). Accordingly, the relative area of the medulla increased by 15.5 % and 9.0 %, respectively, exceeding the similar parameters of the intact group of animals (see Tables 1, 2). CMI in both male and female rats was 22.3 % and 13.3 %, respectively, smaller than the intact animal parameter.

Histologically in the parenchyma of the lymph nodes of rats revealed that the number of secondary lymph nodes is slightly reduced compared with the previous group of animals, decreases the proportion of adipose tissue around the organ. However, the vessels are full-blooded, dilated, deformed. B-lymphocytes, plasmocytes and macrophages are densely located in the medullary cord. The number of monocytes, plasmocytes and macrophages increases (Fig. 4). An increase in the proportion of B-dependent zones and a decrease in T-dependent zones were detected. Such changes can lead to a redistribution

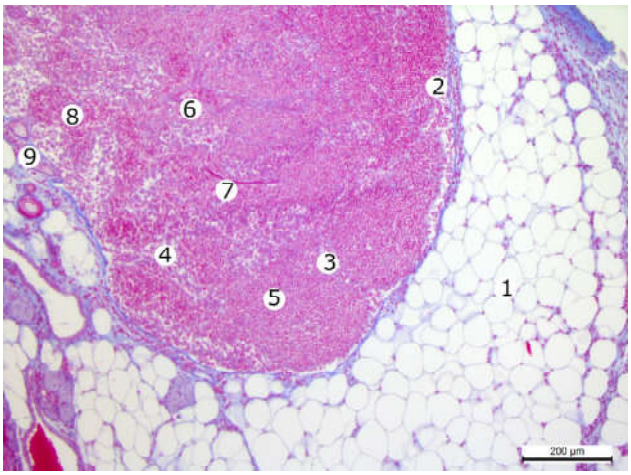

Fig. 2. Fragment of a lymph node of a white rat male after 8 weeks of HCD. 1 - adipose tissue in the thickness of the capsule and around the lymph node; 2 - marginal sinus; 3 - cortex sinus; 4 - medullary sinus; 5 - secondary lymph node; 6 - capillary venula; 7 - hemocapillary; 8 - medullary cord; 9 - hilum of the lymph node. Heidenhain's azan staining. Objective x10, eyepiece x10.

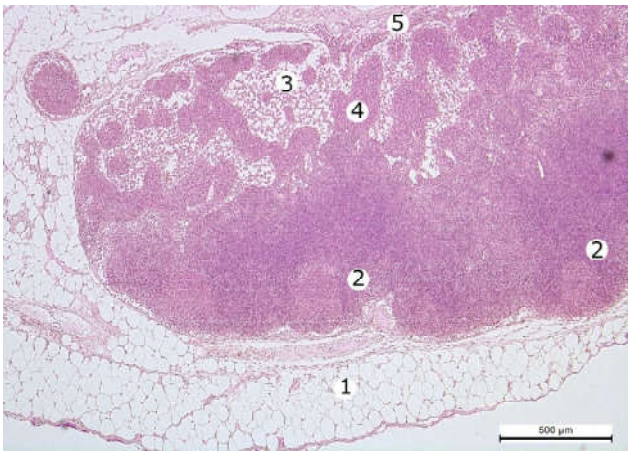

Fig. 3. Fragment of the lymph node of the white rat male after 8 weeks of HCD, followed by its cancellation after 8 weeks. 1 - adipose tissue in the thickness of the capsule and around the lymph node; 2 - secondary lymph node in the cortex; 3 - enlarged medullary sinus; 4 - medullary cord; 5 - hilum of the lymph node. Hematoxylin-eosin. Objective x5, eyepiece x10.

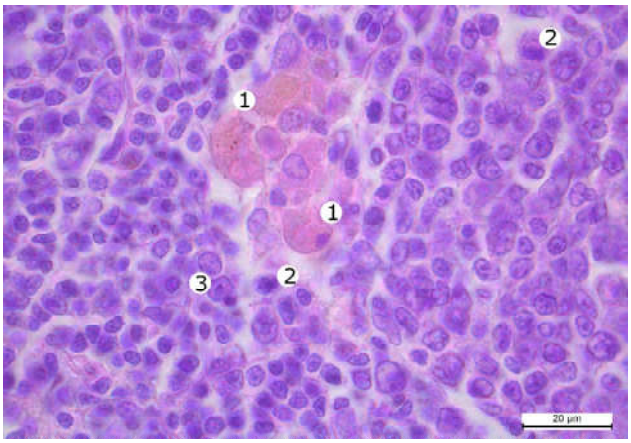

Fig. 4. Fragment of the cortex of the white rat female lymph node after 6 weeks of HCD and subsequent administration of melatonin for 2 weeks. 1 - macrophages; 2 - cells with signs of apoptosis; 3 - lymphocytes. Hematoxylin-eosin. Objective x100, eyepiece x10.

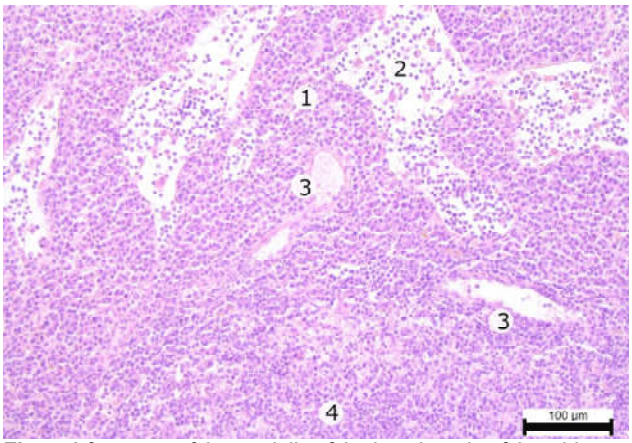

Fig. 5. A fragment of the medulla of the lymph node of the white rat female after 6 weeks HCD, followed by the introduction of melatonin for 6 weeks. 1 - medullary cord; 2 - medullary sinus; 3 - arterioles with thickened wall. Hematoxylin-eosin. Objective x10, eyepiece x10.

of activity toward a humoral immune response.

Morphometric indices in the fourth group of animals (6 weeks of HCD followed by 4 weeks of melatonin administration) indicate that the relative area of the cortex in the lymph nodes parenchyma of white rats in male and female rats increased by 7.1 % and 2.3 %, respectively compare with the previous group of animals. These figures are 3.5 % and 3.6 % lower than similar parameters of intact animals (see Tables 1, 2). Accordingly, the relative area of the medulla in the parenchyma of lymph nodes of white rats-males and females decreased by 8.7 % and 3.1 % compared with the previous group of animals, which is 5.5 % and 5.6 % higher than the same parameter of intact animals (see Tables 1, 2). CMI in both male and female rats was 8.3 % and 8.7 %, respectively, smaller than the intact animal group parameter.

Morphometric indices in the fifth group of animals (6 weeks of HCD followed by 6 weeks of melatonin administration) indicated that the relative area of the cortex in the lymph node parenchyma of white rats in males and females increased by 5.7 % and 6.7 %, respectively compare with the previous group of animals and is on 2.0 % and 2.9 % higher similar parameters of the intact group of animals (see Tables 1, 2). Accordingly, the relative area of the medulla decreases by 8.2 % and 9.7 % compared to the previous group of animals and is 3.1 % and 4.6 % less than the parameters of the intact group of animals (see Tables 1, 2). CMI in both male and female rats was 5.1 % and 7.6 %, respectively, greater than the intact animal parameter. Histologically, both full-blood veins and arteries occur in male and female rats of the fifth experimental group of animals, the artery and arterioles wall are thickened (Fig. 5). In the paracortex, the number of high endothelial capillary venules decreases. Empty hemocapillaries with thickened wall are found.

Discussion

Obesity reduces the size of inguinal lymph nodes, impairs lymphatic transport and migration of dendritic cells to peripheral lymph nodes, and reduces the number of T lymphocytes in lymph nodes. In general, obesity disrupts the integrity of the immune system and leads to changes in the development of leukocytes and lymphocytes, their migration and diversity [3].

Diet-induced obesity in mice leads to significant disruption of the lymphatic system, which is reflected by a decrease in lymph flow, changes in lymph node architecture and impaired dendritic cell migration. Using different research methods, it was discovered [23] that obesity leads to impaired lymphatic transport in the subcutaneous tissue and drainage it to the lymph nodes.

It has been found that body weight gain has a linear negative correlation with lymphatic function and that obesity leads to a decrease in lymphatic vessel density and a decrease in vascular filling. In addition, it has been found that increasing body weight and the degree of obesity lead to the progression of the surrounding lymphatic accumulation

of inflammatory cells [14].

Some authors [21] have argued that melatonin can correct structural and functional changes in the small intestinal wall that are caused by obesity. They also note that evening administration of the drug to experimental animals with obesity is more effective than morning administration.

In experiments on type 2 diabetes mellitus with resistant hypertension and in rats with metabolic syndrome [17], it was shown that the administration of melatonin significantly facilitates the course of hypertension.

Experimentally, [10] it was found that administration of melatonin leads to a decrease in body weight of rats, triglyceride levels, LDL, and an increase in plasma cholesterol and HDL. Ghada M. et al. [10] concluded that melatonin should be used as a treatment to prevent the harmful effects of obesity and related metabolic disorders such as dyslipidemia and insulin resistance.

The prospects for further development are related to the further study of the morphometric and submicroscopic changes in the structural organization of the lymph nodes of rats at different times of experimental obesity and its correction.

Conclusions

1. After 8 weeks of HCD a significant decrease in the relative area of the cortex in the parenchyma of lymph nodes of white rats of males and females by 10.3 % and 8.3 %, respectively, and an increase in the relative area of the medulla by 16.1 % and 13.2 % compared with an intact group of animals.

2. After 6 weeks of HCD, followed by melatonin for 6 weeks, the relative area of the cortex in the parenchyma of lymph nodes of white rats in males and females increased by 2.0 % and 2.9 %, respectively, compared with the intact group of animals. Accordingly, the relative area of the medulla decreased by 3.1 % and 4.6 %.

3. Under conditions of melatonin correction, it was found that the histological samples of lymph nodes in both male rats and female rats revealed full-blooded veins and arteries. Empty hemocapillars with thickened wall are available. In the paracortex, the number of high endothelial capillary venules decreases. Thus, long-term administration of melatonin "improves" the morphometric parameters of the parenchyma of the lymph nodes of rats and restores the morphological structure of the organ.

References

[1] Andersen, C. J., Murphy, K. E., & Fernandez, M. L. (2016). Impact of Obesity and Metabolic Syndrome on Immunity. *Adv. Nutr.*, 7(1), 66-75. doi: 10.3945/an.115.010207

[2] Aylamazyan, E. K., Evsyukova, I. I., & Yarmolinskaya, M. I. (2018). The role of melatonin in the development of gestational diabetes. *Zhurnal akusherstva i zhenskih bolezney,* 67(1), 85-91. doi: 10.17816/JOWD67.185-191

[3] Beltiukova, S. V. (2016). Determination of monosodium glutamate thin-layer chromatography method with detection fluorescent. Visnyk ONU. *Khimiia,* 57(1), 50-58.

[4] Cardinali, P., & Hardeland, R. (2017). Inflammaging, metabolic syndrome and melatonin: a call for treatment studies. *Neuroendocrinology,* 104(4), 382-397. doi: 10.1159/000446543

[5] Do Amaral, F. G., Andrade-Silva, J., Kuwabara, W., & Cipolla-Neto, J. (2019). New insights into the function of melatonin and its role in metabolic disturbances. *Expert Review of Endocrinology & Metabolism,* 14(4), 299-303. doi: 10.1080/17446651.2019.1631158

[6] El-Aziza, R., Naguiba, M., & Rashedb, L. (2018). Spleen size in patients with metabolic syndrome and its relation to metabolic and inflammatory parameters. *The Egyptian Journal of Internal Medicine*, 30, 78-82. doi: 10.4103/ejim.ejim_86_17

[7] Escobedo, N., & Oliver, G. (2017). The Lymphatic Vasculature: Its Role in Adipose Metabolism and Obesity. *Cell metabolism,* 26(4), 598-609. doi: 10.1016/j.cmet.2017.07.020

[8] Favero, G., Franceschetti, L., Buffoli, B., Moghadasian, M. H., Reiter, R. J., Rodella, L. F., & Rezzani, R. (2017). Melatonin: protection against age-related cardiac pathology. *Ageing Research Reviews,* 35, 336-349. doi: 10.1016/j.arr.2016.11.007

[9] Fedecostante, M., Spannella, F., Giulietti, F., Espinosa, E, Dessi-Fulgheri, P., & Sarzani, R. (2015). Associations between body mass index, ambulatory blood pressure findings, and changes in cardiacstructure: relevance of pulse and nighttime pressures. *J. Clin. Hypertens*. (Greenwich), 17(2), 147-153. doi: 10.1111/jch.12463

[10] Ghada, M., Fard, A., Madi, N. M., & El-Saka, M. H. (2013). Effect of Melatonin on Obesity and Lipid Profile in High Fat-Fed Rats. *Journal of American Science,* 9(10), 61-67.

[11] Inoue, H., Kodani, E., Atarashi, H., Okumura K., Yamashita, T., & Origasa, H. (2016). Impact of Body Mass Index on the Prognosis of Japanese Patients with Non-Valvular Atrial Fibrillation. *Am. J. Cardiol.,* 118(2), 215-221. doi: 10.1016/j.amjcard.2016.04.036

[12] Khaksar, M., Oryan, A., Sayyari, M., Rezabakhsh, A., & Rahbarghazi, R. (2017). Protective effects of melatonin on long-term administration of fluoxetine in rats. *Experimental and toxicologic pathology.* 69(8), 564-574. doi: 10.1016/j.etp.2017.05.002

[13] Magnuson, A. M., Regan, D. P., Fouts, J. K., Booth, A. D., Dow, S. W., & Foster, M. T. (2017). Diet-Induced Obesity Causes Visceral, But Not Subcutaneous, Lymph Node Hyperplasia via Increases in Specific Immune Cell Populations. *Cell Prolif.,* 50(5). doi: 10.1111/cpr.12365

[14] Nitti, M. D., Hespe, G. E., Kataru, R. P., Nores, G. D., Savetsky, I. L., Torrisi, J. S., & Mehrara, B. J. (2016). Obesity induced lymphatic dysfunction is reversible with weight loss. *J. Physiol.,* 594(23), 7073-7087. doi: 10.1113/JP273061

[15] Oliveira, E., Castro, S., Ayupe, C. M., Ambrósio, G. E., Souza, P. V., Macedo, C. G., & Ferreira, A. P. (2019). Obesity affects peripheral lymphoid organs immune response in murine asthma model. Immunology, 157(3), 268-279. doi: 10.1111/imm.13081

[16] Prado, N., Ferder, L., Manucha, W., & Diez, E. (2018). Anti-inflammatory effects of melatonin in obesity and hypertension. *Curr. Hypertens. Rep.,* 20(5), 45. doi: 10.1007/s11906-018-0842-6

[17] Rahman, M. M., Kwon, H. S., Kim, M. J., Go, H. K., Oak, M. H., & Kim, D. H. (2017). Melatonin supplementation plus exercise behavior ameliorate insulin resistance, hypertension and fatigue in a rat model of type 2 diabetes mellitus. *Biomedicine & pharmacotherapy,* 92, 606-614. doi: 10.1016/j.biopha.2017.05.035

[18] Suami, H., & Scaglioni, M. F. (2017). Lymphatic Territories

(Lymphosomes) in the Rat: an Anatomical Study for Future Lymphatic Research. *Plast. Reconstr. Surg.,* 140(5):945-951. doi: 10.1097/PRS.0000000000003776

[19] Tordjman, S., Chokron, S., Delorme, R., Charrier, A., Bellissant, E., Jaafari, N., & Fougerou, C. (2017). Melatonin: pharmacology, functions and therapeutic benefits. *Current neuropharmacology.* 15(3), 434-443. doi: 10.2174/1570159X14666161228122115

[20] Valko, O. O., & Holovatskyi, A. S. (2018). Changes in the cell squad of iliac lymph nodes of white rats in case of longterm influence of nalbufin. *EUREKA: Health Sciences,* 2, 8-16. doi: 10.21303/2504-5679.2018.00573

[21] Vareniuk, I., Shevchuk, N., Roslova, N., & Dzerzhynskyi M. (2019). Effect of morning and evening administration of melatonin on the condition of the mucous membrane and small intestine crypts in obese rats. *Bulletin of Taras Shevchenko National University of Kyiv*, 1, 50-53.

[22] Wan, H., Wu, S., Wang, J., Yang, Y., Zhu, J., Shao, X., … & Zhang, H. (2017). Body mass index and the risk of all-cause mortality among patients with nonvalvular atrial fibrillation: a multicenter prospective observational study in China. *Eur. J. Clin. Nutr.,* 71(4), 494-499. doi: 10.1038/ejcn.2016.183

[23] Weitman, E. S., Aschen, S. Z., Farias-Eisner, G., Albano, N., Cuzzone, D. A., Ghanta, S., & Mehrara, B. J. (2013). Obesity Impairs Lymphatic Fluid Transport and Dendritic Cell Migration to Lymph Nodes. *PLoS One.* 8(8), 700-703. doi: 10.1371/journal.pone.0070703

[24] Zaichenko, H. V., Horchakova, N. O., Klymenko, O. V., Yakovleva, N. Iu., & Sinitsyna, O. S. (2019). Melatonin as a potential cardioprotector: an experimental clinical analysis of efficiency. *Visnyk problem biolohii i medytsyny,* 2, 1(150), 26-35. doi: 10.29254/2077-4214-2019-2-1-150-26-35

СТРУКТУРНІ ЗМІНИ ЛІМФАТИЧНИХ ВУЗЛІВ ЗА УМОВ ВИСОКОКАЛОРІЙНОЇ ДІЄТИ ТА КОРЕКЦІЇ МЕЛАТОНІНОМ

Гарапко Т.В., Матешук-Вацеба Л.Р., Головацький А.С.

В статті наведені та проаналізовані дані експериментального дослідження, яке проводили на 80 білих щурах-самицях і самцях репродуктивного віку. Мета дослідження - вивчити морфометричні та гістологічні зміни паренхіми лімфатичних вузлів щурів за умови висококалорійної дієти (ВКД) та при корекції мелатоніном. Мікроанатомію структурних компонентів лімфатичних вузлів білих щурів за умов фізіологічної норми дослідили на 10 інтактних тваринах. Експериментальні тварини поділені на 5 груп. Статистичну обробку цифрових даних проводили за допомогою програмного забезпечення "Excel" та "STATISTICA 6.0" з використанням параметричного методу. Через 8 тижнів ВКД спостерігали достовірне зменшення відносної площі кіркової речовини у паренхімі лімфатичних вузлів білих щурів-самців та самиць на 10,3 % та 8,3 % та відповідно, збільшення відносної площі мозкової речовини на 16,1 % та 13,2 % у порівнянні з інтактною групою тварин. Корково-мозковий індекс (КМІ) зменшився на 22,9 % та 19,0 %. Через 6 тижнів ВКД і наступних 6 тижнів стандартного харчового раціону віварію та введення мелатоніну відносна площа коркової речовини в паренхімі лімфатичних вузлів білих щурів-самців та самиць становила відповідно на 2,0 % та 2,9 % більше параметрів інтактної групи тварин. Відповідно відносна площа мозкової речовини зменшилася на 3,1 % та 4,6 % порівняно з інтактною групою тварин. Корково-мозковий індекс (КМІ) як в щурів-самців, так і в щурів-самиць збільшився, відповідно, на 5,1 % та 7,6 % порівняно з інтактною групою тварин. Після корекції мелатоніном виявлено, що на гістологічних препаратах лімфатичних вузлів вени та артерії повнокровні. Наявні "порожні" гемокапіляри з потовщеною стінкою. У прикірковій ділянці кількість закапілярних венул з високим ендотелієм зменшується. Таким чином, тривале введення мелатоніну "покращує" морфометричні показники паренхіми лімфатичних вузлів щурів, відновлює морфологічну будову органу.

Ключові слова: *експеримент, лімфатичний вузол, глутамат натрію, мелатонін, корекція.*

СТРУКТУРНЫЕ ИЗМЕНЕНИЯ ЛИМФАТИЧЕСКИХ УЗЛОВ В УСЛОВИЯХ ВЫСОКОКАЛОРИЙНОЙ ДИЕТЫ И КОРРЕКЦИИ МЕЛАТОНИНОМ

Гарапко Т.В., Матешук-Вацеба Л.Р., Головацкий А.С.

В статье приведены и проанализированы данные экспериментального исследования, которое проводилось на 80 белых крысах самках и самцах репродуктивного возраста. Цель исследования - изучить морфометрические и гистологические изменения паренхимы лимфатических узлов крыс в условиях высококалорийной диеты (ВКД) и при коррекции мелатонином. Микроанатомию структурных компонентов лимфатических узлов белых крыс в условиях физиологической нормы исследовали на 10 интактных животных. Экспериментальные животные разделены на 5 групп. Статистическую обработку цифровых данных проводили с помощью программного обеспечения "Excel" и "STATISTICA 6.0" с использованием параметрического метода. Через 8 недель ВКД наблюдали достоверное уменьшение относительной площади коркового вещества в паренхиме лимфатических узлов белых крыс-самцов и самок на 10,3 % и 8,3 % и, соответственно, увеличение относительной площади мозгового вещества на 16,1 % и 13,2 % по сравнению с интактной группой животных. Корково-мозговой индекс (КМИ) уменьшился на 22,9 % и 19,0 %. Через 6 недель ВКД и последующих 6 недель стандартного пищевого рациона вивария с применением мелатонина относительная площадь коркового вещества в паренхиме лимфатических узлов белых крыс самцов и самок составляла на 2,0 % и 2,9 % больше параметров интактной группы животных. Соответственно относительная площадь мозгового вещества на 3,1 % и 4,6 % меньше параметров интактной группы животных. КМИ как у крыс-самцов, так и у крыс-самок на 5,1 % и 7,6 % соответственно больше параметра интактной группы животных. В условиях коррекции мелатонином выявлено, что на гистологических препаратах лимфатических узлов вены и артерии полнокровные. Наблюдаются "пустые" гемокапилляры с утолщенной стенкой. В околокорковом веществе количество закапиллярных венул с высоким эндотелием уменьшается. Таким образом, длительное введение мелатонина "улучшает" морфометрические показатели паренхимы лимфатических узлов крыс, восстанавливает морфологическое строение органа.

Ключевые слова: *эксперимент, лимфатический узел, глутамат натрия, мелатонин, коррекция.*

DOI: 10.31393/morphology-journal-2019-25(3)-03 Reports of Morphology, Vol. 25, №3, Pages 16-20

ISSN 1818-1295 eISSN 2616-6194

REPORTS OF MORPHOLOGY

Official Journal of the Scientific Society of Anatomists, Histologists, Embryologists and Topographic Anatomists of Ukraine

journal homepage: https://morphology-journal.com

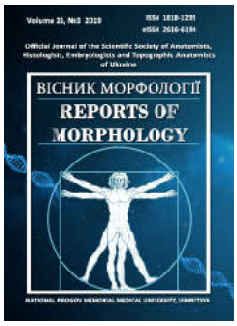

Submicroscopic changes of alveoli of respiratory department of lungs a day after experimental thermal trauma

Nebesna Z.M.[1], Bashynska O.I.[2], Ocheretna N.P.[2], Galunko G.M.[2], Slyvka O.Ya.[2]

[1]Ivan Horbachevsky Ternopil National Medical University of the Ministry of Health of Ukraine, Ternopil, Ukraine

[2]National Pirogov Memorial Medical University, Vinnytsya, Ukraine

ARTICLE INFO

Received: 15 June, 2019

Accepted: 20 July, 2019

UDC: 618.173-039.11-053.7/.84

CORRESPONDING AUTHOR

e-mail: nebesna_zm@tdmu.edu.ua

Nebesna Z.M.

Deep, large thermal burns are not limited to local lesions of tissues, they cause significant disruption of all systems and organs of the organism, change in metabolic processes. It is revealed that the primary links in the pathogenesis of burn disease are destruction of the skin, impaired neuroendocrine regulation and significant hemodynamic disorders. The reorganization of structures and impaired lung function, in response to a pathological process in the body, is attracting increasing attention of scientists. The aim of the study was to establish a submicroscopic rearrangement of the alveoli after a thermal lesion for 1 day after the experimental thermal trauma. Grade III burns were applied under ketamine anesthesia with copper plates heated in boiled water to a temperature of 97-100°C. The size of the lesion area was 18-20 % of the epilated surface of the body of rats. An experimental study of the structural components of lung alveoli after burn injury was performed on laboratory white male rats weighing 160-180 g. Euthanasia of rats was performed after ketamine anesthesia by decapitation. In the experiment, the study of the submicroscopic state of the walls of the alveoli of the lungs after thermal trauma was done. It is established that in the stage of shock after the application of burn injury - 1 day, in the alveoli of the respiratory department of the lung, there are adaptive compensatory and initial destructive changes of all structural components of the alveoli. Damage to the ultrastructure of the aerohematical barrier is manifested by intracellular edema and edema of the organelles of the endothelial cells, respiratory and secretory epitheliocytes, and the amount of heterochromatin increases in their deformed nuclei. The basement membrane also has signs of edema, sometimes homogeneous, fuzzy. The decrease in the number of vesicles and micropinocytotic vesicles in endothelial and respiratory epitheliocytes leads to impaired endothelial and alveolar metabolism. Numerous actively phagocytic alveolar macrophages with a well-expressed lysosomal apparatus are found in the alveoli. Initial alternative alterations of the ultrastructure of the components of the air-barrier barrier lead to disruption of gas exchange in the respiratory department of the lungs

Keywords: *lung alveoli, aerohematic barrier, submicroscopic changes, thermal trauma.*

Introduction

Burns are the most common type of injury and are accompanied by significant changes in the structure and function of organs and systems of the affected organism [1, 3, 4, 5, 9, 11, 16]. In the early term after the injury disturbance of the enzyme homeostasis is caused by the disintegration of tissues in the lesion area, the subsequent destruction of the internal organs [10, 12, 18]. The disorders are directly related to changes in the burned skin as a source of biologically active substances that enter the bloodstream. Other sources of biologically active substances are organs and tissues that are not directly exposed to thermal effects, but are in a state of ischemia and circulatory hypoxia [3, 8, 13]. In the area of the lesion, after a thermal injury, a significant inflammatory reaction occurs, which is accompanied by the formation of biologically active substances, tissue breakdown products, specific and nonspecific toxins, which is the trigger mechanism of burn intoxication [8, 13, 15].

In the affected organism occurs centralization of circulation, which is adaptive in nature, but at the same time leads to significant disorders of regional and peripheral circulation. Not compensated disorders of microcirculation,

which accrue in time, lead to disorders of the systemic circulation and impaired function of all organs and systems [3, 7]. Hypovolemia is one of the leading factors leading to impaired lung respiratory function [14, 17, 19]. In a small circle of circulation the peripheral vascular resistance increases congestion develops. The decrease in circulating blood volume occurs mainly due to plasma loss [2]. Due to the loss of skin barrier function, as well as increased vascular permeability due to the action of vasoactive substances (histamine, serotonin, bradykinin, etc.), there is a pronounced plasma loss.

Given that the components of the respiratory department of the lungs after thermal trauma are not fully understood, it is advisable to conduct an in-depth study of the submicroscopic state of the cells of the alveoli wall of the respiratory department of the lungs.

Therefore, *the purpose* of the work was to establish a submicroscopic rearrangement of alveoli of the lungs of animals after thermal lesion in the shock stage after the experimental burn injury.

Materials and methods

The experiments were performed on 15 adult white male rats. The animals were kept on the standard diet of the vivarium of Ivan Horbachevsky Ternopil National Medical University of the Ministry of Health of Ukraine. Animal care and all manipulations were carried out in accordance with the provisions of the "European Convention for the Protection of Vertebrate Animals Used for Experiments and for Other Scientific Purposes" (Strasbourg, 1986) and in accordance with the provisions of the "General Ethical Principles for Experiments on animals", approved by the First National Congress on Bioethics (Kyiv, 2001). Grade III burns were applied under ketamine anesthesia with copper plates heated in boiled water to a temperature of 97-100°C. The size of the lesion area was 18-20 % of the epilated surface of the body of rats. On a daily examination, we monitored their general condition, the extent of local changes in the area of the burn wound, body weight, and mortality. The object of the study was the lungs. To study submicroscopic changes, animals were decapitated under ketamine anesthesia for 1 day, which, according to modern concepts, corresponds to the stage of shock of burn disease [13].

For ultrastructural studies, lung pieces were collected, fixed in 2.5 % glutaraldehyde solution, postfixed with 1 % osmium tetroxide solution on phosphate buffer. Further processing was carried out according to conventional methods [5]. Ultra-thin sections made on an LKB-3 ultramicrotome were counterstained with uranyl acetate, lead citrate according to the Reynolds method, and studied in an electron microscope PEM-125K.

Results

Electron microscopic studies have shown that the stage of shock for hemocapillaries is characterized by reactive

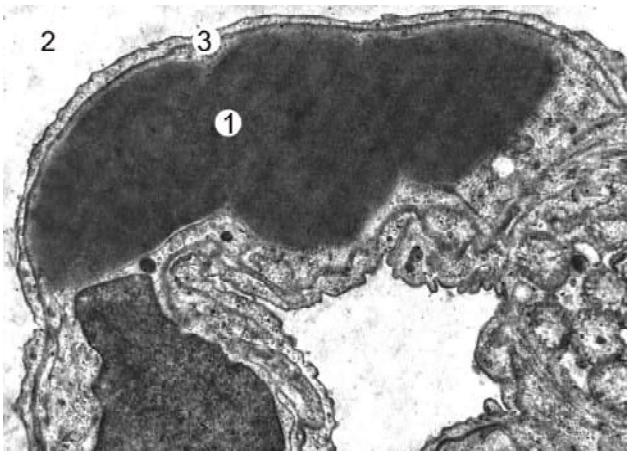

Fig. 1. Submicroscopic condition of the hemocapillary of the respiratory department of the lung animal a day after thermal trauma. Hemopapillary lumen (1), alveoli lumen (2), aerohematic barrier (3). x12000.

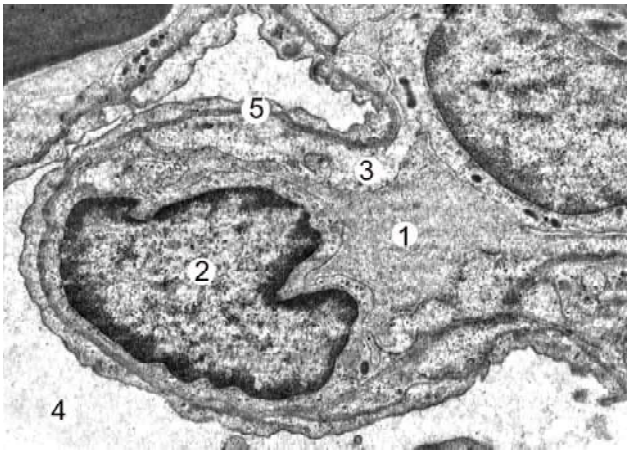

Fig. 2. The ultrastructural state of the hemocapillary of the respiratory compartment of the animal lung a day after thermal trauma. Hemocapillary lumen (1), endothelial cell nucleus (2), endothelial cell cytoplasm swollen (3), alveoli lumen (4), aerohematic barrier (5). x11000.

changes, which are manifested by the enlargement of the lumen, significant blood filling and stasis formation. In endothelial cells, the initial signs of the destructive changes that are manifested by the disruption of the nucleus and cytoplasmic organelles are established. The hypertrophied nuclei have a rounded shape, with some of the invasions of karyolemma and the indistinct outlines of its membranes. Perinuclear space in some areas is expanded. The karyoplasm contains mainly euchromatin, however, in the part of the nuclei, marginally located tubercles of heterochromatin are noted. Enlarged tubules of the endoplasmic reticulum are located in the perinucleus zone, and the Golgi complex is represented by thickened cisterns and large vesicles. Peripheral, cytoplasmic areas of the endothelial cells were characterized by enlightenment and focal edema and a decrease in the number of pinocytosis vesicle and caveolae (Fig. 1).

The nuclei of the respiratory alveolocytes have a rounded

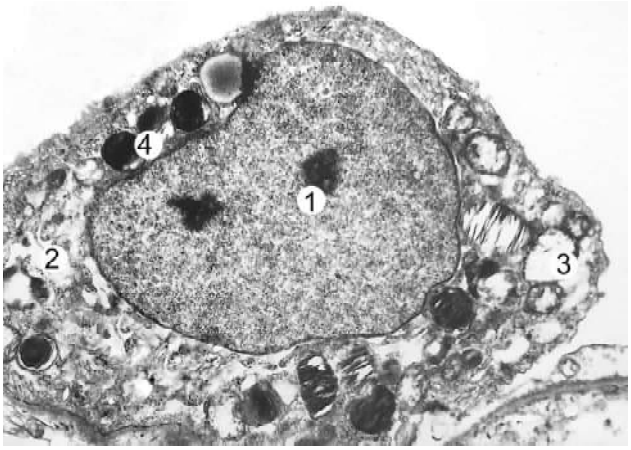

Fig. 3. Ultrastructural state of the secretory alveolocyte of the respiratory department of the lungs a day after thermal trauma. Nuclei with nucleolus (1), dilated tubules of the endoplasmic reticulum (2), emptied lamellar bodies (3), young lamellar bodies (4). x26000.

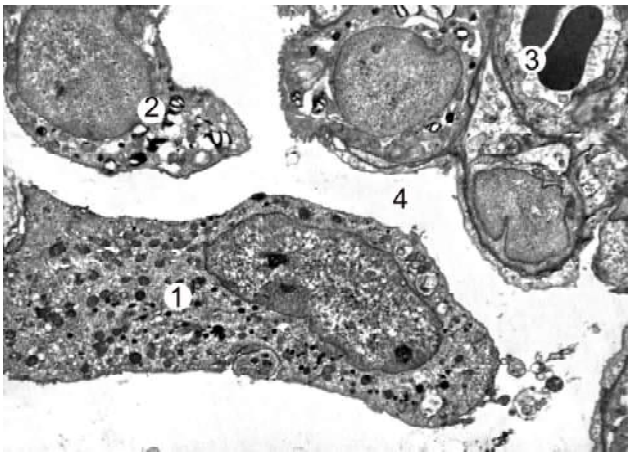

Fig. 4. Ultrastructural condition of alveoli of respiratory department of lungs a day after thermal trauma. Alveolar macrophage (1), type II alveolocytes (2), hemocapillary lumen (3), alveolar lumen (4). x6000.

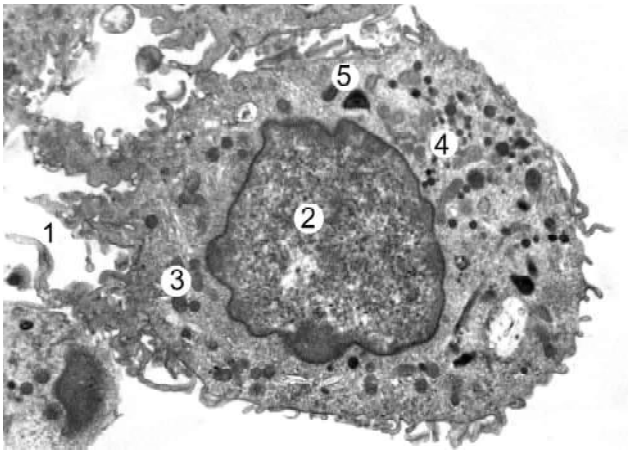

Fig. 5. Ultrastructural state of alveolar macrophage of respiratory department of lungs a day after thermal trauma. Plasmalemma staining (1), nucleus (2), mitochondria (3), primary lysosomes (4), phagosomes (5). x8000.

shape, fuzzy contours of the cariole membrane and invaginations. In moderately electron-dense karyoplasm, euchromatin prevails. The cytoplasm of cells is swollen, enlightened, especially in the peripheral regions. The integrity and structural organization of most organelles is partially impaired, with little pinocytosis vesicles. The basement membrane of the aerohematic lung barrier is characterized by swelling, thickening, or some areas of thinning (Fig. 2).

In the stage of burn shock in the secretory alveolocytes rounded nuclei are observed, membranes of the karyolemma are fuzzy, form shallow indentations, in the karyoplasm, euchromatin prevails, nucleolus are found. At some loci, the perinuclear space is enlarged and few nuclear pores are detected. In the cytoplasm of the secretory epitheliocytes, degranulation is observed, which is accompanied by a decrease in the amount of osmiophilic material in the lamellar bodies, and young forms are also present. The tubules of the endoplasmic reticulum are unevenly expanded, with few ribosomes on their membranes. The Golgi complex of type II alveolocytes is represented by expanded cisterns and a small number of vesicles and vacuoles. The mitochondria are hypertrophied, with electron-light matrix and fuzzy crystals. The apical surface of the cells contains few small microvilli (Fig. 3).

In the lumen of the alveoli, there is an increase in the number of alveolar macrophages that are in a state of increased functional activity. A considerable number of cytoplasmic outgrowths are found on their surface. Macrophage nuclei have irregularly shaped and invasive karyolemma. In the karyoplasm prevail euchromatin, there is one or two nuclei. The cytoplasm contains small, osmiophilic primary lysosomes and small secondary lysosomes. Small mitochondria have different shapes and their matrix is electron-dense. Dictyosomes of the Golgi complex are located mainly in the paranuclear space of the cytoplasm and are formed by expanded cisterns, small vesicles and vacuoles. The tubules of the granular endoplasmic reticulum are non-stretchable and thickened, with a moderate number of ribosomes on their membranes (Fig. 4, Fig. 5).

Discussion

Conducted submicroscopic studies of the components of the alveoli of the lungs in the stage of burn shock in thermal trauma revealed that the pathological link is impaired microcirculation in the walls of the alveoli, and causes the development of local hypoxia and increased proteolysis, permeability of the wall of microvessels with access to the alveoli of plasma components having lipolytic and proteolytic properties, which is fully consistent with scientific works [7, 13]. The expressed disturbances of microcirculation in the lungs during burn shock are accompanied by blockage of the capillary bed, stasis, bypass of blood flow, as well as violation of the aerohematic barrier. Interstitial edema creates hypoxia conditions for alveoli cells and, first of all, for large alveolocytes that produce surfactant.

In the stage of burn shock in the secretory alveolocytes in the cytoplasm there is degranulation, which is accompanied by a decrease in the number of lamellar bodies and osmiophilic material in them. Submicroscopically, there is an increase in the number of alveolar macrophages in the alveolar lumen that are in a state of increased functional activity.

During the period of shock after skin burns, pulmonary edema is detected as a violation of vascular permeability. Significant in this belongs to the segmented leukocytes. Violation of the permeability of microvessels develops as a result of the complex action of a number of factors that are in the blood and released locally by cellular elements during their degradation. The second component of the system of phagocytic cells, together with leukocytes, which are subject to urgent mobilization under conditions of burn shock are alveolar macrophages. Their increase is an adaptation reaction, a manifestation of the tension of all protective systems in a situation critical to the body [14, 17].

In the swollen areas of the lung, in the alveoli there is perfusion, but there is no aeration, which contributes to the strengthening of arterial hypoxemia in the period of shock. Thus, pulmonary edema is one of the links in the pathogenesis of burn shock.

However, the lungs are the only organ where not only blood circulation provides the vital function of the organ, but the organ itself exists for the circulation of the main function - gas exchange. Therefore, the unity of the functioning of the circulatory and respiratory systems is a necessary, adaptive pattern [13].

Thus, the results obtained from our own studies correlate with the scientific data of other researchers [13, 14, 17] and allow to conclude that severe thermal trauma in the early term of the experiment leads to disturbances of the ultrastructure of the aerohematical lung barrier. At the stage of shock in the experimental burns, adaptive compensatory changes and the initial signs of destructive ones were established. Hemocapillaries within the alveoli wall have enlarged blood-filled lumps, stasis formation is detected. Swelling of respiratory epitheliocytes and endothelial cells, disturbances in their cytoplasm of organelles, reduction of pinocytosis leads to the deterioration of gas exchange processes in the lungs.

Further studies plan to determine the degree of morphological changes in the structural components of the lung alveoli in dynamics after experimental thermal trauma under the condition of using corrective drugs.

Conclusions

Severe thermal injury leads to disruption of the ultrastructure of the aerohematic lung barrier. In the stage of shock during the experimental burns, adaptive-compensatory processes and signs of destructive changes of the alveolar epithelium, macrophages and the wall of the hemocapillaries are established, which leads to disruption of gas exchange processes in the lungs.

References

[1] Cherkasov, V. G., Kovalchuk, A. I., Dzevulskaya, I. V., Malikov, A. V., Lakhtadyr, T. V., & Matkivskaya, R. M. (2015). Structural transformations in the internal organs with infusion therapy for burn disease. *Medical science of Ukraine,* 11(3-4), 4-11.

[2] Dzevulska, I. V., Kovalchuk, O. I., Cherkasov, E. V., Majewskyi, O. Ye., Shevchuk, Yu. G., Pastukhova, V. A., & Kyselova, T. M. (2018). Influence of lactoproteinum solution with sorbitol on dna content of cells of endocrine glands on the background of skin burn in rats. *World of Medicine and Biology,* 2(64), 33-39. doi:10.26724/2079-8334-2018-2-64-33-39

[3] Evers, L. H., Bhavsar, D., & Mail?nder, P. (2010). The biology of burn injury. *Experimental dermatology,* 19(9), 777-783. doi: 10.1111/j.1600-0625.2010.01105.x

[4] Gavryluk, A. O., Gunas, I. V., Galunko, G. M., Chereshniuk, I. L., & Lysenko, D. A. (2017). Indicators of the cell cycle and fragmentation of DNA of cells of small intestinal mucosa through 14, 21 and 30 days after burn skin damage on the background of infusion of 0,9 % NaCl solution. *Biomedical and Biosocial Anthropology,* 29, 104-108.

[5] Goralskiy, L. P., Homich, V. T., & Kononskiy, O. I. (2011). *Fundamentals of histological technique and morphofunctional methods of research in normal and in pathology.* Zhitomir: Polissya.

[6] Gunas, I. V., Guminskiy, Yu. I., Ocheretna, N. P., Lysenko, D. A., Kovalchuk, O. I., Dzevulska, I. V., & Cherkasov, E. V. (2018). Indicators cell cycle and dna fragmentation of spleen cells in early terms after thermal burns of skin at the background of introduction 0.9 % NaCl solution. *World of Medicine and Biology,* 1(63), 116-120. doi: 10.26.724/2079-8334-2018-1-63-116-120

[7] Herold, S., Gabrielli, N. M., & Vadász, I. (2013). Novel concepts of acute lung injury and alveolar-capillary barrier dysfunction. *American Journal of Physiology-Lung Cellular and Molecular Physiology,* 305(10), L665-L681. doi: 10.1152/ajplung.00232.2013

[8] Janak, J. C., Clemens, M. S., Howard, J. T., Le, T. D., Cancio, L. C., Chung, K. K., ... Stewart, I. J. (2018). Using the injury severity score to adjust for comorbid trauma may be double counting burns: implications for burn research. *Burns,* 44(8), 1920-1929. doi: 10.1016/j.burns.2018.03.012

[9] Jeschke, M. G., Pinto, R., Kraft, R., Nathens, A. B., Finnerty, C. C., Gamelli, R. L., ... Herndon, D. N. (2015). Morbidity and survival probability in burn patients in modern burn care. *Critical care medicine,* 43(4), 808-815. doi: 10.1097/CCM.0000000000000790

[10] Kallinen, O., Maisniemi, K., Bohling, T., Tukiainen, E., & Koljonen, V. (2012). Multiple organ failure as a cause of death in patients with severe burns. *Journal of burn care & research,* 33(2), 206-211. doi: 10.1097/BCR.0b013e3182331e73

[11] Kearney, L., Francis, E. C., & Clover, A. J. (2018). New technologies in global burn care-a review of recent advances. *International journal of burns and trauma,* 8(4), 77-87. PMID: 30245912

[12] Maievskyi, O. Y., Bobruk, S. V., & Gunas, I. V. (2018). Dynamics of histochemical changes in the skin of rats within a month after the burning of II-III degrees on the background of the injection first 7 days HAES-LX-5% solution. *World of Medicine and Biology,* 4(66), 180-184. doi: 10.26724/2079-8334-2018-4-66-180-184

[13] Netyukhailo, L. G., Kharchenko, A. G., & Kostenko, S. V. (2011). Pathogenesis of burn disease (in 2 parts). *World of Medicine*

and Biology, 1, 127-131.
[14] Ocheretnyuk, A. O., Palamarchuk, O. V., Lysenko, D. A., Vashchuk, G. I., & Stepanyuk, G. I. (2018). Influence of solution of lactoprotein with sorbitol on ultrastructural changes in lungs of rats in the condition of burn shock. *Regulatory Mechanisms in Biosystems,* 9(3), 440-445. https://doi.org/10.15421/021866
[15] Porter, C., Tompkins, R. G., Finnerty, C. C., Sidossis, L. S., Suman, O. E., & Herndon, D. N. (2016). The metabolic stress response to burn trauma: current understanding and therapies. *The Lancet,* 388(10052), 1417-1426. doi: 10.1016/S0140-6736(16)31469-6
[16] Rowan, M. P., Cancio, L. C., Elster, E. A., Burmeister, D. M., Rose, L. F., Natesan, S., ... & Chung, K. K. (2015). Burn wound healing and treatment: review and advancements. *Critical care,* 19(1), 243. doi: 10.1186/s13054-015-0961-2
[17] Sousse, L. E., Herndon, D. N., Andersen, C. R., Zovath, A., Finnerty, C. C., Mlcak, R. P., ... & Hawkins, H. K. (2015). Pulmonary histopathologic abnormalities and predictor variables in autopsies of burned pediatric patients. *Burns,* 41(3), 519-527. doi: 10.1016/j.burns.2014.09.014
[18] Tiwari, V. K. (2012). Burn wound: How it differs from other wounds? *Indian journal of plastic surgery,* 45(02), 364-373. doi: 10.4103/0970-0358.101319
[19] Zhang, D., Chang, Y., Han, S., Yang, L., Hu, Q., Yu, Y., ... & Chai, J. (2018). The microRNA expression profile in rat lung tissue early after burn injury. *Turkish Journal of Trauma and Emergency Surgery,* 24(3), 191-198. doi: 10.5505/tjtes.2018.98123

СУБМІКРОСКОПІЧНІ ЗМІНИ АЛЬВЕОЛ РЕСПІРАТОРНОГО ВІДДІЛУ ЛЕГЕНЬ ЧЕРЕЗ ДОБУ ПІСЛЯ ЕКСПЕРИМЕНТАЛЬНОЇ ТЕРМІЧНОЇ ТРАВМИ

Небесна З.М., Башинська О.І., Очеретна Н.П., Галунко Г.М., Сливка О.Я.

Глибокі, великі за площею термічні опіки не обмежуються тільки місцевими ураженнями тканин, вони викликають значні порушення всіх систем і органів організму, змінюють обмінні процеси. Виявлено, що первинними ланками у патогенезі опікової хвороби є руйнування шкірного покриву, порушення нейроендокринної регуляції та значні гемодинамічні розлади. Реорганізація структур і порушення функцій легень, як реакція на патологічний процес в організмі, привертає все більшу увагу науковців. Метою дослідження було встановлення субмікроскопічної перебудови альвеол після термічного ураження на 1 добу після експериментальної термічної травми. Опік III ступеня наносили під кетаміновим наркозом мідними пластинами, нагрітими у киплячій воді до температури 97-100°С. Розміри ділянки ураження складали 18-20 % епільованої поверхні тіла щурів. Експериментальне вивчення структурних компонентів альвеол легень після опікової травми було виконано на лабораторних білих щурах-самцях масою 160-180 г. Евтаназію щурів проводили після кетамінового наркозу, шляхом декапітації. В експерименті проведено вивчення субмікроскопічного стану стінок альвеол легень після термічної травми. Встановлено, що в стадії шоку після нанесення опікової травми - 1 доба, в альвеолах респіраторного відділу легень виявляються пристосувально-компенсаторні та початкові деструктивні зміни усіх структурних компонентів альвеол. Пошкодження ультраструктури аерогематичного бар'єру проявляється інтрацелюлярним набряком та набряком органел ендотеліоцитів, респіраторних та секреторних епітеліоцитів, в їх деформованих ядрах зростає кількість гетерохроматину. Базальна мембрана також має ознаки набряку, подекуди гомогенна, нечітка. Зменшення числа везикул та мікропіноцитозних пухирців в ендотеліальних та респіраторних епітеліоцитах призводить до порушення ендотеліального та альвеолярного обміну. В альвеолах виявляються чисельні активно фагоцитуючі альвеолярні макрофаги із добре вираженим лізосомальним апаратом. Встановлені початкові альтеративні зміни ультраструктури компонентів аерогематичного бар'єру призводять до порушення газообміну у респіраторному відділі легень.

Ключові слова: *альвеоли легень, аерогематичний бар'єр, субмікроскопічні зміни, термічна травма.*

СУБМИКРОСКОПИЧЕСКИЕ ИЗМЕНЕНИЯ АЛЬВЕОЛ РЕСПИРАТОРНОГО ОТДЕЛА ЛЕГКИХ ЧЕРЕЗ СУТКИ ПОСЛЕ ЭКСПЕРИМЕНТАЛЬНОЙ ТЕРМИЧЕСКОЙ ТРАВМЫ

Небесная З.М., Башинская Е.И., Очеретная Н.П., Галунко А.М., Сливка О.Я.

Глубокие, большие по площади термические ожоги не ограничиваются только местными поражениями тканей, они вызывают значительные нарушения всех систем и органов организма, изменяют обменные процессы. Выявлено, что первичными звеньями в патогенезе ожоговой болезни являются разрушение кожного покрова, нарушение нейроэндокринной регуляции и значительные гемодинамические расстройства. Реорганизация структур и нарушение функций легких, как реакция на патологический процесс в организме, привлекает все большее внимание ученых. Целью исследования было установление субмикроскопической перестройки альвеол после термического поражения на 1 сутки после экспериментальной термической травмы. Ожог III степени наносили под кетаминовым наркозом медными пластинами, нагретыми в кипящей воде до температуры 97-100°С. Размеры участка поражения составляли 18-20 % эпилированной поверхности тела крыс. Экспериментальное изучение структурных компонентов альвеол легких после ожоговой травмы было выполнено на лабораторных белых крысах-самцах массой 160-180 г. Эвтаназию крыс проводили после кетаминового наркоза путем декапитации. В эксперименте проведено изучение субмикроскопического состояния стенок альвеол легких после термической травмы. Установлено, что в стадии шока после нанесения ожоговой травмы - 1 сутки, в альвеолах респираторного отдела легких определяются приспособительно-компенсаторные и начальные деструктивные изменения всех структурных компонентов альвеол. Повреждения ультраструктуры аэрогематического барьера проявляется интрацеллюлярным отеком и отеком органелл эндотелиоцитов, респираторных и секреторных эпителиоцитов, в их деформированных ядрах растет количество гетерохроматина. Базальная мембрана также имеет признаки отека, иногда гомогенная, нечеткая. Уменьшение числа везикул и микропиноцитозных пузырьков в эндотелиальных и респираторных эпителиоцитах приводит к нарушению эндотелиального и альвеолярного обмена. В альвеолах определяются многочисленные активно фагоцитирующие альвеолярные макрофаги с хорошо выраженным лизосомальным аппаратом. Установленные начальные альтеративные изменения ультраструктуры компонентов аэрогематического барьера приводят к нарушению газообмена в респираторном отделе легких.

Ключевые слова: *альвеолы легких, аэрогематический барьер, субмикроскопические изменения, термическая травма.*

DOI: 10.31393/morphology-journal-2019-25(3)-04 Reports of Morphology, Vol. 25, №3, Pages 21-26

ISSN 1818-1295 eISSN 2616-6194

REPORTS OF MORPHOLOGY

Official Journal of the Scientific Society of Anatomists, Histologists, Embryologists and Topographic Anatomists of Ukraine

journal homepage: https://morphology-journal.com

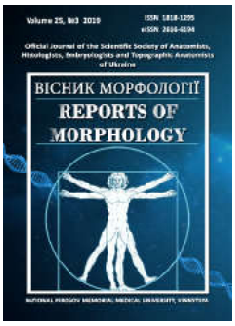

Changes of the ultrastructural organization of cells of rats esophagus in the modeling of second-degree esophageal stricture

Shaprynskyi Ye.V.
National Pirogov Memorial Medical University, Vinnytsya, Ukraine

ARTICLE INFO
Received: 17 June, 2019
Accepted: 22 July, 2019

UDC: 616-001.37-089.844

CORRESPONDING AUTHOR
e-mail: evgensh20078@gmail.com
Shaprynskyi Ye.V.

Scar strictures that lead to obstruction of the esophagus do not tend to decrease lately, but on the contrary, the number of such patients is increasing, which is caused by the use of a large range of chemicals in human life. The results of treatment of scarring strictures depend on the degree of stenosis. With complete obstruction of the esophagus, the question arises about conducting surgical treatment. Methods of correction of esophageal strictures have a considerable number of postoperative complications and lethal consequences - from 5.0 % to 15.0 %. Therefore, in order to create a unified pathogenetic tactic for the management and treatment of esophageal strictures, we were offered to study the ultrastructural changes of the mucous membrane of the stricture of the second stage during its modeling in the experiment. The purpose of the work is to investigate the dynamics of ultrastructural changes of the mucous membrane of the esophagus wall in the normal and second stage of its stricture. The experimental study was performed on adult white male rats weighing between 250 and 300 g. A total of 16 animals were operated on, which were divided into 2 groups: a control group (6 rats) and a study group (10 rats). The studies were performed under ketamine anesthesia. In animals of the control group performed only laparotomy, followed by layer-by-layer suturing of the anterior abdominal wall. In animals of the study group created a model of obstruction of the esophagus of the second stage. Electron microscopic examination was performed on days 3, 4, and 5 of the experiment, eliminating animals by overdosing on ketamine. As a result of the electron microscopic study of the ultrastructural organization of basal, spinosum, superficial epitheliocytes of stratified squamous epithelium without keratin, smooth muscle myocytes of the muscular plate and contractile elements of the muscular layer of the esophagus of rats with simulated stricture of the second degree revealed dystrophic and destructive disorders that varied in depth and severity. It was established that mitochondrial dysfunction leads to a decrease in the activity of reparative, metabolic and synthetic processes of the cell, which is indirectly manifested by a decrease in ribosomes and polysomes in the cytoplasm, loosening and focal lysis of membranes of the granular endoplasmic reticulum. Stricture of esophagus of the second stage causes activation of catabolic intracellular processes in all cells, which is morphologically confirmed by the appearance in the cytoplasm of secondary lysosomes and inclusions of lipids.
Keywords: *esophageal cell ultrastructure, esophageal stricture, mitochondrial dysfunction.*

Introduction

Scar strictures that lead to obstruction of the esophagus do not tend to decrease lately, but on the contrary, the number of such patients is increasing, which is caused by the use of a large range of chemicals in human life [4, 8, 10, 24, 27, 30]. The results of treatment of scarring strictures depend on the degree of stenosis. In the first and second stage of esophageal obstruction it is possible to carry out dilatation therapy, with complete obstruction of the esophagus the question arises about conducting surgical treatment [2, 3, 5, 11, 16, 17, 25]. However, both dilatation and operative methods of correcting esophageal strictures still have a significant number of postoperative complications and lethal consequences - from 5% to 15% [1, 6, 9, 12, 13, 14, 15, 20, 29].

Therefore, in order to create a single pathogenetic tactic for the management and treatment of esophageal strictures, we were offered to study the ultrastructural changes of the mucous membrane of the stage of stricture of the second degree in its modeling in the experiment, which is most common in clinical practice [18, 19, 26].

The purpose of the work is to investigate the dynamics of ultrastructural changes of the mucous membrane of the esophagus wall in the normal and second stage of its stricture.

Materials and methods

The experimental study was performed on adult white rats, males weighing 250 g to 300 g, in accordance with the general principles of animal experiments approved by the First National Congress on Bioethics (Kyiv, 2001) and in accordance with the provisions of the European Convention for the Protection of Vertebrate Animals used for experimental and other scientific purposes (Strasbourg, 1986).

A total of 16 animals were operated on, which were divided into two groups: control (6 rats) and studies (10 rats). Before the experiment began, animals were observed in the same conditions in the vivarium for a week. The studies were performed under ketamine anesthesia. In animals, the control group performed only laparotomy, followed by layer-by-layer suturing of the anterior abdominal wall. On days 3, 4, 5 of the experiment, the animals were removed from the experiment by an overdose of ketamine and performed a relaparotomy to collect material for electron microscopic examination - the wall of the unchanged abdominal part of the esophagus. The animals of the study group created a model of second-degree esophageal obstruction as follows: performed a median laparotomy, isolated the abdominal esophagus, and then took the conductor from the adult subclavian catheter through the mouth into the stomach and tied the abdominal esophagus. Electron microscopic examination was performed on days 3, 4, and 5 of the experiment, eliminating animals by overdosing on ketamine. The material for electron microscopic examination was a section of the simulated stricture of the II degree of the esophagus wall of rats.

The method of preparation of the material was that for pre-fixation pieces of tissue after their collection was immediately immersed in 2.5 % buffered solution glutaraldehyde retainer at a temperature of 4°C. After treatment in the buffer solution, the tissue was transferred for final fixation in 1 % buffered solution of osmium tetroxide for 3-4 hours, followed by dehydration in alcohols of increasing concentration and acetone. The fabric was placed in a mixture of epoxy resins according to conventional methods. The polymerization of the blocks was carried out in a thermostat at 60°C for two days. Sections were made from the blocks obtained using a UMTP-3M ultramicrotome, mounted on electrolytic grids and, after contrast with lead citrate, examined under an electron microscope EMV-100 BR at a voltage of 75 kW. Quality control of histological processing of the material was performed using pieces of the mucous membrane of the abdominal esophagus of intact experimental animals.

Results

The study of the ultrastructural organization of the organs of cells of the mucous membrane of the esophagus of the control group of rats indicated the adequacy of the chosen method of histological tissue processing and met modern requirements.

In submicroscopic organization of basal cells of the mucous membrane of the wall of the esophagus of rats on the site of the second-stage simulated stricture, degenerative changes of organelles were combined with the foci of destruction of intracellular membranes. Nuclear chromatin in the basal epitheliocytes was in a condensed state, and its clusters were concentrated along the periphery of the nucleus matrix and evenly distributed along the slice plane. The nuclear membrane, except for the loosening cells, had lysis cells. Perinuclear spaces were moderately expanded. The nuclear matrix was highly enlightened. In the central region of the matrix were concentrated granules of decondensed chromatin. Tanks of the granular endoplasmic reticulum were greatly expanded and presented as vacuoles of various shapes and sizes, the contents of which were of low electron density. A small number of ribosomes are attached to the membranes of the granular endoplasmic reticulum. When compared with the control group in the cytoplasm was reduced the number of free ribosomes and the polysomes. Total destruction of the membranes of the granular endoplasmic reticulum in some basal epitheliocytes was observed, secondary lysosomes were detected in the cytoplasm (Fig. 1).

The mitochondria were of various shapes and sizes, moderately swollen. Their matrix had a rough structure with

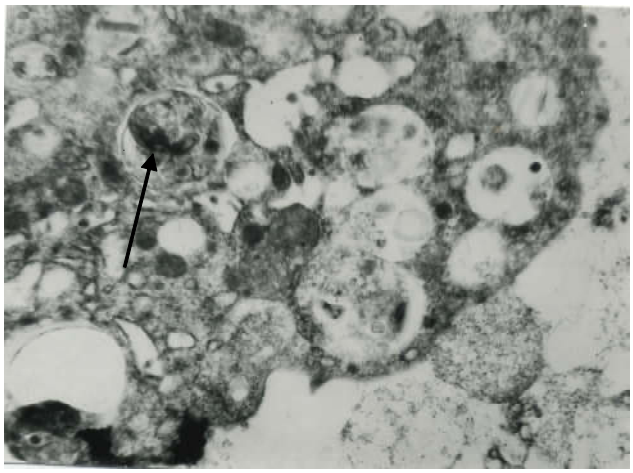

Fig. 1. Ultrastructure of basal epitheliocytes of stratified squamous epithelium without keratin with simulated second-degree stricture. Destruction of granular endoplasmic reticulum membranes, secondary lysosomes and lipid incorporation into the cytoplasm (arrow). x43000.

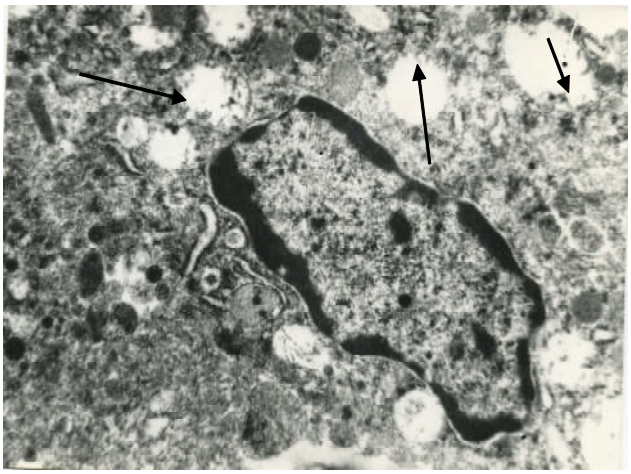

Fig. 2. Ultrastructure of basal epitheliocytes of stratified squamous epithelium without keratin with simulated second-degree stricture. Enlightenment of the matrix of mitochondria and destruction of the cristae (arrow). x43000.

Fig. 3. Ultrastructure of basal epitheliocytes of stratified squamous epithelium without keratin with simulated second-degree stricture. Inclusion of lipids in the cytoplasm (arrow). x34000.

an average electron density. A small number of cristae in the mitochondria were disorganized and deformed, the outer membranes in some mitochondria and the cristae were lysed. Sometimes in the cytoplasm of basal epitheliocytes, mitochondria were present whose cristae were destroyed. Such mitochondria looked like electronically transparent vacuoles (Fig. 2).

The lamellar cytoplasmic Golgi complex was moderately reduced. The parallel orientation of the smooth membranes is impaired. A small number of small vacuoles were found in the location of the plate cytoplasmic Golgi complex. Sometimes the inclusion of lipids was detected in the cytoplasm (Fig. 3).

Violation of the parallel orientation of the tonofibrils was observed. Intercellular spaces remained enlarged. The spinosum epitheliocytes of the esophageal mucosa had a polygonal shape and contained a centrally located nucleus.

The nuclear membrane had deep invaginations, loose structure, and lysis cells. The nuclear matrix was finely granular with an average electron density. Nuclear chromatin was in a decondensed state and its granules were diffusely distributed along the plane of the nucleus slice. The mitochondria were swollen, containing an electron-transparent matrix and single cristae. The outer membranes and cristae of the mitochondria were loosened (Fig. 4).

In the cytoplasm there was a large number of parallel-oriented tonofibrils and glycogen granules. Secondary lysosomes were sometimes found in the area of the plate cytoplasmic Golgi complex. Tanks of the granular endoplasmic reticulum were vacuolated, the membranes moderately loosened with lysis cells. Spinosum epitheliocytes with fragmented membranes of the granular endoplasmic reticulum were encountered. Free ribosomes and polysomes are extremely rare in the cytoplasm. Occasions of lipids and secondary lysosomes in the cytoplasm of the spinosum layer epitheliocytes were sometimes found. The intercellular spaces were greatly expanded. Cytoplasmic and intracellular membranes of superficial epitheliocytes are strongly thickened, loosened and osmiophilous.

In smooth muscle myocytes of the muscle plate and the muscle layer of the rat esophagus in the second-degree stricture, the ultrastructural organization had moderately pronounced dystrophic changes. Higher number of nuclear chromatin was in a decondensed state. Separate areas of the nuclear membrane were loosened. There were almost no foci of nuclear membrane lysis. Perinuclear spaces were uniformly expanded. The deformation of the nuclear membrane was observed in the form of its deep invaginations. The cytoplasmic membrane was strongly loosened with areas of lysis (Fig. 5).

The mitochondria had an electron-transparent matrix and contained a small number of shortened cristae. The

Fig. 4. Ultrastructure of the spinosum epitheliocytes of the stratified squamous epithelium without keratin with simulated second-degree stricture. Nuclear membrane invagination, matrix enlightenment and mitochondrial membrane lysis. x32000.

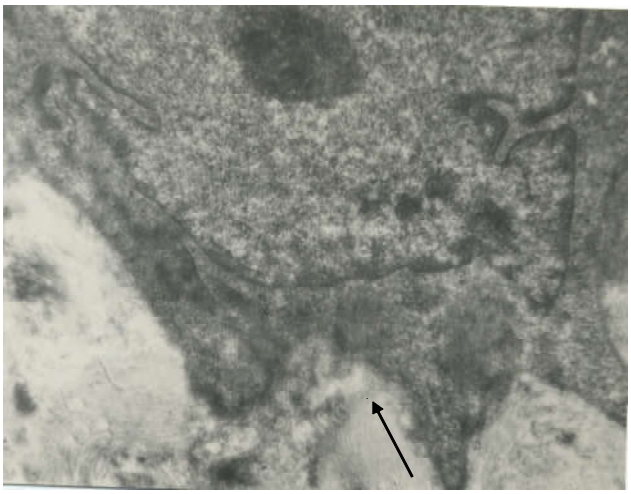

Fig. 5. Ultrastructure of smooth rat esophageal myocytes with modeled second-degree stricture. Nuclear membrane invagination, loosening and cytoplasmic membrane lysis (arrow). x32000.

sites of outer membrane lysis and mitochondrial cristae were relatively rare. The lamellar cytoplasmic Golgi complex was moderately reduced. Single micropinocytotic vesicles were detected near the cytoplasmic membrane.

In the ultrastructural organization of the endothelial cells of the blood capillaries, distinct dystrophic changes were determined in the stricture region. Endotheliocyte nuclei contained condensed chromatin diffusely scattered across the matrix. The nuclear membrane had multiple small invaginations. The mitochondria were small with an electron-transparent matrix and single cristae. Tanks of the granular endoplasmic reticulum were filled with electronically transparent material. In comparison with the group of intact animals, fewer ribosome-bound ribosomes were observed on the surface of the granular endoplasmic reticulum membranes in the animals of the study group. Free-standing ribosomes and polysomes are very rare. In the cytoplasm of the processes of endothelial cells of the blood capillaries were micropinocytotic vesicles.

Discussion

As a result of the electron microscopic study of the ultrastructural organization of basal, spinosum, superficial epitheliocytes of stratified squamous epithelium without keratin, smooth myocytes of the muscular plate and contractile elements of the muscular layer of the esophagus of rats with simulated stricture of the second degree revealed dystrophic and destructive disorders that varied in depth and severity. Unlike the first-degree stricture, as shown by Shaprynsky Y. V. et al. in 2013 [21], dystrophic and destructive disorders were more pronounced.

When the esophagus is completely obstructed, that is, in animals with a third-degree modeled stricture, destructive disorders prevail to a greater extent. Stein H. J. et al. (1995) and Shaprynsky Y. V. in 2016 confirmed the fact that the focal lysis was subject to a nuclear membrane, mitochondrial membrane, endoplasmic reticulum and lamellar cytoplasmic Golgi complex [22, 23].

The leading point in the development of these processes in the stratified squamous epithelium without keratin is mitochondrial dysfunction, which morphologically manifests focal destruction of the outer membranes and the cristae. Mitochondrial dysfunction leads to a decrease in the activity of the reparative, metabolic and synthetic processes of the cell, which is indirectly manifested by a decrease in ribosomes and polysomes in the cytoplasm, loosening and focal lysis of membranes of the granular endoplasmic reticulum. As shown in their works Shaprinsky Y. V. et al. [21] and Chandrasoma P.T. et al. [7], in animals with first-degree modeled stricture, there are deformations of the nuclear membrane, mitochondrial membranes, membranes of the granular endoplasmic reticulum and the lamellar cytoplasmic Golgi complex, which is explained by the inclusion of redundant intracellular mechanisms related to the phenomena of piezobiosynthesis. Cells under conditions of insufficient energy supply of metabolic processes use the piezoelectric energy, which occurs during deformation of membranes, which are liquid crystals. In the simulated stricture of the third degree, total lysis of membranes of the granular endoplasmic reticulum was sometimes observed [14, 22, 28].

Ultrastructural changes of smooth myocyte organelles and cross-striated muscle fibers in the region of the second-degree esophageal stricture indicate a decrease in the contractile capacity of these cells. Submicroscopic disorders of the endothelial cells of the capillary bed of the esophagus are characterized by a decrease in the electron density of the cytoplasm due to the development of intracellular edema, the absence in the cytoplasm of appendages of endothelial cells of micropinocytosis vesicles, which is characteristic for the decrease in the activity of transcellular transport of substances, water and electrolytes up to its termination under the condition of modeling of the third-degree esophageal stricture [22]. That is, the organelles of smooth myocytes and skeleton muscles and endothelial cells of the esophageal capillary are undergoing similar changes.

The esophageal stricture of the second stage causes activation of catabolic intracellular processes of the mucous membrane epithelium, which is structurally confirmed by the appearance of secondary lysosomes in the cytoplasm and inclusions of lipids. With third-degree stricture, there is an even greater increase in catabolic processes, and the changes become irreversible [22]. And disturbances of submicroscopic architectonics of rat esophagus cells with simulated first-degree stricture are reversible after elimination of an external, negative factor [21].

In the future, we also plan to investigate the ultrastructural changes of esophageal cells in the dynamics after removal of the stricture.

Conclusions

1. It is established that in the area of the simulated stricture of the second degree, degenerative and destructive

disorders of the ultrastructural organization of the epithelial cells of the stratified squamous epithelium without keratin, smooth muscle cells of the muscular plate and contractile elements of the muscular layer of the esophagus, which vary in degree and depth, develop.

2. Mitochondrial dysfunction is a major element in reducing the activity of reparative, metabolic and synthetic intracellular processes.

3. The esophageal stricture of the second stage causes activation of catabolic intracellular processes in all cells, which is morphologically confirmed by the appearance in the cytoplasm of secondary lysosomes and lipid inclusions.

References

[1] Andreeshchev, S.A., Myasoedov, S.D., Usenko, A. Yu. & Movchan, B. B. (2008). Repeated operations on the artificial esophagus. *Clinical surgery,* 4-5.

[2] Boyko, V. V., Korolevska, A. Y., Savvi, S. O., Korolevska, A. Y., & Zhidetsky, V. V. (2018). Features of surgical tactics at long scarring of esophagus. *Clinical surgery*, 85(1), 52-55.

[3] Boyko, V. V., Savvi, S. O., Lazirsky, V. O., & Likhman, V. M. (2014). *Artifical stomach: Gastric plastic is an ileocecal segment of the intestine.* Kharkiv: Promin'.

[4] Boyko, V. V., Shaprinsky, V. O., & Shaprinsky, E. V. (2015). Treatment of scarring of esophagus. *Kharkov Surgical School*, 73(4), 152-155.

[5] Cerfolio, R. J., Wei, B., Hawn, M. T., Minnich D. J. (2016). Robotic esophagectomy for cancer: early results and lessons learned. *Semin. Thorac. Cardiovasc. Surg.,* 28(1), 160-169. doi: 10.1053/j.semtcvs.2015.10.006

[6] Chadi, S. A., Fingergut, A., Berho, M., DeMeester, S. R., Fleshman, J. W., Hyman, N. H. … Wexner, S. D.. (2016). Emerging trends in the etiology, prevention and treatment of gastrointestinal anastomotic leakage. *J. Gastrointest. Surg.*, 20(12), 2035-2051. doi: 10.1007/s11605-016-3255-3

[7] Chandrasoma, P. T., Der, R., Ma, Y., Peters, J., & DeMeester, T. (2003). Histologic classification of patients based on mapping biopsies of the gastroesophageal junction. *Am. J. Surg. Pathol.,* 27, 929-936.

[8] Iskit, S. H., Ozcelik, Z., Alkan, M., Türker, S., & Zorludemir, U. (2014). Factors affecting the prevalence of gastro-oesophageal reflux in childhood corrosive oesophageal strictures. *Balkan Med. J.*, 31(2), 137-142. doi: 10.5152/balkanmedj.2014.13276

[9] Kachmar, W. M. (2016). Esophageal ruptures, mediastinitis - an individual approach to treatment. *Hospital surgery. Journal of the name of L.Y. Kovalchuk*, 1, 116-117.

[10] Kim, S. H., Jeong, J. B., Kim, J. W., Koh, S. J., Kim, B. G., Lee, K. L. … Shin, C. M. (2014). Clinical and endoscopic characteristics of drug-induced esophagitis. *World J. Gastroenterol*. 20(31), 10994-10999.

[11] Lazirsky, V. A., Boyko, V. V., Kryvorotko, I. V. & Savvi, S. A. (2014). The use of the ileocecal segment of bowel for reconstruction after combined gastrectomy. *European Journal of Surgical Oncology,* 40, 11, 156. doi: 10.1016/j.ejso.2014.08.395

[12] Low, D. E., Alderson, D., Cecconello, I., Chang, A. C., Darling, G. E., D?Journo X. B. … van Lanschot, J. J. (2015). International consensus of standardization of data collection for complications associated with esophagectomy: Esophagectomy Complications Consensus Group (ECCG). *Ann. Surg.,* 262, 286-294.

[13] Melnyk, V. M., & Poida, O. I. (2016). Surgical tactics for the failure of sutures of intestinal anastomoses. *Clinical surgery,* 6, 8-12.

[14] Mori, H., Koike, M., Gotow, T., Ichimura, K., Asaoka, D., Oguro, M. ... Watanabe, S. (2011). Ultrastructural analyses of the rat esophageal stratified epithelium under normal conditions and in chronic reflux esophagitis, *Archives of Histology and Cytology,* 73(4-5), 199-214. doi: 10.1679/aohc.73.199

[15] Newton, N. J., Sharrock, A., Rickard, R., & Mughal M. (2017). *Systematic review of the use of endo-luminal topical negative pressure in oesophageal leaks and perforations.* Dis. Esophagus, 30(3), 1-5. doi: 10.1111/dote.12531

[16] Perbtani, Y., Suarez, A. L., & Wagh, M. S. (2016). Emerging techniques and efficacy of endoscopic esophageal reconstruction and lumen restoration for complete esophageal obstruction. *Endosc. Int. Open.,* 4(2), 136-142. doi: 10.1055/s-0041-107898.

[17] Reavis K. M. (2009). The esophageal anastomosis: how improving blood supply affects leak rate. *J. Gastrointest. Surg.,* 13, 1558-1560. doi: 10.1007/s11605-009-0906-7

[18] Savvi, S. A., & Nevzorova, O. V. (2009). The clinical significance of ultrastructural changes in the esophagus after a chemical burn. *International Medical Journal,* 27(2), 73-74.

[19] Sarkisov, D. S., & Perov, Yu. L. (1996). *Microscopic technique. Leadership*. Moscow: Medicine.

[20] Senyutovich, R. V., Barannikov, K. V., Bodiak, V. Y., Shumko, B. I., Unguryan, V. P., & Chorny, O. V. (2016). Stapler esophageal anastomosis. Current trends. *Hospital surgery. Journal of the name of L.Y. Kovalchuk,* 2, 103-107. Режим доступу: http://nbuv.gov.ua/UJRN/shpkhir_2016_2_26

[21] Shaprynskyi, E. V., Nevzorov, V. P., & Nevzorova, A. F. (2013). Violation of the ultrastructure of esophageal cells with simulated esophageal stricture in experiment. *Bulletin of problems of biology and medicine*, 2(105), 4, 226-230.

[22] Shaprynskyy, Ye. V. (2016). Changes in the ultrastructural organization of cells of the mucous membrane of the esophagus of rats with simulated third-degree stricture. *Clinical anatomy and surgery,* 15(3), 6-10.

[23] Stein, H. J., Liebermann-Meffert, D., DeMeester, T. R., & Siewert, J. R. (1995). Threedimensional pressure image and muscular structure of the human lower esophageal sphincter. *Surgery,* 117, 692-698.

[24] Shafa, S., Sharma, N., Keshishian, J., & Dellon, E. S. (2016). The black esophagus: a rare but deadly disease. *ACG Case Rep J.*, 3(2), 88-91. doi: 10.14309/crj.2016.9

[25] Swanson, E. W., Swanson, S. J., & Swanson R. S. (2012). Endoscopic pyloric balloon dilatation obviates the need for pyloroplasty at esophagectomy. *Surg. Endosc.,* 26(7), 2023-2028. doi: 10.1007/s00464-012-2151-5

[26] Tertychny, A. S., Mamchenko, S. I., & Dubrovskaya, M. I. (2014). Morphological characteristics of the mucous membrane of the esophageal-gastric transition zone in children with gastroesophageal reflux disease. *Experimental and clinical gastroenterology,* 1, 30-34.

[27] Usenko, A. Yu., Lavrik, A. S., Andreeshchev, S. A., Movchan, B. B., & Doskuch, O. A. (2010). *Comparative evaluation of various types of total and subtotal esophagoplasty.* All-Ukrainian scientific-practical conference with international participation "Modern problems of breast surgery". Kharkov: Promin'.

[28] Weickert, U., Wolf, A., Schröder, C., Autschbach, F., Vollmer, H. (2011). *Frequency, histopathological findings, and clinical*

significance of cervical heterotopic gastric mucosa (gastric inlet patch): a prospective study in 300 patients. Dis. Esophagus, 24, 63.
[29] Worrell, S., Mumtaz, S., Tsuboi, K., Lee, T. H., & Mittal, S. K. (2010). Anastomotic complications associated with stapled versus hand-sewn anastomosis. *J. Surg. Res.,* 161(1), 9-12. doi: 10.1016/j.jss.2009.07.004
[30] Zhang, D. H., Zhou, L. Y., Dong, X. Y., Cui, R. L., Xue, Y., & Lin, S. R. (2010). Factors influencing intercellular spaces in the rat esophageal epithelium. *World J. Gastroenterol.*, 16, 1063-1069. doi: 10.3748/wjg.v16.i9.1063

ЗМІНИ УЛЬТРАСТРУКТУРНОЇ ОРГАНІЗАЦІЇ КЛІТИН СТРАВОХОДУ ЩУРІВ ПРИ МОДЕЛЮВАННІ СТРИКТУРИ СТРАВОХОДУ ДРУГОГО СТУПЕНЯ

Шапринський Є.В.

Рубцеві стриктури, що призводять до непрохідності стравоходу, останнім часом не мають тенденції до зменшення, а навпаки, кількість таких хворих збільшується, що зумовлено використанням великого спектру хімічних речовин у побуті людини. Результати лікування рубцевих стриктур залежать від ступеня стенозування. При повній непрохідності стравоходу постає питання про проведення оперативного лікування. Методи корекції стриктур стравоходу мають значну кількість післяопераційних ускладнень і летальних наслідків - від 5,0 % до 15,0 %. Тому для створення єдиної патогенетичної тактики ведення і лікування стриктур стравоходу нами було запропоноване дослідження ультраструктурних змін слизової оболонки ділянки стриктури II ступеня при її моделюванні в експерименті. Мета роботи - дослідити динаміку ультраструктурних змін слизової оболонки стінки стравоходу в нормі та при другому ступені її стриктури. Експериментальне дослідження проводили на статевозрілих білих щурах-самцях, масою від 250 до 300 г. Всього було прооперовано 16 тварин, котрих розподілили на 2 групи: контрольну групу (6 щурів) і групу дослідження (10 щурів). Дослідження проводили під кетаміновим наркозом. У тварин контрольної групи виконували тільки лапаротомію з подальшим пошаровим ушиванням передньої черевної стінки. У тварин групи дослідження створювали модель непрохідності стравоходу другого ступеня. Забір матеріалу для електронно-мікроскопічного дослідження виконували на 3, 4 та 5 добу експерименту, виводячи тварин шляхом передозування кетаміну. В результаті проведеного електронно-мікроскопічного дослідження ультраструктурної організації базальних, шипуватих, поверхневих епітеліоцитів багатошарового незроговілого епітелію, гладеньких міоцитів м'язової пластинки і скорочувальних елементів м'язового шару стравоходу щурів з модельованою стриктурою другого ступеня виявлено дистрофічні та деструктивні порушення, які варіювали за глибиною та ступенем виразності. Встановлено, що мітохондріальна дисфункція призводить до зниження активності репаративних, метаболічних та синтетичних процесів клітини, що опосередковано проявляється зменшенням кількості рибосом і полісом у цитоплазмі, розпушенням і вогнищевим лізисом мембран гранулярного ендоплазматичного ретикулума. Стриктура стравоходу другого ступеню викликає активацію катаболічних внутрішньоклітинних процесів у всіх клітинах, що морфологічно підтверджується появою у цитоплазмі вторинних лізосом та включень ліпідів.

Ключові слова: *ультраструктура клітин стравоходу, стриктура стравоходу, мітохондріальна дисфункція.*

ИЗМЕНЕНИЯ УЛЬТРАСТРУКТУРНОЙ ОРГАНИЗАЦИИ КЛЕТОК ПИЩЕВОДА КРЫС ПРИ МОДЕЛИРОВАНИИ СТРИКТУРЫ ПИЩЕВОДА ВТОРОЙ СТЕПЕНИ

Шапринский Е.В.

Рубцовые стриктуры, которые приводят к непроходимости пищевода, в последнее время не имеют тенденции к уменьшению, а наоборот, количество таких больных увеличивается, что обусловлено использованием большого спектра химических веществ в быту человека. Результаты лечения рубцовых стриктур зависят от степени стенозирования. При полной непроходимости пищевода встает вопрос о проведении оперативного лечения. Методы коррекции стриктур пищевода имеют значительное количество послеоперационных осложнений и летальных последствий - от 5,0 % до 15,0 %. Поэтому, для образования единой патогенетической тактики ведения и лечения стриктур пищевода нами было предложено исследование ультраструктурных изменений слизистой оболочки участка стриктуры II степени при ее моделировании в эксперименте. Цель работы - исследовать динамику ультраструктурных изменений слизистой оболочки стенки пищевода в норме и при второй степени ее стриктуры. Экспериментальные исследования проводили на половозрелых белых крысах-самцах, массой от 250 до 300 г. Всего было прооперировано 16 животных, которых разделили на 2 группы: контрольную группу (6 крыс) и группу исследования (10 крыс). Исследования проводили под кетаминовым наркозом. У животных контрольной группы выполняли только лапаротомию с последующим послойным ушиванием передней брюшной стенки. У животных группы исследования создавали модель непроходимости пищевода второй степени. Забор материала для электронно-микроскопического исследования выполняли на 3, 4 и 5 сутки эксперимента, выводя животных путем передозировки кетамина. В результате проведенного электронно-микроскопического исследования ультраструктурной организации базальных, шиповатых, поверхностных эпителиоцитов многослойного неороговевающего эпителия, гладких миоцитов мышечной пластинки и сократительных элементов мышечного слоя пищевода крыс с моделируемой стриктурой второй степени обнаружены дистрофические и деструктивные нарушения, которые варьировали по глубине и степени выраженности. Установлено, что митохондриальная дисфункция приводит к снижению активности репаративных, метаболических и синтетических процессов клетки, косвенно проявляется уменьшением количества рибосом и полисом в цитоплазме, разрыхлением и очаговым лизисом мембран гранулярного эндоплазматического ретикулума. Стриктура пищевода второй степени активизирует катаболические внутриклеточные процессы, что морфологически подтверждается появлением в цитоплазме клеток вторичных лизосом и включений липидов.

Ключевые слова: *ультраструктура клеток пищевода, стриктура пищевода, митохондриальная дисфункция.*

DOI: 10.31393/morphology-journal-2019-25(3)-05 Reports of Morphology, Vol. 25, №3, Pages 27-32

ISSN 1818-1295 eISSN 2616-6194

REPORTS OF MORPHOLOGY

Official Journal of the Scientific Society of Anatomists, Histologists, Embryologists and Topographic Anatomists of Ukraine

journal homepage: https://morphology-journal.com

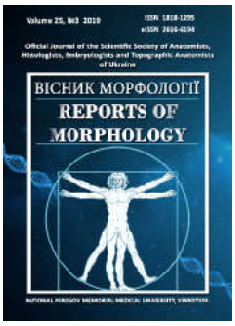

Electronic microscopic research on periodont in experimental two-weight opioid action and after its over for four weeks

Fik V.B.[1], Paltov Ye.V.[1], Kryvko Yu.Ya.[2]

[1]Danylo Halytsky Lviv National Medical University, Lviv, Ukraine
[2]Higher Educational Communal Institution of Lviv Regional Council "Andrey Krupynsky Lviv Medical Academy", Lviv, Ukraine

ARTICLE INFO
Received: 22 June, 2019
Accepted: 23 July, 2019

UDC: 611.311-018.73:615.214.24:616-076.4

CORRESPONDING AUTHOR
e-mail: fikvolodymyr@ukr.net
Fik V.B.

Due to the harmful effects of opioid agents in the uncontrolled use of them, it is impossible to ease the early manifestations of damage to the tissues and organs of the oral cavity, which is a pressing problem of today. The purpose of this work was to investigate the features of the sub-microscopic organization of the structural components of the periodontium under the action of an opioid analgesic for two weeks and its four-week withdrawal in the experiment. The study was conducted on 22 adult rats-males of the Wistar line, weighing 160 g, 4.5-6 months of age. Animals were administered intramuscularly daily, once a single opioid analgesic nalbuphine for the first two weeks, in terms of the mean therapeutic dose for the rat, as well as for the mean weight of the test group (0.212 mg/kg), and subsequent four weeks. The fragments of soft periodontal tissue were used for electron microscopic examination. Submicroscopically expressed destructive changes in periodontal tissues were not observed. However, the positive dynamics of regeneration of periodontal components at the ultrastructural level were also not revealed. In the cytoplasm of cells of the epithelium of the free part of the gums, there is destruction of organelles, partially damaged mitochondrial cristae, poorly contoured tonofilaments, shallow karyolemma invaginations, thickened areas and damaged desmosomal contacts. In the surface areas of the periodontium, the collagen fibers are partially stratified, there is moderate swelling of the intercellular substance of the connective tissue, part of the fibrocytes invaginating the karyolemma of the nucleus and placement of heterochromatin in the periphery. Ultrastructurally in the cytoplasm of the macrophage, lysosomes are detected, phagosomes are scarce, indicating a slight damage to the structures. In the gaps of the blood capillaries, blood cells are formed, mainly erythrocytes, in the perinuclear part of the cytoplasm of organelles are few, mitochondria with electron-light matrix and small cristae, perivascular edema is insignificant, there are destructively altered mitochondria in the cytoplasm of endothelial cells of venules, the basement membrane is thickened, the perivascular spaces are enlarged. Thus, at the end of the sixth week of the experiment, no short-term irreversible changes in the ultrastructural organization of the periodontal components were detected in the short-term effect of the opioid for two weeks and its subsequent four-week cancellation. However, the complete restoration of the structural components of the periodontium is not observed, there are signs of reactive changes, reparative processes are slowed.

Keywords: *periodontium, opioid, abolition of the opioid, ultrastructure, experiment.*

Introduction

The tissues and organs of the oral cavity are especially responsive to any harmful stimuli in the body [9, 18, 26]. Under the influence of factors of exogenous origin disturbances of gums resistance arise, which causes pathological changes in periodontium tissues [14, 19]. It should be noted that periodontium diseases and gums bleeding are more common in drug abusers compared to the general population [10, 20, 21, 25]. Important are the issues of therapeutic tactics of inflammatory periodontal diseases in drug addicts, as well as the abolition of the drug, which is necessary for both local and general action on the tissues of the periodontal complex [5, 6, 16, 21, 23]. However, the mapping of the pathomorphological pattern in periodontal tissues is a rather complicated process and

changes in this case occur over a period of time with the involvement of different mechanisms of pathogenesis [3, 7]. Therefore, experimental studies related to the study of the ultrastructural organization of the periodontium and the correction of pathological changes that occur during the action of opioids are particularly important today and will help to develop an adequate scheme of corrective effects to stabilize the morphofunctional condition of periodontium tissues.

The aim of the study was to determine the features of the submicroscopic organization of the structural components of the periodontium under the action of an opioid analgesic for two weeks and its four-week withdrawal in the experiment.

Materials and methods

The study was conducted on 22 adult rats-males of the Wistar line, weighing 160 g, aged 4.5-6 months. Animals were divided into 2 groups. The first group included intact rats (n=10). The second group included 12 animals, which were administered intramuscularly opioid analgesic nalbuphine daily for the first two weeks, based on the mean therapeutic dose for the rat, and considering the mean weight of the experimental group (0.212 mg/kg) and its subsequent 4 weeks. Controls were 3 male rats administered intramuscularly saline. Sampling was performed after 6 weeks of the experiment.

All animals were kept under standard vivarium conditions and all experiments were carried out in accordance with the provisions of the "European Convention for the Protection of Vertebrate Animals Used for Experimental and Other Scientific Purposes" (Strasbourg, 1985). Before sampling the biopsy material, the animals were primed with intraperitoneal administration of sodium thiopental (25 mg/kg).

For electron microscopic examination, pieces of soft periodontal tissue were used in the gums papilla. The tissue fragments were fixed in a 2.5 % solution of glutaraldehyde and in a 1 % solution of osmium tetroxide on phosphate buffer pH = 7.2-7.4, dehydrated in alcohols and propylene oxide and poured into a mixture of epoxy resins with araldite [24]. Ultra-thin sections were made on a UMPT3m ultramicrotome, which was counterstained with uranyl acetate and lead citrate and studied in a PEM-100-01 electron microscope.

Results

Electron microscopic studies have shown that the structural changes in the epithelium of the different sites studied were similar in nature, but not as significant as in the subgroup of animals without opioid withdrawal. The cells of the basal layer of the epithelial plate of its free part have an enlarged nucleus area, the karyoplasm of which includes the osmiophilic regions of heterochromatin, but they are located mainly near the nuclear envelope. Small, compact nucleolus are available. The karyolemma has

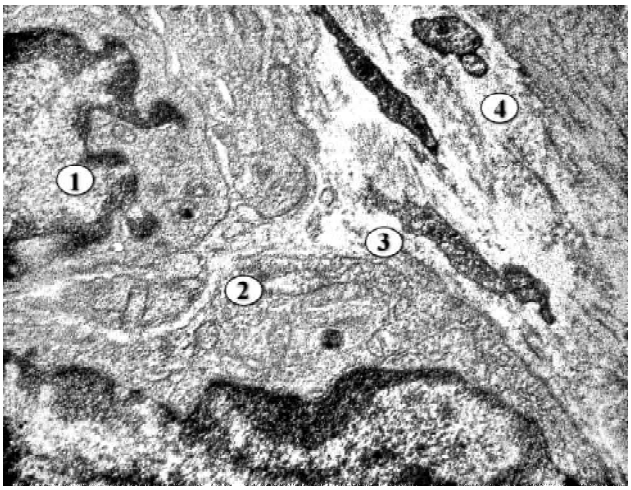

Fig. 1. The ultrastructure of the free epithelium of the rat gingiva after six weeks: two weeks of opioid administration and four weeks after its abolition. 1 - basal layer epitheliocyte nucleus, 2 - cytoplasm of epitheliocyte, 3 - basement membrane, 4 - connective tissue. x14000.

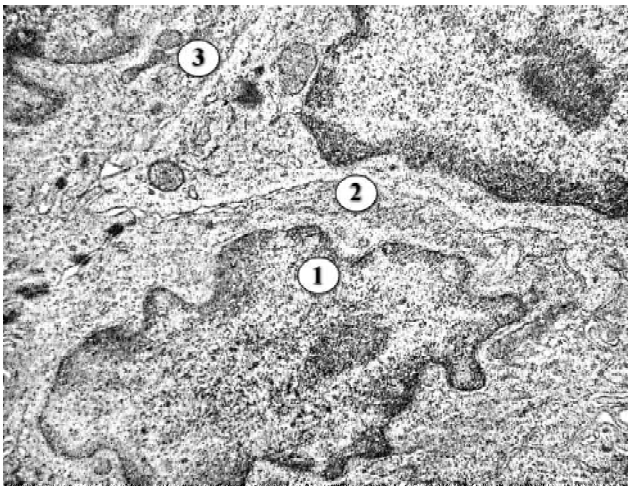

Fig. 2. Ultrastructure of the rat gingival sulcus epithelium after six weeks: two weeks of opioid administration and four weeks after its abolition. 1 - nucleus with invagination of karyolemma, 2 - cytoplasm of epitheliocytes, 3 - desmosomes. x9000.

shallow invaginations, and its perinuclear spaces are enlarged only in some places. In the cytoplasm there is a normalization of organelles, damaged ultrastructures are small in number. Part of the mitochondria has a focal electron-light matrix and partially damaged cristae. In the hyaloplasm, areas with poorly contoured tonofilaments were detected, some of them homogenized. Thick areas with fuzzy intercellular contacts (Fig. 1) are noted between plasmalemmas. The epitheliocytes of the spinosum and granulosum layers are also less altered, the structure of the nucleus and cytoplasm normalizing.

The nuclei have a shallow invagination of the karyolemma, euchromatin predominates in the karyoplasm. There are different sizes of cells in the granular layer, sometimes large clumps of keratohyalin. The desmosomal contacts are sometimes damaged. The

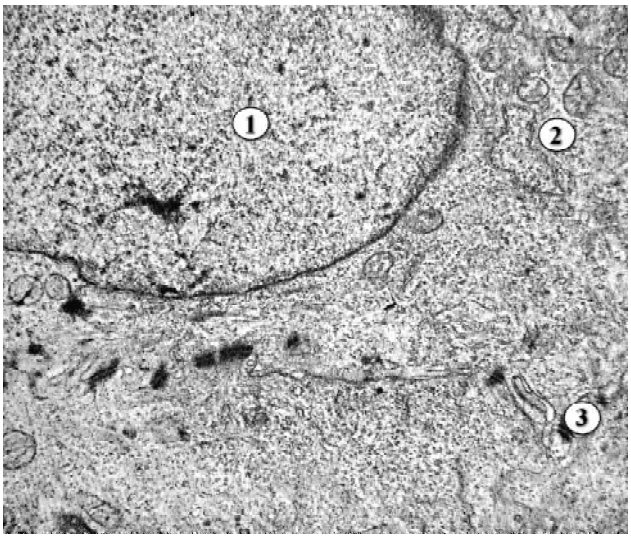

Fig. 3. The ultrastructure of the epithelium of the attached part of the rat gingiva is six weeks: two weeks of opioid administration and four weeks after its abolition. 1 - oblong nucleus, 2 - mitochondria, 3 - plasmolemmas connected by desmosomes. x12000.

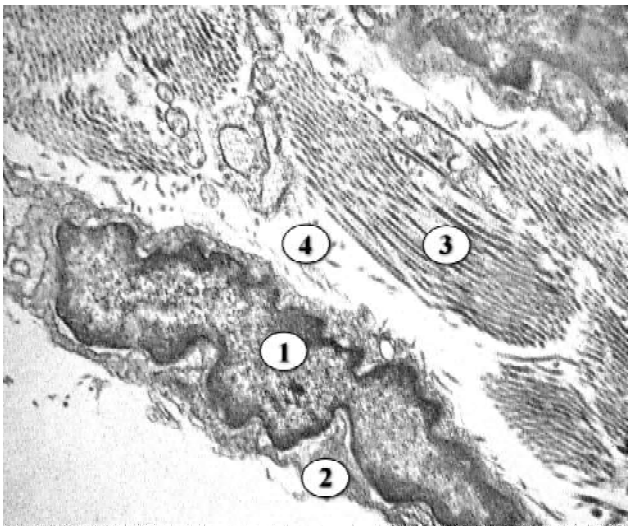

Fig. 4. The ultrastructure of the rat periodontium after six weeks: two weeks of opioid administration and four weeks after its abolition. 1 - fibrocyte nucleus, 2 - fibrocyte cytoplasm, 3 - collagen fibril bundle, 4 - light amorphous electron component. x14000.

ultrastructural organization of the gums epithelium of this group is also unchanged. There is no swelling of the cytoplasm of the epitheliocytes of the basal and spinosum layers. Only the nuclei of the superficial layers of cells have karyolemma invaginations, and the cytoplasm is virtually unchanged. Clear contours of plasmolemma and desmosomal contacts (Fig. 2). Submicroscopically, the epithelium of the attached part of the gums of the animals is found to be unaltered. Epitheliocytes include the oblong-shaped nucleus with shallow invasions of the karyolemma, and euchromatin is noted in the karyoplasm. In the cytoplasm, there are small mitochondria, a few cristae. The clear contours of the plasmolemma, the intercellular contacts are osmiophilic, appear enlarged (Fig. 3).

Electron microscopic studies of the periodontium of animals have found that its structural components are unchanged. Collagen fibers are characterized by a tufted arrangement of fibrils, only in the superficial area they are partially stratified and moderate swelling of the amorphous component of the intercellular substance of the connective tissue is present. Fibroblasts of the usual structure, and some fibrocytes have irregular shape with invaginations of karyolemma of the nucleus and placement of heterochromatin on the periphery. The cytoplasm contains ribosomes, enlarged tubules of the granular endoplasmic reticulum, part of the mitochondria with the enlightened matrix (Fig. 4). Lymphocytes, neutrophils and macrophages are observed in connective tissue surrounding the periodontium. Ultrastructurally, the cytoplasm of the macrophage reveals lysosomes, a little phagosome, indicating little damage to the structures. Plasmolemma forms protrusion in the form of outgrowths and has the invaginations required for phagocytosis of damaged structures (Fig. 5).

Submicroscopic studies of the mucous membrane of the rats gums of this group found that moderate reactive changes are characteristic of the hemomicrocirculatory bed of the gums. The lumps of the blood capillaries are small, in them the formed elements of blood, mainly erythrocytes are found. The nucleus and cytoplasm of endothelial cells have their own structural organization. In the wide cytoplasmic areas of the cells, there are many foam pinocytosis vesicles, caveolae.

In the perinuclear part of the cytoplasm organelles are small in number. The tubules of the endoplasmic reticulum are moderately dilated, mitochondria with electron-light matrix and small cristae. The elongated nucleus is well contoured, the perinuclear spaces are small, and

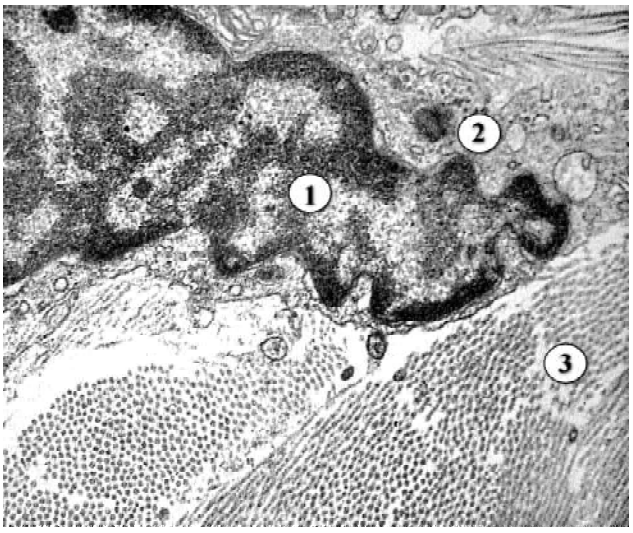

Fig. 5. The ultrastructure of the rat periodontal after six weeks: two weeks of opioid administration and four weeks after its abolition. 1 - macrophage nucleus, 2 - macrophage cytoplasm, 3 - collagen fibril bundle. x14000.

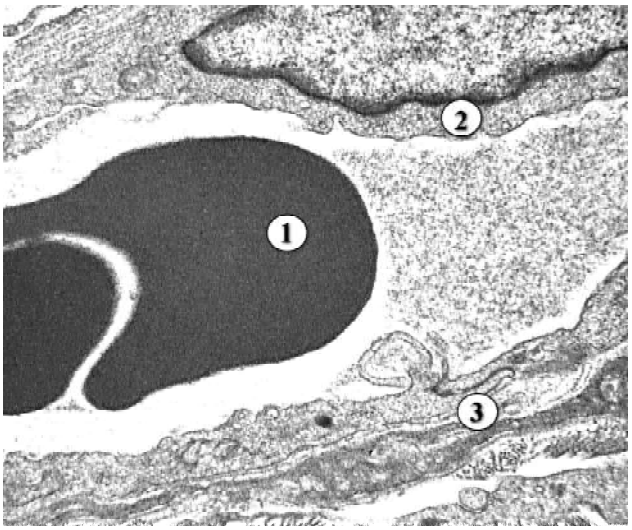

Fig. 6. The ultrastructure of the hemocapillary of the mucous membrane of the gingival mucosa of the rat after 6 weeks: two weeks of opioid administration and four weeks after its abolition. 1 - lumen with red blood cells, 2 - nucleus and cytoplasm of endothelial cells, 3 - basement membrane. x12000.

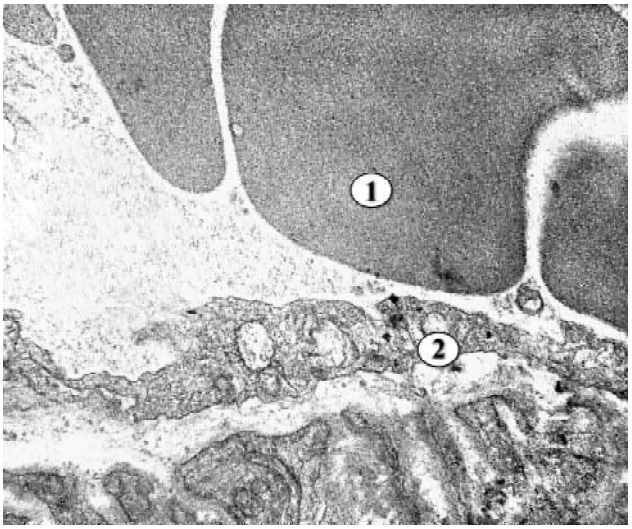

Fig. 7. Ultrastructure of the lamina propria venules of the mucous membrane of the rat gums after six weeks: two weeks opioid use and four weeks after its withdrawal. 1 - a lumen with erythrocytes, 2 - cytoplasm of endothelial cells. x14000.

euchromatin prevails in the karyoplasm. The basal membrane is wide, wavy and has clear contours. Perivascular edema is insignificant; collagen fibers and an amorphous component are present in the loose connective tissue of the advent (Fig. 6). Venules have moderately blood-filled lumps, the cytoplasm of endothelial cells is preserved, however, here and there destructively altered mitochondria are present. Separate areas of the cytoplasm protrude into the lumen, which increases the area of interaction of endothelial cells with the internal contents of the vessel. The basal membrane is thickened, but is well contoured, the perivascular spaces are slightly enlarged (Fig. 7).

Discussion

In the modern professional literature there are more and more studies devoted to the study of the effect of opioid drugs on various organs and systems [1, 8, 12, 17, 22], but their effect on the structural organization of the of oral cavity and periodontium remains unknown [6, 10, 20, 21]. Scientific research is mainly aimed at studying the changes in the internal organs that develop as a result of the introduction of such classic opioids as morphine, tramadol and codeine using significantly high doses [4, 5, 8, 15]. In addition, studies on the effects of the opioid analgesic nalbuphine on tissues and organs of the oral cavity are virtually absent in the literature. Preferably, such studies have been performed to study the characteristics of pharmacodynamics and pharmacokinetics both in experiment and in volunteers [2, 11, 13].

As a result of our studies of the experimental effect of opioid for two weeks and its 4-week cancellation, we found no significant destructive changes in periodontium. However, the positive dynamics of regeneration of periodontal components at the ultrastructural level were also not observed. Submicroscopically, there are reactive changes, which are manifested by focal sites of expansion of perinuclear spaces, fuzzy intercellular contacts, partial damage of the cristae in the mitochondria of epitheliocytes and endothelial cells, as well as swelling of the intercellular substance and minor constituents of periodontium.

In the available medical literature there are no results of studies of the ultrastructural organization of periodontal tissues in dynamics at different terms of opioid exposure and after its abolition, which makes it impossible to perform a comparative analysis of the data obtained. Given the relevance of this problem, the study of periodontal tissues in drug addicts is insufficient and requires further scientific research [5-7, 16, 21, 25]. Therefore, we believe that the method of creating a biological experimental model of opioid exposure will help to find out the peculiarities of submicroscopic organization in periodontal tissues, which is relevant and necessary in modern dentistry and periodontology.

Prospects for further research are to study the features of ultrastructural reorganization in periodontal tissues when exposed to opioid, after its abolition, and at the application of medical correction at an early date.

Conclusions

1. At the end of week 6 of the experiment, no irreversible changes in the ultrastructural organization of periodontal components were detected in the short-term effect of the opioid for two weeks and its subsequent cancellation of.

2. Submicroscopically, it was found that the abolition of opioid analgesic at longer periods (3-6 weeks) does not lead to complete restoration of the structural components of the periodontium, regenerative processes are slow, there are signs of reactive changes.

References

[1] Alinejad, S., Kazemi, T., Zamani, N., Hoffman, R.S., Mehrpour, O. (2015). A systematic review of the cardiotoxicity of methadone. *EXCLI J.,* 14, 577-600. doi: 10.17179/excli2015-553.

[2] Attia, J. Z., Kamel, M. Y., Yousef, R. K. (2015). Safety of nalbuphine on neural tissues of rats and its efficacy in the treatment of acute herpetic pain in children with acute lymphoblastic leukemia. *Res. Opin. Anesth. Intensive Care,* 2, 89-95. doi: 10.4103/2356-9115.172801

[3] Avdeev, O. V. (2010). Structural changes of periodontal tissues in experiment. *Bulletin of dentistry,* 71(2), 2.

[4] Carnaval, T. G., Sampaio, R. M., Lanfredi, C. B., Borsatti, M. A., & Adde, C. A. (2013). Effects of opioids on local anesthesia in the rat: a codeine and tramadol study. *Braz. Oral. Res.,* 27(6), 455-462. doi: 10.1590/S1806-83242013000600003.

[5] Dolova, A. I. (2006). *The use of the antioxidant of Mexidol in the complex treatment of chronic generalized periodontitis in patients suffering from opiate drug dependence (experimental clinical study).* (Master's thesis). Moskva

[6] Fedun, I. R. (2019). *Features of clinic and treatment of periodontal diseases in drug addicted patients.* (Master's thesis). Danylo Halych National Medical University, Ministry of Health of Ukraine, Lviv.

[7] Fik, V. B., Paltov, E. V., & Kryvko, Y. Y. (2018). Morphofunctional peculiarities of the periodontal tissue under conditions of simulated eight-week opioid effect. *Deutscher Wissenschaftscherold German Science Herald*, 1, 14-17. doi: 10.19221/201814

[8] Ghoneim, F. M., Khalaf, H. A., Elsamanoudy, A. Z., & Helaly, A. N. (2014). Effect of chronic usage of tramadol on motor cerebral cortex and testicular tissues of adult male albino rats and the effect of its withdrawal: histological, immunohistochemical and biochemical study. *Int. J. Clin. Exp. Pathol.*, 7, 7323-7341. PMID: 25550769 PMCID: PMC4270590

[9] Hasturk, H., & Kantarci, A. (2015). Activation and resolution of periodontal inflammation and its systemic impact. *Periodontol.* 2000, 69(1), 255-273. doi:10.1111/prd.12105

[10] Kayal, R. A., Elias, W. Y., Alharthi, K. J., Demyati, A. K., & Mandurah, J. M. (2014). Illicit drug abuse affects periodontal health status. *Saudi Med. J.,* 35(7), 724-728. PMID: 25028230

[11] Liaqat, N., & Dar, S. H. (2017). Comparison of single-dose nalbuphine versus tramadol for postoperative pain management in children: a randomized, controlled trial. *Korean J. Anesthesiol,* 70, 184-187. doi: 10.4097/kjae.2017.70.2.184

[12] Mallappallil, M., Sabu, J., Friedman, E. A., & Salifu, M. (2017). What Do We Know about Opioids and the Kidney? *Int. J. Mol. Sci.,* 18(1), 223. https://doi.org/10.3390/ijms18010223

[13] Mello, N. K., Mendelson, J. H., Sholar, M. B., Jaszyna-Gasior, M., Goletiani, N., & Siegel, A. J. (2005). Effects of the mixed mu/kappa opioid nalbuphine on cocaine-induced changes in subjective and cardiovascular responses in men. *Neuropsychopharmacology,* 30(3), 618-632. doi: 10.1038/sj.npp.1300631

[14] Nagpal, R., Yamashiro, Y., & Izumi, Y. (2015). The two-way association of periodontal infection with systemic disorders: an overview. *Mediators Inflamm.* 2015:793898. doi: 10.1155/2015/793898

[15] Pacheco, C. M. F., Queiroz-Junior, C. M., Maltos, K. L. M., Calliari, M. V., Rocha, O. A., & Francischi, J. N. (2007). Local opioids in a model of periodontal disease in rats. *Archives of Oral Biology,* 52(7), 677-683. doi: 10.1016/j.archoralbio.2006.12.012

[16] Patalakha, O. V. (2019). *Features of the immune response and optimization of treatment of generalized periodontitis in patients with toxic opioid hepatitis*. (Master's thesis). State Institution "I.I. Mechnikov Institute of Microbiology and Immunology of the National Academy of Medical Science of Ukraine", Kharkiv.

[17] Radke, J. B., Owen, K. P., Sutter, M. E., Ford, J. B., & Albertson, T. E. (2014). The effects of opioids on the lung. *Clin. Rev. Allergy Immunol.*, 46, 54-64. doi: 10.1007/s12016-013-8373-z

[18] Ranjan, R., Abhinay, A., & Mishra, M. (2018). Can oral microbial infections be a risk factor for neurodegeneration? A review of the literature. *Neurol.* India, 66, 344-351. doi: 10.4103/0028-3886.227315

[19] Rosier, B. T., de Jager, M., Zaura, E., & Krom, B. P. (2014). Historical and contemporary hypotheses on the development of oral diseases: are we there yet? *Front Cell Infect. Microbiol.,* 4, 92. doi: 10.3389/fcimb.2014.00092

[20] Rotemberg, E., Salveraglio, I., Kreiner, M., Piovesan, S., Smaisik, K., Ormaechea, R., & Varela, A. (2015). Estado dental y periodontal de poblacion en tratamiento por consumo de drogas: Estudio piloto. *Rev. Odontoestomatologia,* 17(25), 34-39. http://www.scielo.edu.uy/scielo.php.

[21] Saini, G. K., Gupta, N. D., & Prabhat, K. C. (2013). Drug addiction and periodontal diseases. *J. Indian Soc. Periodontol.,* 17, 587-591. doi: 10.4103/0972-124X.119277.

[22] Seltenhammer, M. H., Marchart, K., Paula, P., Kordina, N., Klupp, N., Schneider, B. … Risser, D. U. (2013). Micromorphological changes in cardiac tissue of drug-related deaths with emphasis on chronic illicit opioid abuse. *Addiction,* 108(7), 1287-1295. doi: 10.1111/add.12106

[23] Shekarchizadeh, H., Khami, M.R., Mohebbi, S. Z., Ekhtiari, H., & Virtanen, J. I. (2013). Oral health of drug abusers: A review of health effects and care. *Iran J. Public Health,* 42(9), 929-40. PMCID: PMC4453891 PMID: 26060654

[24] Stempak, J. G., & Ward, R. T. (1964). An improved staining method for electron microscopy. *J. Cell. Biol.,* 22(3), 697-701. doi: 10.1083/jcb.22.3.697

[25] Sun, D., Ye, T., Ren, P., & Yu, S. (2018). Prevalence and etiology of oral diseases in drug-addicted populations: a systematic review. Int. J. Clin. Exp. Med., 11(7), 6521-6531 www.ijcem.com /ISSN:1940-5901/IJCEM0075796

[26] Vinogradova, O. M., & Shkrebniuk, R. Yu. (2015). Differential methods of treatment of periodontal tissue diseases on the background of diabetes. *Clinical and experimental pathology,* 51(1),205-208. http://nbuv.gov.ua/UJRN/kep_2015_14_149

ЕЛЕКТРОННО-МІКРОСКОПІЧНІ ДОСЛІДЖЕННЯ ПАРОДОНТУ ПРИ ЕКСПЕРИМЕНТАЛЬНІЙ ДВОТИЖНЕВІЙ ДІЇ ОПІОЇДУ ТА ПІСЛЯ ЙОГО ВІДМІНИ ВПРОДОВЖ ЧОТИРЬОХ ТИЖНІВ

Фік В.Б., Пальтов Є.В., Кривко Ю.Я.

Зважаючи на шкідливий вплив опіоїдних речовин при неконтрольованому їх вживанні, неможливо легковажити ранніми проявами ушкоджень тканин і органів ротової порожнини, що складає актуальну проблему сьогодення. Метою цієї роботи було дослідити особливості субмікроскопічної організації структурних компонентів пародонту при дії опіоїдного аналгетика впродовж двох тижнів та його 4-тижневої відміни в експерименті. Дослідження проведено на 22 статевозрілих щурах-

самцях лінії Wistar, масою 160 г, віком 4,5-6 місяців. Тваринам протягом перших двох тижнів вводили щоденно внутрішньом'язово одноразово опіоїдний аналгетик налбуфін у перерахунку середньої терапевтичної дози для щура, а також з урахуванням середньої ваги піддослідної групи (0,212 мг/кг) та його подальшою відміною протягом наступних 4 тижнів. Для електронно-мікроскопічного дослідження використали фрагменти м'яких тканин пародонту. Субмікроскопічно виражених деструктивних змін у тканинах пародонту виявлено не було. Позитивної динаміки регенерації компонентів пародонту на ультраструктурному рівні також не виявили. В цитоплазмі клітин епітелію вільної частини ясен спостерігали деструкцію органел, частково ушкоджені кристи мітохондрій, погано контурувались тонофіламенти, встановлені неглибокі інвагінації каріолеми, між плазмолемами спостерігали потовщені ділянки та пошкоджені десмосомальні контакти. У поверхневих ділянках періодонту колагенові волокна були частково розшарованими, спостерігали помірний набряк міжклітинної речовини сполучної тканини, у частини фіброцитів встановлені інвагінації каріолеми ядра та розміщення гетерохроматину по периферії. Ультраструктурно у цитоплазмі макрофага відмічено лізосоми, фагосом небагато, що свідчить про незначне ушкодження структур. У просвітах кровоносних капілярів виявляються форменні елементи крові, переважно еритроцити, в перинуклеарній частині цитоплазми органел небагато, мітохондрії з електронно світлим матриксом та невеликими кристами, периваскулярний набряк незначний, у цитоплазмі ендотеліоцитів венул спостерігались деструктивно змінені мітохондрії, базальна мембрана потовщена, периваскулярні простори збільшені. Таким чином, наприкінці 6 тижня експерименту при короткотривалій дії опіоїду впродовж двох тижнів та його подальшій 4-тижневій відміні глибоких незворотніх змін ультраструктурної організації компонентів пародонту не виявлено. Слід відмітити, що повного відновлення структурних компонентів пародонту не спостерігається, наявні ознаки реактивних змін, репаративні процеси сповільнені.

Ключові слова: *пародонт, опіоїд, відміна опіоїду, ультраструктура, експеримент.*

ЭЛЕКТРОННО-МИКРОСКОПИЧЕСКИЕ ИССЛЕДОВАНИЯ ПАРОДОНТА ПРИ ЭКСПЕРИМЕНТАЛЬНОМ ДВУХНЕДЕЛЬНОМ ВЛИЯНИИ ОПИОИДА И ПОСЛЕ ЕГО ОТМЕНЫ В ТЕЧЕНИЕ ЧЕТЫРЕХ НЕДЕЛЬ

Фик В.Б., Пальтов Е.В., Кривко Ю.Я.

Учитывая вредное воздействие опиоидных веществ при неконтролируемом их употреблении, невозможно пренебрегать ранними проявлениями повреждений тканей и органов ротовой полости, что составляет актуальную проблему современности. Целью работы было исследовать особенности субмикроскопической организации структурных компонентов пародонта при действии опиоидного анальгетика в течение двух недель и после его 4-недельной отмены в эксперименте. Исследование проведено на 22 половозрелых крысах-самцах линии Wistar, массой 160 г, в возрасте 4,5-6 месяцев. Животным в течение первых двух недель вводили ежедневно внутримышечно однократно опиоидный анальгетик налбуфин в перерасчете средней терапевтической дозы для крысы, а также с учетом среднего веса подопытной группы (0,212 мг/кг) и его последующей отменой в течение следующих 4 недель. Для электронно-микроскопического исследования использовали фрагменты мягких тканей пародонта. Субмикроскопически выраженных деструктивных изменений в тканях пародонта выявлено не было. Положительной динамики регенерации компонентов пародонта на ультраструктурном уровне также не выявили. В цитоплазме клеток эпителия свободной части десны наблюдали деструкцию органелл, частично поврежденные кристы митохондрий, плохо контурировались тонофиламенты, установлены неглубокие инвагинации кариолеммы, между плазмолеммами наблюдали утолщенные участки и поврежденные десмосомальные контакты. В поверхностных участках периодонта коллагеновые волокна были частично расслоенными, наблюдали умеренный отек межклеточного вещества соединительной ткани, у части фиброцитов установлены инвагинации кариолеммы и наличие гетерохроматина на периферии. Ультраструктурно в цитоплазме макрофага отмечены лизосомы, фагосом немного, что свидетельствует о незначительном повреждении структур. В просветах кровеносных капилляров выявляются форменные элементы крови, преимущественно эритроциты, в перинуклеарной части цитоплазмы органелл немного, митохондрии с электронно светлым матриксом и небольшими кристами, периваскулярный отек незначительный, в цитоплазме эндотелиоцитов венул наблюдаются деструктивно измененные митохондрии, базальная мембрана утолщена, периваскулярные пространства увеличены. Таким образом, в конце 6 недели эксперимента при кратковременном действии опиоида в течение двух недель и его дальнейшей 4-недельной отмене, глубоких необратимых изменений ультраструктурной организации компонентов пародонта не обнаружено. Следует отметить, что полного восстановления структурных компонентов пародонта не наблюдается, в наличии явные признаки реактивных изменений и замедленные репаративные процессы.

Ключевые слова: *пародонт, опиоид, отмена опиоида, ультраструктура, эксперимент.*

DOI: 10.31393/morphology-journal-2019-25(3)-06 Reports of Morphology, Vol. 25, №3, Pages 33-39

ISSN 1818-1295 eISSN 2616-6194

REPORTS OF MORPHOLOGY

Official Journal of the Scientific Society of Anatomists, Histologists, Embryologists and Topographic Anatomists of Ukraine

journal homepage: https://morphology-journal.com

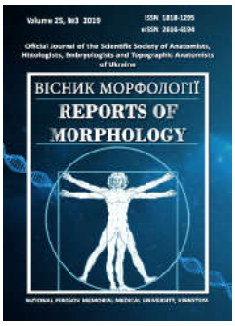

Analysis of the dynamics of the structural changes development in the humerus of guinea pigs under modeling biomechanical disturbances

Sergienko R.A.[1], Strafun S.S.[2], Savosko S.I.[3], Makarenko A.M.[3]

[1]Medical center "Modern orthopedics" SPE Firm "Rehabilitation", Kyiv, Ukraine
[2]GA "Institute of traumatology and orthopedics NAMS of Ukraine", Kyiv, Ukraine
[3]Bogomolets A.A. National Medical University, Kyiv, Ukraine

ARTICLE INFO
Received: 25 June, 2019
Accepted: 27 July, 2019

UDC: 616.727.2-007.233-02-092

CORRESPONDING AUTHOR
e-mail: ruslan.sergienko.md@gmail.com
Serghiyenko R.O.

Today, the role of the traumatic factor and inflammation in the development and progression of osteoarthrosis is generally recognized, but the available research results do not allow to establish the role of impaired biomechanics as a monofactor in the development of deforming osteoarthrosis of the shoulder joint. Violation of the function of the bone and bone-cartilage elements of the joint, which is compensated by soft tissue formations, leads to overloads of the joints, upsets the normal balance of the load forces in the joint, creates abnormal biomechanics and the resulting pathological manifestations of deforming osteoarthrosis. The aim of the study is research of the dynamics of the disturbed biomechanics influence of the shoulder joint on the development of deformation osteoarthrosis and the features of the development of its structural changes. The experiments were conducted on guinea pigs weighing 380-420 grams at the age of 5 months. A model of surgical restriction of joint mobility was reproduced, which caused the formation of contracture. Using the methods of histology and scanning electron microscopy, we studied the relief of the articular surface, the topography of degenerative changes, and structural changes in the articular cartilage and subchondral bone. A statistical evaluation of the obtained data samples was carried out using Student t-test. The results were considered reliable at $p<0.05$. The results of an experimental study demonstrated a decrease in the thickness and structure of articular cartilage when modeling deforming osteoarthrosis and confirmed the hypothesis that pathological limitation of the mobility of the shoulder joint and violation of biomechanics is an independent factor in the formation of osteoarthrosis. After surgery on day 30, degenerative changes and their progression with the formation of contracture on day 90 of observation were found in the articular cartilage. The features of the development of articular surface degeneration, the dynamics of the pathological changes and topography, which can expand the understanding of the pathogenesis of the disease, were established. The loss of the superficial zone caused the progression of dystrophic changes in the articular cartilage and sclerosis of the subchondral bone at 60 and 90 days.

Keywords: *osteoarthrosis, humerus, topography, dynamics, lesion area.*

Introduction

Deforming osteoarthrosis is a group of diseases of joints of different etiology with degeneration of hyaline cartilage and subchondral bone layer, obvious or hidden synovitis and subsequent loss of joint functionality [2, 16]. Numerous modern methods of treatment of the pathology of the shoulder joints are often not effective enough, which may be due to untimely treatment and insufficient assessment of pathogenetic components in the appearance and progression of pathological changes [17, 18]. However, the place of biomechanical disorders in the development of osteoarthritis of the shoulder joint as a monofactor of the pathological condition remains unknown. Experimental studies on animals allow us to determine the pathogenetic links of this complex process on the basis of reproduction of different models of osteoarthrosis [17, 27].

In clinical practice, there is often a correlation between impaired biomechanics of the shoulder joint and the development of shoulder-scapula arthrosis [8, 21, 22]. This may be due to a violation of the balance of forces on the shoulder, resulting in a change in rotation of the humerus head and subsequent formation of an abnormal load on the joint surfaces [13, 17].

Today, the role of traumatic factor and inflammation in the development and progression of osteoarthritis is generally recognized [14, 17]. The results of experimental studies have shown the similarity of the main pathogenetic units of these processes in animal models with those that develop in the most common forms of slowly progressing human arthrosis [4, 18, 24]. However, the available research results do not allow us to establish the role of impaired biomechanics as a single factor in the development of deforming osteoarthrosis of the shoulder joint [6]. In view of this, it became necessary to develop another methodological approach in the study of the site of abnormal loading in the appearance and progression of osteoarthritis. The shoulder joint is known to be the most mobile in the human body due to its superiority in the biomechanics of the soft tissue elements over the bone [10].

The peculiarities of the morphological structure cause the possibility of powerful compensation in the case of pathological changes of one of the joints by other biomechanical units [7, 19, 28]. However, the violation of the function of the bone and cartilage elements of the joint, which is compensated by soft tissue formation, leads to overload of the latter, disrupts the normal balance of forces of the joints, creates abnormal biomechanics and caused by pathological manifestations of deforming osteoarthritis [3]. Reducing the thickness of the cartilage, its elasticity in the future becomes a cause of instability of the joint and the progression of osteoarthritis [18, 24, 25]. The metabolic flexibility of the joint chondrocytes normally allows to generate energy and maintain cell viability under the initial stages of pathology by increasing the regulation of mitochondrial respiration and reducing the rate of formation of reactive nitrogen and oxygen [11], however, at later stages of the disease, chondrocytes lose this metabolic flexibility [15].

The purpose of the study was to investigate the dynamics of the impact of disturbed biomechanics of the shoulder joint on the development of deformity osteoarthrosis and the features of its structural changes.

Materials and methods

The studies were performed on Guinea pigs (Cavia porcellus) weighing 380-420 grams at the age of 5 months. Animals were divided into groups according to the objectives of the experiment. The control group (n=5) and the main experimental group (n=19) were formed. The experimental group included operated animals, which were withdrawn from the experiment at 30 day (n=5), 60 day (n=5) and 90 day (n=9). Before operative reproduction of the model of osteoarthrosis of the shoulder joint of the animals was anesthetized with sodium thiopental (50-60 mg/kg, intraperitoneally). The sequence of surgical procedures was performed according to the technique described in 2013 by E.J. Kramer et al. [9]. First, the skin and subcutaneous tissue were cut, and then the interval of the capsule was separated between the anterior margin of the supraspinatus muscle and the upper edge of the subscapularis muscle. On the edge of the foregoing muscles, the sutures were sutured with vicryl № 2.0 and stitched together to form a capsular contracture. The cavity of the joint was not opened. The wound was sutured in layers.

Animals were removed from the experiment at 30, 60 and 90 days after surgery by administering a lethal dose of sodium thiopental.

Histological examination. The histological material (humerus) was fixed in 10% formalin solution on 0.1M phosphate buffer (pH=7.4) for 24 hours at 4°C, then washed with running water. In order to investigate the structural changes of the shoulder joint, the test specimens were decalcified according to the Freiman method in a 5% aqueous solution of EDTA calibrated with sodium hydroxide to pH 6.0-6.5. Decalcification in the first 24 hours was performed at 4°C, then at room temperature for 20-30 days [20]. The solution was changed every 5 days. From decalcified specimens of the humerus were made cryosections 12-15 μm thick (cryostat-microtome MK-25, USSR). Cryosections were stained with picrofuxin, toluidine blue, hematoxylin and eosin [26].

Morphometric study. Morphometric analysis consisted of quantitative assessment of the thickness of the articular surface of the humerus. To do this, the histological sections of all experimental animals from the surface to the subchondral measured its thickness at 20 points. Microphotographs were obtained on an Olympus BX 51 microscope. Morphometric analysis was performed using CarlZeiss software (AxioVision SE64 Rel.4.9.1) at magnification x200 and x400.

Scanning electron microscopy. For the methods of scanning electron microscopy SEM, the samples underwent a number of methodological procedures. The samples were dehydrated with ethanol solution in increasing concentrations (25%, 50%, 75% and 100%). The material was then dried in a Samdri-780A installation at a CO_2 critical point. The dried samples were coated with 15 nm gold using a Gatan 682 PECS device. SEM studies were performed on a Tescan Mira 3 LMU microscope in the electron microscopy laboratory of "NanoMedTech" LLC under the guidance of M.A. Skoryk.

Criteria for assessing structural changes in the joint:

- capsule changes: inflammatory infiltrate (appearance of monocytes, macrophages, neutrophils, basophils and lymphocytes); angiogenesis (increase in microvascular density); plethora of microvessels in capsule;

- articular cartilage changes: change in cartilage thickness (loss of superficial and/or deep cartilage layer), reduction of cartilage cellular composition;

- subchondral bone changes: the appearance of foci of bone reorganization or reduction.

Statistical processing. Statistical evaluation of the obtained data samples was performed using Student's t-test. Results $p<0.05$ were considered valid. Data are presented as mean ± standard deviation.

Bioethics. All experimental manipulations were carried out in accordance with the provisions of the European Convention for the Protection of Vertebrate Animals Used for Experimental and Other Scientific Purposes (Strasbourg, 1986), Council of Europe Directive 86/609/EEC (1986), Law of Ukraine No. 3447-IV "On protection of animals from ill-treatment", General Ethical Principles of Animal Experiments, approved by the First National Congress of Ukraine on Bioethics (2001).

Results

By surgical limitation of the biomechanics of the shoulder joint in the experimental animals, an abnormally altered (disturbed) projection of rotation of the humerus head in the hollow of the scapula was achieved.

Proliferation changes of the articular capsule and tendons of the skeletal muscles, as well as the increase of the microvascular density, were found in the study of the structural changes of the shoulder joint. These changes are the result of traumatic damage and reorganization of the connective tissue of the capsule of the joint (Fig. 1).

The results of histological examination confirmed our working hypothesis that surgical limitation of the biomechanics of the shoulder joint is an isolated factor in the appearance and progression of deforming osteoarthrosis.

Morphometric analysis allowed us to quantify the structural changes of the shoulder joint. The value of the thickness of the cartilage surface of the humerus in the group of operated animals was statistically significantly smaller compared to the control group by an average of 48% (127.9±38.3 μm^2 versus 255.9±26.7 μm^2 in control, $p<0.01$). In general, the quantitative indicators were lower in the lower area of the joint surface of the humerus, which is associated with the formation of non-physiological (abnormal) load on this area of the joint.

Histogram 1 shows the number of structural change criteria identified in each comparison group. On the 60th day most of the samples confirmed the presence of structural changes in the joint, and on the 90th day progression or no difference on the 60 day of the experiment.

However, the histological method made it possible to establish the appearance and frequent localization of degenerative changes of hyaline cartilage, but for a more complete assessment of the topography of the established changes, a scan of the surface of the humerus was performed using the SEM method. The application of the method yielded the following results.

On the 30th day after surgery, focal destructive changes of the cartilage surface area at the lower or anterior pole were observed on the articular surface of the humerus (mean lesion area 8.3% of the articular surface area). The thickness of the cartilage surface at 60 day decreased significantly at the anterior lower pole and to a lesser extent at the posterior lower (lesion area averaged 25.9%, $p<0.05$). At 90 day, the deformation zone increased in area (an average of 54.2%, $p<0.05$), and deformation changes of the articular surface progressed from the central zone of

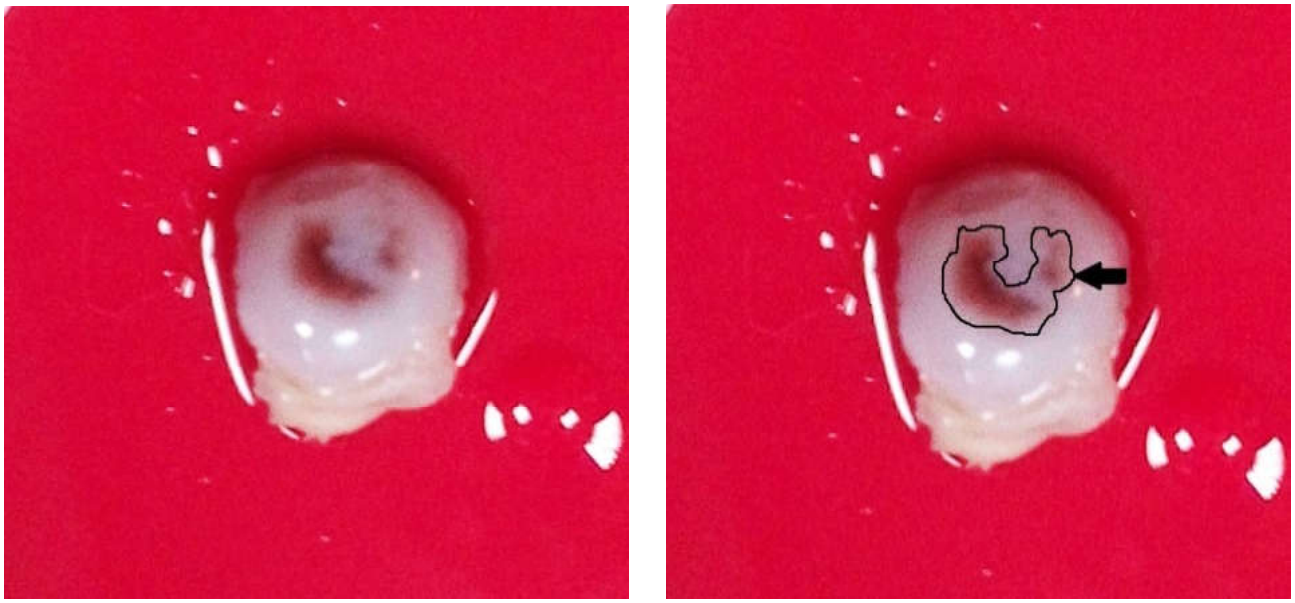

Fig. 1. Native preparation of Guinea pig humerus head on 90 day after modeling of deforming osteoarthrosis of the shoulder joint. (⬅) - the area of deforming osteoarthritis.

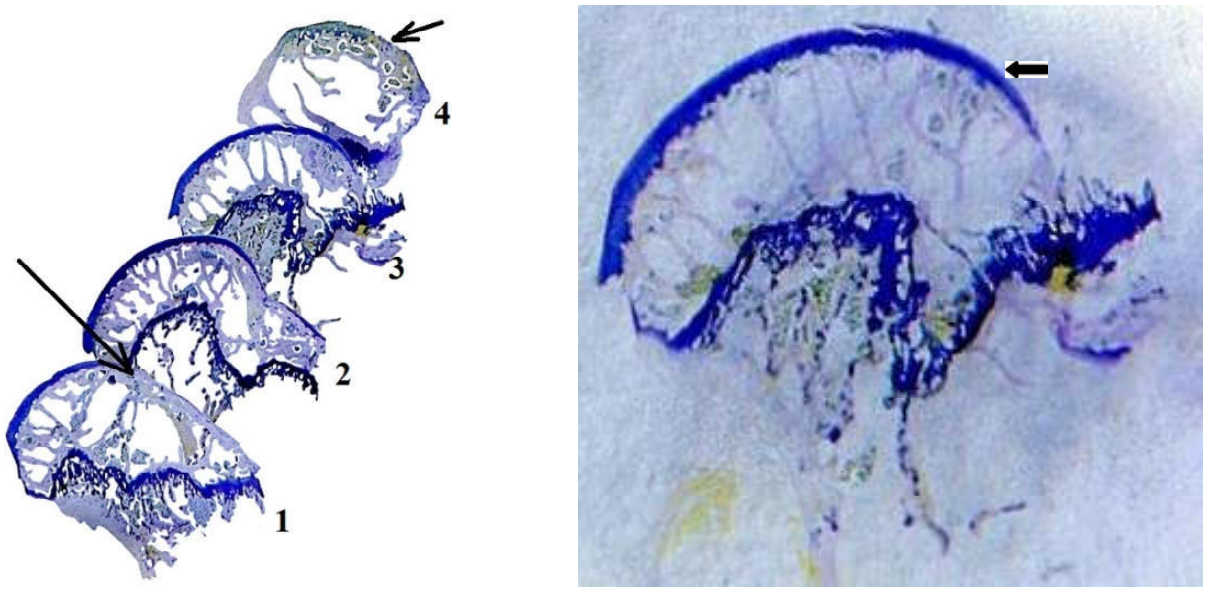

Fig. 2. Histological sections of the humerus in lateral projection (60 day of observation). Arrows (⟵) indicate areas of thinning or loss of articular surface: 1 - anterior surface; 2 and 3 - central part of the head; 4 - back surface (x 5) (left side). Positive staining of toluidine blue hyaline cartilage of the articular surface (⟵) and metaphyseal plate (x 11) (right side).

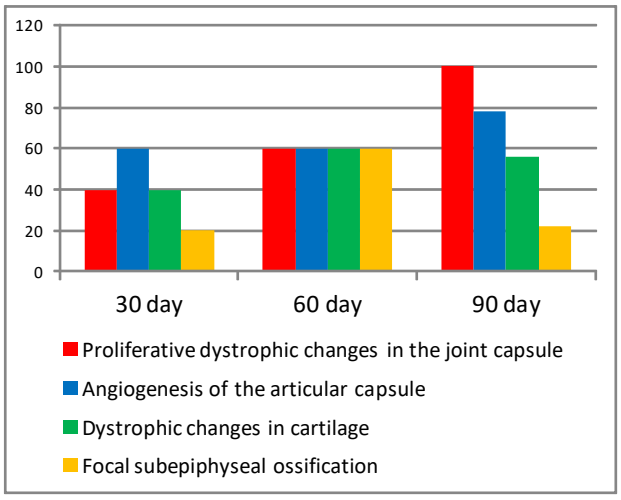

Histogram 1. Histological changes of the shoulder joint at the level of the cartilage surface (% of animals).

the articular surface to the outer contour, which was previously described at 60 day. The scan results of the humerus head are clearly shown in Figure 2.

Figure 2 shows histological sections of the head of the humerus, reflecting the change in thickness of hyaline cartilage on different surfaces of the head. Thus, at 60 day marked dystrophic changes more developed on the anterior and/or posterior surface of the head. These data should be confirmed by scanning the articular depression of the scapula.

In the study of the topography and the degree of degenerative changes, considerable attention was paid to the study of the surface area of the articular surface, because of its localization, the latter experiences the bulk of the load in anomalous biomechanics and therefore rapidly loses elasticity, density and degenerates.

Histological picture of the anterior and posterior articular lower surfaces was characterized by signs of focal or diffuse destruction of cartilage. A decrease in the thickness of the articular cartilage over a considerable area of the surface of the humeral head was noted. The deep area of the cartilage surface contained newly formed foci of paravascular ossification. In the resorptive cavities of the articular cartilage, foci of loose connective tissue were located next to the vessels, the density of such areas was increased in calcified cartilage and deep sections of non-calcified cartilage. The density of chondrocytes was low, they were unevenly located within the matrix. The expressed changes were observed in the cellular composition of the articular cartilage. Most isogenic chondrocyte groups were in a state of edema and necrosis. The ossification zones extended from the epiphyseal foci of the subchondral bone to its surface; in the formed gaps blood vessels with osteogenic cells grew; surrounding matrix with signs of compaction and ossification; the contour of the border of cartilage and bone tissue towards the epiphyseal cartilage has changed. On the opposite side, that is, the surface of the epiphysis, the structural changes of the cartilage were characterized by a sharp change in the relief of the articular surfaces, as confirmed by SEM studies.

At the ultrastructural level, the loss of the superficial zone of cartilage was established against the background of its deformation, matrix and cell structure. Since the 60th day of observation, there has been a sharp increase in the degree of degenerative changes of the shoulder joint, which progressed from the central zone of the articular surface to the outer contour. On average, reduction of the epiphyseal

cartilage was 15.9%, 25.3%, and 49.3% ($p<0.05$) according to the observation period.

Discussion

The experimental study evaluated the role of immobilization of the shoulder joint as a monopathogenetic factor in the development of osteoarthrosis. Today there is a considerable amount of research on the analysis of the nature and features of the development of dystrophic changes in the joint. Researchers focus on the mechanical and histochemical factors of these disorders [2, 16]. Mechanical factors include traumatic compression, mechanical overload, etc. [17, 18], and enzymatic dysfunction, microcirculation, denervation, and metabolic disorders, including genetically predetermined ones, are quite conditional on histochemical [3, 6].

The analysis of literary sources revealed quite similar features of the development of histostructural changes in the shoulder joint in different models of osteoarthrosis reproduction in experimental animals [4, 14]. In particular, a decrease in the content of collagen, proteoglycans and other polysaccharides and proteins has been observed, providing strength and resistance to compression and loading [19, 25, 28]. The authors explain this by increasing the activity of local collagenases and metalloproteinases, ie enzymes of the catabolic (proteolytic) plan [7]. Together with abnormal loading and non-physiological biomechanics of the joint, all these factors cause changes in the cartilage surfaces of the humerus head and are considered as a prerequisite for joint instability [21, 22].

The development of osteoarthrosis is accompanied by increased expression of vascular endothelial growth factor (VEGF) in articular cartilage [29]. VEGF is an angiogenic factor directly or indirectly involved in all links of angiogenesis. Under normal physiological conditions hypertrophied chondrocyte can secrete VEGF, which promotes angiogenesis in the area of calcified articular cartilage and bone formation.

The vascular growth, ossification foci formation, resorption cavities revealed in our study are signs of osteoarthrosis, which is also accompanied by increased production of inflammatory cytokines, change in macromolecular structure of the articular cartilage matrix coincides with other researchers [12].

Conclusions

1. The results of the experimental study showed a decrease in the thickness and structure of articular cartilage in the modeling of deforming osteoarthrosis. The features of the development of joint surface degeneration, the dynamics of the pathological changes and the topography established and which can expand the understanding of the pathogenesis of the disease.

2. The results of the experimental study confirmed the hypothesis that pathological limitation of shoulder joint mobility and disturbance of biomechanics is an independent factor in the formation of osteoarthrosis. At the same time, according to the results of dynamic observation, the most critical is the period from 30 to 60 days, because it is at this interval of time that degenerative phenomena reached the most vulnerable to ossification of articular cartilage. The exposure of the latter in the projection to the area of loading of the articular surface and concomitant sclerosis caused a rapid progression of degenerative changes in the shoulder joint. Given these data, the first 30 days can be considered as a therapeutic window to correct the pathological process.

References

[1] Anderson, D. E., & Johnstone, B. (2017). Dynamic mechanical compression of chondrocytes for tissue engineering: A critical review. *Frontiers in Bioengineering and Biotechnology,* 5, 76. doi: 10.3389/fbioe.2017.00076

[2] Birrell, F., Howells, N., & Porcheret, M. (2011). Osteoarthritis: pathogenesis and prospects for treatment. *Rep. Rheumatic. Dis.*, 10, 1-2. doi: 10.1177/2040622312462734

[3] Cooke, M. E., Lawless, B. M., Jones, S. W., & Grover, L. M. (2018). Matrix degradation in osteoarthritis primes the superficial region of cartilage for mechanical damage. *Acta Biomaterialia,* 78, 320-328. doi: 10.1016/j.actbio.2018.07.037

[4] Cope, P. J., Ourradi, K., Li, Y., & Sharif, M. (2019). Models of osteoarthritis: the good, the bad and the promising. *Osteoarthritis and Cartilage,* 27(2), 230-239. doi: 10.1016/j.joca.2018.09.016

[5] Goldring, M. B., & Berenbaum, F. (2015). Emerging targets in osteoarthritis therapy. *Current Opinion in Pharmacology,* 22, 51-63. doi: 10.1016/j.coph.2015.03.004

[6] Guilak, F., Nims, R. J., Dicks, A., Wu, C. L., & Meulenbelt, I. (2018). Osteoarthritis as a disease of the cartilage pericellular matrix. *Matrix Biology,* 71, 40-50. doi: 10.1016/j.matbio.2018.05.008

[7] Hall, A. C. (2019). The Role of Chondrocyte Morphology and Volume in Controlling Phenotype-Implications for Osteoarthritis, Cartilage Repair, and Cartilage Engineering. *Current Rheumatology Reports,* 21(8), 38. doi: 10.1007/s11926-019-0837-6

[8] Hsu, H. C., Luo, Z. P., Stone, J. J., Huang, T. H., & An, K. N. (2003). Correlation between rotator cuff tear and glenohumeral degeneration. *Acta Orthopaedica Scandinavica,* 74(1), 89-94. doi: 10.1080/00016470310013725

[9] Kramer, E. J., Bodendorfer, B. M., Laron, D., Wong, J., Kim, H. T., Liu, X., & Feeley, B. T. (2013). Evaluation of cartilage degeneration in a rat model of rotator cuff tear arthropathy. *Journal of Shoulder and Elbow Surgery,* 22(12), 1702-1709. doi: 10.1016/j.jse.2013.03.014

[10] Krishnan, Y., & Grodzinsky, A. J. (2018). Cartilage diseases. *Matrix Biology,* 71, 51-69. doi: 10.1016/j.matbio.2018.05.005

[11] Lane, R. S., Fu, Y., Matsuzaki, S., Kinter, M., Humphries, K. M., & Griffin, T. M. (2015). Mitochondrial respiration and redox coupling in articular chondrocytes. *Arthritis Research & Therapy,* 17(1), 54. doi: 10.1186/s13075-015-0566-9.

[12] Liu, J., Dai, J., Wang, Y., Lai, S., & Wang, S. (2017). Significance of new blood vessels in the pathogenesis of temporomandibular joint osteoarthritis. *Experimental and Therapeutic Medicine,* 13(5), 2325-2331. doi: 10.3892/etm.2017.4234

[13] Mazor, M., Best, T. M., Cesaro, A., Lespessailles, E., & Toumi,

H. (2019). Osteoarthritis biomarker responses and cartilage adaptation to exercise: A review of animal and human models. *Scandinavian Journal of Medicine & Science in Sports*, 29(8), 1072-1082. doi: 10.1111/sms.13435

[14] Miyaki, S., & Lotz, M. K. (2018). Extracellular vesicles in cartilage homeostasis and osteoarthritis. *Current Opinion in Rheumatology,* 30(1), 129. doi: 10.1097/BOR.0000000000000454

[15] Mobasheri, A., Matta, C., Zakany, R., & Musumeci, G. (2015). Chondrosenescence: definition, hallmarks and potential role in the pathogenesis of osteoarthritis. *Maturitas,* 80(3), 237-244. doi: 10.1016/j.maturitas.2014.12.003

[16] Paterson, S. I., Eltawil, N. M., Simpson, A. H. R. W., Amin, A. K., & Hall, A. C. (2016). Drying of open animal joints in vivo subsequently causes cartilage degeneration. *Bone & Joint Research,* 5(4), 137-144. doi: 10.1302/2046-3758.54.2000594

[17] Prieto-Alhambra, D., Judge, A., Javaid, M. K., Cooper, C., Diez-Perez, A., & Arden, N. K. (2014). Incidence and risk factors for clinically diagnosed knee, hip and hand osteoarthritis: influences of age, gender and osteoarthritis affecting other joints. *Annals of the Rheumatic Diseases,* 73(9), 1659-1664. doi: 10.1136/annrheumdis-2013-203355

[18] Reuther, K. E., Thomas, S. J., Tucker, J. J., Sarver, J. J., Gray Ch. F., Rooney, S. I., … Soslowsky, L. J. (2014). Disruption of the anterior-posterior rotator cuff force balance alters joint function and leads to joint damage in a rat model. J*ournal of Orthopaedic Research,* 32(5), 638-644. doi: 10.1002/jor.22586

[19] Rosenthal, A. K. (2016). Articular cartilage vesicles and calcium crystal deposition diseases. *Current Opinion in Rheumatology,* 28(2), 127. doi: 10.1097/BOR.0000000000000244

[20] Sarkisov, D. S. & Perov, Yu. L. (Ed.) (1996). *Microscopic Technique: Manual*. M.: Medicine.

[21] Sears, B. W., Johnston, P. S., Ramsey, M. L., & Williams, G. R. (2012). Glenoid bone loss in primary total shoulder arthroplasty: evaluation and management. *JAAOS-Journal of the American Academy of Orthopaedic Surgeons*, 20(9), 604-613. doi: 10.5435/JAAOS-20-09-604

[22] Simon, T. M., & Jackson, D. W. (2018). Articular cartilage: injury pathways and treatment options. *Sports Medicine and Arthroscopy Review*, 26(1), 31-39. doi: 10.1097/JSA.0000000000000182

[23] Tkach, M., & Théry, C. (2016). Communication by extracellular vesicles: where we are and where we need to go. *Cell,* 164(6), 1226-1232. doi: 10.1016/j.cell.2016.01.043

[24] Van Den Berg, W. B. (2001). Lessons from animal models of osteoarthritis. *Current Opinion in Rheumatology,* 13(5), 452-456. doi: 10.1097/00002281-200109000-00019

[25] Van Der Kraan, P. M. (2017). The changing role of TGFβ in healthy, ageing and osteoarthritic joints. *Nature Reviews Rheumatology,* 13(3), 155. doi: 10.1038/nrrheum.2016.219

[26] Wang, C., Wang, X., Xu, X. L., Yuan, X. L., Gou, W. L., Wang, A. Y., ... & Lu, S. B. (2014). Bone microstructure and regional distribution of osteoblast and osteoclast activity in the osteonecrotic femoral head. *PloS-one,* 9(5). doi: 10.1371/journal.pone.0096361

[27] Wang, W. J., Liu, F., Zhu, Y. W., Sun, M. H., Qiu, Y., & Weng, W. J. (2016). Sagittal alignment of the spine-pelvis-lower extremity axis in patients with severe knee osteoarthritis: A radiographic study. *Bone & Joint Research,* 5(5), 198-205. doi: 10.1302/2046-3758.55.2000538

[28] Wang, X., Zhai, M., Zhao, Y., & Yin, J. (2018). A review of articular cartilage and osteoarthritis studies by Fourier transform infrared spectroscopic imaging. *Ann. Joint,* 3(2), 9. doi: 10.21037/aoj.2018.01.04

[29] Zhang, S., Cao, W., Wei, K., Liu, X., Xu, Y., Yang, C., ... & Chen, W. (2013). Expression of VEGF-receptors in TMJ synovium of rabbits with experimentally induced internal derangement. *British Journal of Oral and Maxillofacial Surgery,* 51(1), 69-73. doi: 10.1016/j.bjoms.2012.01.014

АНАЛІЗ ДИНАМІКИ РОЗВИТКУ СТРУКТУРНИХ ЗМІН ПЛЕЧОВОЇ КІСТКИ МУРЧАКІВ ПРИ МОДЕЛЮВАННІ ПОРУШЕННЯ БІОМЕХАНІКИ

Сергієнко Р.О., Страфун С.С., Савосько С.І., Макаренко О.М.

Сьогодні роль травматичного чинника і запалення у розвитку і прогресуванні остеоартрозу є загальновизнаною, проте існуючі результати досліджень не дозволяють встановити роль порушеної біомеханіки як монофактора у розвитку деформуючого остеартрозу плечового суглоба. Порушення функції кісткових та кістково-хрящових елементів суглоба призводить до їх перевантаження, порушуючи рівновагу сил навантажень в суглобі, і створює аномальну біомеханіку. Мета роботи: дослідити динаміку впливу порушеної біомеханіки плечового суглоба на розвиток деформуючого остеоартрозу та особливості розвитку його структурних змін. Експерименти проведені на морських свинках вагою 380-420 грам у віці 5 місяців. Відтворювали модель хірургічного обмеження рухливості суглоба, що спричиняло формування контрактури. Методами гістології та скануючої (растрової) електронної мікроскопії досліджували рельєф суглобової поверхні, топографію дегенеративних змін, структурні зміни суглобового хряща і субхондральної кістки. Статистичну оцінку отриманих вибірок даних проводили із застосуванням t-критерію Стьюдента. Достовірними вважались результати за умови p<0,05. При моделюванні деформуючого остеоартрозу встановлено зменшення товщини та зміну структури суглобового хряща. Отримано підтвердження гіпотези: самостійним чинником у формуванні остеоартрозу є патологічне обмеження рухомості плечового суглоба та порушення його біомеханіки. Після оперативного втручання на 30 добу в суглобовому хрящі виявлено дегенеративні зміни та їх прогресування з формуванням контрактури на 90 добу спостереження. Таким чином, встановлено особливості розвитку дегенерації суглобових поверхонь і динаміки перебігу патологічних змін. Втрата поверхневої зони сприяла прогресуванню дистрофічних змін в суглобовому хрящу та склерозу субхондральної кістки у терміни 60 та 90 діб.

Ключові слова: *остеоартроз, плечова кістка, топографія, динаміка, площа ураження.*

АНАЛИЗ ДИНАМИКИ РАЗВИТИЯ СТРУКТУРНЫХ ИЗМЕНЕНИЙ ПЛЕЧЕВОЙ КОСТИ МОРСКИХ СВИНОК ПРИ МОДЕЛИРОВАНИИ НАРУШЕНИЯ БИОМЕХАНИКИ

Сергиенко Р.А., Страфун С.С., Савосько С.И., Макаренко А.Н.

Сегодня роль травматического фактора и воспаления в развитии и прогрессировании остеоартроза является общепризнанной, однако имеющиеся результаты исследований не позволяют установить роль нарушенной биомеханики как монофактора в развитии деформирующего остеартроза плечевого сустава. Нарушение функции костных и костно-хрящевых элементов сустава приводит к их перегрузкам, нарушая равновесие сил нагрузок в суставе, и создает аномальную биомеханику. Цель работы: исследовать динамику влияния нарушенной биомеханики плечевого сустава на развитие

деформирующего остеоартроза и особенности развития его структурных изменений. Эксперименты проведены на морских свинках весом 380-420 грамм в возрасте 5 месяцев. Воспроизводили модель хирургического ограничения подвижности сустава, что вызывало формирование контрактуры. Методами гистологии и сканирующей (растровой) электронной микроскопии исследовали рельеф суставной поверхности, топографию дегенеративных изменений, структурные изменения суставного хряща и субхондральной кости. Статистическую оценку полученных выборок данных проводили с использованием t-критерия Стьюдента. Достоверными считались результаты при условии p<0,05. При моделировании деформирующего остеоартроза установлено уменьшение толщины и изменение структуры суставного хряща. Получено подтверждение гипотезы: самостоятельным фактором в формировании остеоартроза является патологическое ограничение подвижности плечевого сустава и нарушение его биомеханики. После оперативного вмешательства на 30 сутки в суставном хряще обнаружены дегенеративные изменения и их прогрессирование с формированием контрактуры на 90 сутки наблюдения. Таким образом, установлены особенности развития дегенерации суставных поверхностей и динамика развития патологических изменений. Потеря поверхностной зоны способствовала прогрессированию дистрофических изменений в суставном хряще и склерозу субхондральной кости в сроки 60 и 90 суток.

Ключевые слова: *остеоартроз, плечевая кость, топография, динамика, площадь поражения.*

DOI: 10.31393/morphology-journal-2019-25(3)-07 Reports of Morphology, Vol. 25, №3, Pages 40-44

ISSN 1818-1295 eISSN 2616-6194

REPORTS OF MORPHOLOGY

Official Journal of the Scientific Society of Anatomists, Histologists, Embryologists and Topographic Anatomists of Ukraine

journal homepage: https://morphology-journal.com

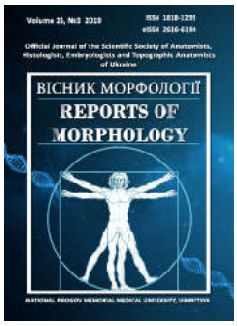

Histological features of the mitral valve in norm and opioid exposure in experiment

Mateshuk-Vatseba L.R.[1], Symivska R.R.[1], Belik N.V.[2], Piliponova V.V.[2]

[1]Lviv National Medical University named after Danylo Halytskyi, Lviv, Ukraine
[2]National Pirogov Memorial Medical University, Vinnytsya, Ukraine

ARTICLE INFO
Received: 30 June, 2019
Accepted: 5 August, 2019

UDC: 611.12.126-018:615.212.7]-08

CORRESPONDING AUTHOR
e-mail: lvatseba@gmail.com
Mateshuk-Vatseba L.R.

To date, pathology of the cardiovascular system is the most common, tends to increase, most often leads to disability and mortality of the population at a young working age and is an important medical and social problem. The purpose of the study was to establish the features of micro organization of the mitral valve in white rat in norm and after opioid action. The study material is presented by histological samples of a mitral valve of the white rat. The study was performed on 30 adult white reproductive age rats weighing 160-220 g. The experimental animals were injected intramuscularly 1 time per day for the same period of 42 days (6 weeks) with the opioid drug analgesic "Nalbuphine". Using histological methods, 30 mitral valves of white rat were examined. Microscopy of histological preparations of the valves of the heart was performed sequentially, assessing the morphological changes in the norm and under the action of the opioid after 6 weeks of the experiment. Emphasis was placed on the presence or absence of endothelial layer, as well as the condition of endothelial cells in normal and at the action of the damaging factor, determining the signs of their dystrophy, desquamation and proliferation. It is established that the normal mitral valve is represented by endocardial folds. The rat endocardium consists of three layers: endothelial (endothelial cells rich layer, attached to the basement membrane), subendothelial (connective tissue rich in fibroblasts) and a muscular-elastic layer (represented by smooth myocytes, plaited collagen fibers). After 6 weeks of administration of Nalbuphine, the mitral valve is in a stage of decompensation, when the outer and inner endothelial layers are destroyed, the endothelial cells are deformed, the subendothelial layer is represented by single bundles of different directions. In the musculo-elastic layer, contact between smooth myocytes and fragmented and thinned, collagen and elastic fibers is lost. This study allows us to conclude on the destructive effect of opioid agents on the valvular apparatus of the heart.

Keywords: *mitral valve, histology, opioid, white rat, norm.*

Introduction

This article presents and analyzes data from studies conducted on white rats of reproductive age. Despite the fact that the average life expectancy in modern society is increasing significantly due to the development of experimental and clinical medicine, cardiovascular diseases have become the leading cause of death in the world over the last 10 years, accounting for 30% of all cases and 45% of all non-communicable causes of death. [1-5, 8]. According to WHO, about 90% of all diseases are associated with pain, and patients with chronic pain are five times more likely to seek medical treatment, compared with the general population [21]. One of the issues remains the use of opioids in clinical practice, in particular for the treatment of postoperative and chronic pain [14, 22, 24, 25]. According to epidemiological studies, the prevalence of chronic pain syndromes is at least 40% of the adult population and these figures tend to increase steadily [7, 10, 20, 21]. A systematic analysis of original studies of the prevalence of symptoms in patients at the terminal stage of the disease, found that 35-96% of cancer patients, 63-80% of patients with AIDS, 41-77% of patients with cardiovascular disease, 34-77% of patients with chronic obstructive pulmonary diseases and 45-70% with kidney diseases - have a pronounced pain syndrome [19]. There is an increasing trend in the world of opioid use, which contributes to the improvement of somatic, visceral and

neuropathic pain. Not infrequently, the opioid arsenal and physicians' knowledge is limited by the use of morphine, which for a long time has been the "gold standard", the most common drug in its group. According to research, there are significant differences in the amount of morphine consumed by high-income countries compared to middle- and low-income countries [11]. For example, the International Narcotics Control Committee (INCC) reports that about 92% of the worldwide use of morphine is consumed in countries with only 17% of the world's population (US, Canada, Western Europe, Australia and New Zealand). About 75% of the world's population in more than 100 countries do not have or have insufficient access to proper treatment for severe pain [12]. However, the biggest problem with using morphine is the lack of a "marginal effect" and linear dose-response. That is why, at the moment, it is important to find alternative methods of analgesia and to study their effects on the human body.

The purpose of the study is to determine the features of the micro organization of mitral valve white rat in norm and after opioid.

Materials and methods

The study material is represented by mitral valve histological samples of the white rat. The study was performed on 30 adult white reproductive rats weighing 160-220 g. The experimental animals were divided into 3 series of 10 animals. In the first series the features of angioarchitectonics of the valves of white rats were normal, in the second series the dynamics of qualitative and quantitative structural changes of the valves against the background of prolonged exposure to opioids in the experiment after 6 weeks, the third series served as a control. Experimental animals were injected intramuscularly 1 time per day for the same period of time for 42 days (6 weeks) by the opioid drug analgesic "Nalbuphine". Each week, the dose of the drug for injection was increased in sequence: 1st week - 8 mg/kg, 2nd week - 15 mg/kg, 3rd week - 20 mg/kg, 4th week - 25 mg/kg, 5th week - 30 mg/kg, 6th week - 35 mg/kg [16]. Animals were withdrawn from the experiment 6 weeks after opioid administration. The sampling of rat heart valves was performed after euthanasia by intraperitoneal anesthesia overdose using sodium thiopental (calculated at 25 mg/kg body weight).

All experimental animals were kept in the vivarium of Lviv National Medical University named after Danylo Halytskyi. The studies were conducted in accordance with the provisions of the European Convention for the Protection of Vertebrate Animals Used for Experimental and Other Scientific Purposes (Strasbourg, 1986), Council of Europe Directives 86/609/EEC (1986), Law of Ukraine No.3447-IV, on the "Protection of Animals from Cruelty behavior", the general ethical principles of animal experimentation, approved by the First National Congress of Ukraine on Bioethics (2001).

Images from histological specimens of the mitral valve on a computer monitor were taken from a MICROmed SEO SSCAN microscope and using a Vision CCD Camera. The studies were performed at certain times of the experiment in preparations stained with hematoxylin-eosin.

Results

Mitral valve consists of two leaflets. Histologically, the left atrioventricular valve is represented by endocardial folds (Fig. 1). The endocardium of the mitral valve consists of 3 layers. Internal and external - endothelial - in the form of a layer of flat polygonal shape, elongated cells with irregular wavy edges. On the inner surface (facing the ventricle cavity), the endothelial cells contain many microvilli. On the outer surface of the valves (facing the atrial cavity), the endothelial cells are located much further apart from the layer of the inner endothelium. The subendothelial layer is represented by a fibroblast-rich connective tissue. As a part of this connective tissue base there are superficial fibrous and deep spongy layers. The superficial fibrous layer is a dense connective tissue with a small number of cells, thick bundles of collagen fibers oriented in different directions, which provides durability under various factors. Collagen fiber bundles are delimited by thin layers of the basic substance, fibrocyte bodies, and single elastic fibers. The thin collagen fibers of the endocardium gradually move into the fibrous plate of the valve leaf, and at the place of attachment of the mitral and tricuspid valves into fibrous rings. The deep spongy layer is a loose connective tissue rich in cells. The musculoelastic layer is represented by smooth myocytes, braided collagen fibers with fibroblasts and large number of elastic fibers.

At the base of the valves, the endocardium is separated from the myocardium by a connective tissue base containing thick elastic, collagen and reticular fibers. Blood vessels and nerves are placed between them. The atrial side of the valves has a smooth surface. The endothelial layer is more pronounced and denser than the ventricular side. The

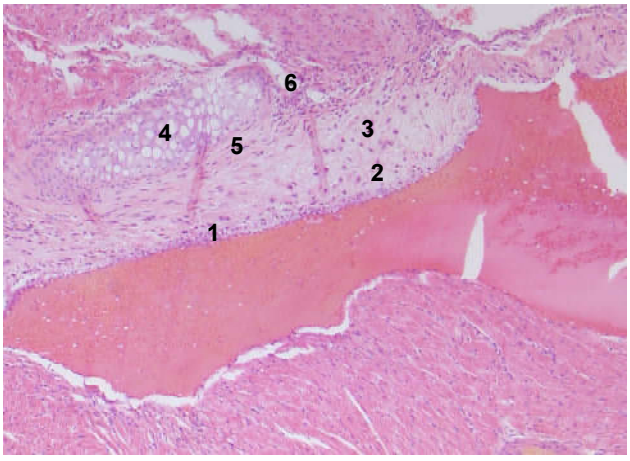

Fig. 1. White rat mitral valve base endocardium. 1 - endothelial cells on the basement membrane; 2 - tufts of collagen fibers; 3 - fibroblast bodies; 4 - fibrous ring; 5 - nuclei of smooth muscle cells; 6 - blood capillaries. Hematoxylin-eosin staining. x200.

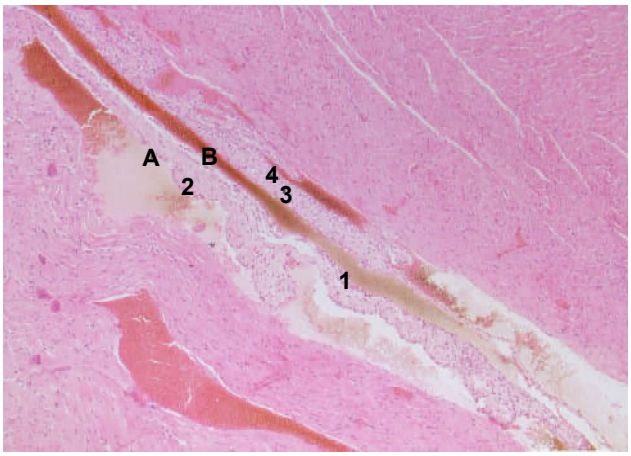

Fig. 2. A - atrial side of leaflets of valve; B - ventricle side leaflets of valve; 1 - layer of endothelial cells on the basement membrane; 2 - tufts of collagen fibers; 3 - elastic fibers; 4 - nuclei of connective tissue cells. Hematoxylin-eosin staining. x200.

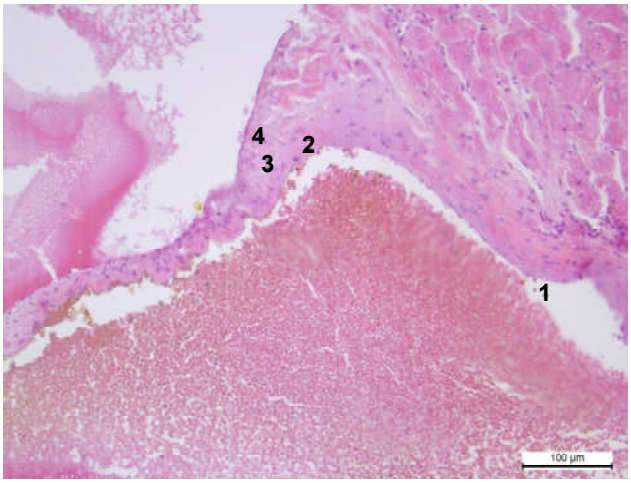

Fig. 3. White rat mitral valve base endocardium, week 6 of the experiment. 1 - detachment of endothelial cells in the lumen of the right ventricle; 2 - single endothelial cells on a thinned basal membrane; 3 - fragmented collagen fibers; 4 - single bodies of fibroblasts. Hematoxylin-eosin staining. x100.

ventricular side has an uneven surface because of the outgrowths from which the tendon filaments begin. In this area, only a few elastic fibers are located below the endothelium (Fig. 2).

After 6 weeks of nalbuphine administration, deep destructive changes are observed: in the inner layer, the endothelial cells are not attached to the basement membrane, irregularly shaped and without processes. The single endothelial cells remaining on the basement membrane lost their polygonal shape and connections. In the outer layer, single, irregularly shaped endothelial cells attach to a thin basal membrane and form valve structures with each other or lose contact with it. In the subendothelial layer there is a small amount of multidirectional collagen fibers, a large amount of basic substance and fibrocytes. Fibroblasts are presented in small numbers. Collagen fiber bundles have become thinner and more fragmented. In the musculoelastic layer, contact between smooth myocytes, thin bundles of collagen and elastic fibers was lost. The gaps between the structural components are taken up by the basic substance. A small amount of collagen fibers and fibroblasts are located between the main substance (Fig. 3).

Discussion

Depending on the extracardiac and intracardiac factors, a number of studies by both morphologists-experimenters and clinicians have been devoted to the study of the adaptive capacity of the injured heart [23]. It should also be noted that in recent years, morphometric methods have been widely used in biomedical research, which allow to study qualitative and quantitative patterns of physiological and pathological processes, to adequately objectify and logically interpret them [6, 13]. However, there are almost no studies that would comprehensively study heart valves at all levels of structural organization and under the conditions of action on the body of opioids. The relevance of this work is that the microscopy of histological preparations of the heart valves was performed sequentially, evaluating the morphological changes in normal and opioid exposure after 6 weeks of the experiment. Emphasis was placed on the presence or absence of endothelial layer, as well as the condition of endothelial cells in normal and at the action of the damaging factor, determining the signs of their dystrophy, desquamation and proliferation. There is sufficient information in the literature regarding the effects of opioid agents on the sense organs [17], the skin [15], and etc. There are experimental works describing the decompensation of the hemomicrocirculatory bed with prolonged exposure to opioids, when the capillary component is destroyed, arterioles are twisted and deformed, venules are enlarged [18]. Fundamental is the work to formulate a list of macro- and microscopic changes in heart valve structures that are characteristic of acquired heart defects of inflammatory and non-inflammatory genesis, and morphological groups that are typical only of rheumatic heart disease, infectious endocarditis, and acquired heart defects of non-inflammatory nature [9]. The novelty of this study is that there are no data on the effect of opioid agents on cardiac function, namely the morphological changes of the valvular apparatus under the influence of opioids, some studies are observational and the findings are insufficiently substantiated.

The prospect of further research in this direction is related to the further study of the histological organization of the valvular apparatus of the heart under the action of opioid agents.

Conclusions

1. In the norm, the mitral valve rat is represented by the folds of the endocardium, consisting of three layers: endothelial, subendothelial and musculoelastic.

2. After six weeks of administration of nalbuphine, mitral valve is in the stage of decompensation - the outer and

inner endothelial layers are destroyed, the endothelial cells are deformed, the subendothelial layer is represented by single bundles of multidirectional and destroyed collagen fibers. In the musculoelastic layer, contact between smooth myocytes and fragmented and thinned collagen and elastic fibers is lost.

References

[1] Abdulkareem, N., Smelt, J., & Jahangiri, M. (2013). Bicuspid aortic valve aortopathy: genetics, pathophysiology and medical therapy. *Interactive Cardiovascular and Thoracic Surgery,* 17(3), 554-559. doi: 10.1093/icvts/ivt196

[2] Akyüz, A. R., & Kul, S. (2015). Bicuspid aortic valve and extremely elongated chordae tendineae protruding into the left ventricular outflow tract. *Anadulu Kardiyoloji Dergisi: AKD*, 15(5), E14. doi: 10.5152/akd.2015.6090

[3] Alegret, J. M., Martinez-Micaelo, N., Aragonés, G., & Beltrán-Debón, R. (2016). Circulating endothelial microparticles are elevated in bicuspid aortic valve disease and related to aortic dilation. *International Journal of Cardiology,* 217, 35-41. doi: 10.1016/j.ijcard.2016.04.184

[4] Alegret, J. M., Masana, L., Martinez-Micaelo, N., Heras, M., & Beltrán-Debón, R. (2015). LDL cholesterol and apolipoprotein B are associated with ascending aorta dilatation in bicuspid aortic valve patients. *QJM: An International Journal of Medicine,* 108(10), 795-801. doi: 10.1093/qjmed/hcv032

[5] Björck, H. M., Du, L., Pulignani, S., Paloschi, V., Lundströmer, K., Kostina, A. S., ... & Teixidó-Tura, G. (2018). Altered DNA methylation indicates an oscillatory flow mediated epithelial-to-mesenchymal transition signature in ascending aorta of patients with bicuspid aortic valve. *Scientific Reports*, 8(1), 1-15. doi: 10.1038/s41598-018-20642-4

[6] Cameli, M., Lisi, M., Righini, F. M., & Mondillo, S. (2012). Novel echocardiographic techniques to assess left atrial size, anatomy and function. *Cardiovascular Ultrasound,* 10(1), 10-14. doi: 10.1186/1476-7120-10-4

[7] Emonet, S., Wuillemin, T., Harbarth, S., Wassilew, N., Cikirikcioglu, M., Schrenzel, J. ... Van Delden, C. (2015). Relapse of Tropheryma whipplei endocarditis treated by trimethoprim/sulfamethoxazole, cured by hydroxychloroquine plus doxycycline. *International Journal of Infectious Diseases,* 30, 17-19. doi: 10.1016/j.ijid.2014.11.003

[8] Endo, M., Nabuchi, A., Okuyama, H., Muto, Y., Hiranuma, S., Miyazaki, T. ... Hashimoto, O. (2015). Differing relationship between hypercholesterolemia and a bicuspid aortic valve according to the presence of aortic valve stenosis or aortic valve regurgitation. *General Thoracic and Cardiovascular Surgery,* 63(9), 502-506. doi: 10.1007/s11748-015-0561-8

[9] Fedoniuk, L. Ya. (2008). *Structural organization of changes of the valve Apparatus at Acquired Heart Defects* (Doctoral dissertation). https://otherreferats.allbest.ru/medicine/00603084_0.html

[10] Gear, R. W., Gordon, N. C., Hossaini-Zadeh, M., Lee, J. S., Miaskowski, C., Paul, S. M., & Levine, J. D. (2008). A subanalgesic dose of morphine eliminates nalbuphine anti-analgesia in postoperative pain. *The Journal of Pain,* 9(4), 337-341. doi: 10.1016/j.jpain.2007.11.011

[11] Gilson, A. M., Maurer, M. A., Ryan, K. M., Rathouz, P. J., & Cleary, J. F. (2013). Using a morphine equivalence metric to quantify opioid consumption: examining the capacity to provide effective treatment of debilitating pain at the global, regional, and country levels. *Journal of Pain and Symptom Management,* 45(4), 681-700. doi: 10.1016/j.jpainsymman.2012.03.011

[12] International Narcotics Control Board. (2011). Report of the International Narcotics Control Board on the availability of internationally controlled drugs: ensuring adequate access for medical and scientific purposes. UN.

[13] Kovalenko, V. M., Nesukai, O. G., Polenova, N. S. (2012). Three-dimensional echocardiography: a technique and a role in the study of the structure and function of the heart valves. *Heart Failure*, (3), 7-13.

[14] Kshirsagar, S., Gear, R., Levine, J., & Verotta, D. (2008). A mechanistic model for the sex-specific response to nalbuphine and naloxone in postoperative pain. *Journal of Pharmacokinetics and Pharmacodynamics,* 35(1), 69-83. doi: 10.1007/s10928-007-9076-y

[15] Mateshuk-Vatseba, L. R., Bekesevych, A. M., Diskovskyi, I. S., Zinko, A. V., Pidvalna, U. E., & Popyk, P. M. (2015). Patterns of structural changes in the links of the hemomicrocirculatory bed of organs under the conditions of opioid exposure in the experiment. T*opical Issues of Medical Science and Practice,* 82, 16(1), 328-335.

[16] Onysko, P. M., Paltov, E. V., & Fik, V. B. (2012). Method for modeling physical opioid dependence in rats. Patent, Ukraine №76564U

[17] Pidvalna, U. E. (2014). Structural organization of organs and systems under the influence of opioids. *Experimental and clinical physiology and biochemistry,* (1), 65, 71-78.

[18] Savchenko, S. V. (2012). Actual issues of expert assessment of heart morphology. Bulletin of Forensic Medicine, 1(3), 5-8.

[19] Solano, J. P., Gomes, B., & Higginson, I. J. (2006). A comparison of symptom prevalence in far advanced cancer, AIDS, heart disease, chronic obstructive pulmonary disease and renal disease. *Journal of Pain and Symptom Management,* 31(1), 58-69. doi: 10.1016/j.jpainsymman.2005.06.007

[20] Stevens, S. M., & Doty, J. R. (2017). New evidence on old drugs; warfarin versus aspirin after bioprosthetic aortic valve placement. *Thrombosis Research,* 150, 102. doi: 10.1016/j.thromres.2016.12.015

[21] Toyama, S., Tagaito, Y., & Shimoyama, M. (2016). Patient-controlled epidural analgesia for labour in a patient after Ross procedure for congenital bicuspid aortic valve. *Journal of Obstetrics and Gynaecology,* 36(8), 1010-1011. doi: 10.1080/01443615.2016.1234441

[22] Voronkov, M., Ocheret, D., Bondarenko, S., & Ivanov, Y. (2008). Administration of nalbuphine to heroin addicts. Feasibility and short-term effects. *Heroin Addiction and Related Clinical Problems,* 10(1), 19-24.

[23] Yasinovskyi, O. B. (2015). *Remodeling of chambers and vascular bed during intoxication with cadmium and aluminum salts* (PhD thesis). http://www.irbis-nbuv.gov.ua

[24] Yeh, Y. C., Lin, T. F., Chang, H. C., Chan, W. S., Wang, Y. P., Lin, C. J., & Sun, W. Z. (2009). Combination of low-dose nalbuphine and morphine in patient-controlled analgesia decreases incidence of opioid-related side effects. *Journal of the Formosan Medical Association,* 108(7), 548-553. doi: 10.1016/S0929-6646(09)60372-7

[25] Yeh, Y. C., Lin, T. F., Lin, F. S., Wang, Y. P., Lin, C. J., & Sun, W. Z. (2008). Combination of opioid agonist and agonist-antagonist: patient-controlled analgesia requirement and adverse events among different-ratio morphine and Nalbuphine admixtures for postoperative pain. *British Journal of Anaesthesia*, 101(4), 542-548. doi: 10.1093/bja/aen213

ГІСТОЛОГІЧНІ ОСОБЛИВОСТІ ДВОСТУЛКОВОГО КЛАПАНА СЕРЦЯ В НОРМІ ТА ПРИ ДІЇ ОПІОЇДУ В ЕКСПЕРИМЕНТІ

Матешук-Вацеба Л.Р., Симівська Р.Р., Белік Н.В., Піліпонова В.В.

На сьогоднішній день патологія серцево-судинної системи є найбільш розповсюдженою, має тенденцію до збільшення, найчастіше призводить до інвалідності та смертності населення у молодому працездатному віці та є важливою медичною і соціальною проблемою. Мета дослідження - встановлення особливостей мікроорганізації двостулкового клапана серця білого щура в нормі та за умови дії опіоїду. Матеріал дослідження представлений гістопрепаратами двостулкового клапана серця білого щура. Дослідження виконано на 30 статевозрілих білих щурах репродуктивного віку масою 160-220 г. Експериментальним тваринам вводили внутрішньом'язово 1 раз на добу в однаковий проміжок часу протягом 42 днів (6 тижнів) опіоїдний наркотичний анальгетик "Налбуфін". За допомогою гістологічних методів були вивчені 30 двостулкових клапанів білого щура. Мікроскопію гістологічних препаратів клапанів серця проводили послідовно, оцінюючи їх морфологію в нормі та при дії опіоїду через 6 тижнів експерименту. Акцентували увагу на присутність чи відсутність ендотеліального шару, а також стан ендотеліоцитів у нормі та при дії пошкоджуючого фактора, визначаючи ознаки їх дистрофії, десквамації та проліферації. Встановлено, що, зазвичай, двостулковий клапан серця щура представлений складками ендокарда. Ендокард щура складається з трьох шарів: ендотеліального (багатого ендотеліоцитами прикріпленими до базальної мембрани), підендотеліального (сполучна тканина, котра багата на фібробласти) та м'язово-еластичного шару (представлений гладкими міоцитами, обплетеними пучками колагенових та еластичних волокон). Двостулковий клапан серця після 6-тижневого введення налбуфіну знаходиться на стадії декомпенсації, коли зовнішній та внутрішній ендотеліальні шари зруйновані, ендотеліоцити деформовані, підендотеліальний шар представлений поодинокими пучками різнонапрямлених та знищених колагенових волокон, невеликою кількістю клітин, які розміщені між основною речовиною. У м'язово-еластичному шарі втрачається контакт між гладкими міоцитами та фрагментованими і стоншеними колагеновими й еластичними волокнами. Дане дослідження дозволяє зробити висновки щодо деструктивного впливу опіоїдних складових на клапанний апарат серця.

Ключові слова: *двостулковий клапан, гістологія, опіоїд, білий щур, норма.*

ГИСТОЛОГИЧЕСКИЕ ОСОБЕННОСТИ ДВУСТВОРЧАТОГО КЛАПАНА СЕРДЦА В НОРМЕ И ПРИ ВОЗДЕЙСТВИИ ОПИОИДА В ЭКСПЕРИМЕНТЕ

Матешук-Вацеба Л.Р., Симивська Р.Р., Белик Н.В., Пилипонова В.В.

На сегодняшний день патология сердечно-сосудистой системы является наиболее распространенной, имеет тенденцию к росту, зачастую приводит к инвалидности и смертности населения в молодом трудоспособном возрасте и является важной медицинской и социальной проблемой. Цель исследования - установление особенностей микроорганизации двустворчатого клапана сердца белой крысы в норме и при воздействии опиоида. Материал исследования представлен гистопрепаратами двустворчатого клапана сердца белой крысы. Исследование выполнено на 30 половозрелых белых крысах репродуктивного возраста массой 160-220 г. Экспериментальным животным вводили внутримышечно 1 раз в сутки в одинаковый промежуток времени в течение 42 дней (6 недель) опиоидный наркотический анальгетик "Налбуфин". С помощью гистологических методов были изучены 30 двустворчатых клапанов белой крысы. Микроскопию гистологических препаратов клапанов сердца проводили последовательно, оценивая их морфологию в норме и при воздействии опиоида через 6 недель эксперимента. Акцентировали внимание на присутствие или отсутствие эндотелиального слоя, а также состояние эндотелиоцитов в норме и при воздействии повреждающего фактора, определяя признаки их дистрофии, десквамации и пролиферации. Установлено, что в норме двустворчатый клапан сердца крысы представлен складками эндокарда. Эндокард крысы состоит из трех слоев: эндотелиального (богатого эндотелиоцитами, прикрепленными к базальной мембране), подэндотелиального (соединительная ткань, которая богата фибробластами), и мышечно-эластического слоя (представлен гладкими миоцитами, оплетенными пучками коллагеновых и эластических волокон). Двустворчатый клапан сердца после 6-недельного введения налбуфина находится на стадии декомпенсации, когда внешний и внутренний эндотелиальные слои разрушены, эндотелиоциты деформированы, подэндотелиальный слой представлен единичными пучками разнонаправленных и уничтоженных коллагеновых волокон, небольшим количеством клеток, расположенных между основным веществом. В мышечно-эластичном слое теряется контакт между гладкими миоцитами и фрагментированными и истонченными коллагеновыми и эластическими волокнами. Данное исследование позволяет сделать выводы относительно деструктивного влияния опиоидных составляющих на клапанный аппарат сердца.

Ключевые слова: *двустворчатый клапан, гистология, опиоид, белая крыса, норма.*

DOI: 10.31393/morphology-journal-2019-25(3)-08 Reports of Morphology, Vol. 25, №3, Pages 45-51

ISSN 1818-1295 eISSN 2616-6194

REPORTS OF MORPHOLOGY

Official Journal of the Scientific Society of Anatomists, Histologists, Embryologists and Topographic Anatomists of Ukraine

journal homepage: https://morphology-journal.com

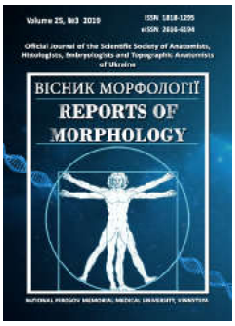

Histostructural organization of the cerebellum of human fetuses for 8-9 weeks of prenatal development

Zalevskiy L.L., Shkolnikov V.S., Prykhodko S.O.
National Pirogov Memorial Medical University, Vinnytsya, Ukraine

ARTICLE INFO
Received: 8 July, 2019
Accepted: 7 August, 2019

UDC: 611.817.1:616.8-091.94:618.231

CORRESPONDING AUTHOR
e-mail: med2@vnmu.edu.ua
Shkolnikov V.S.

The high incidence of anomalies in the hindbrain is due to the fact that neurulation in the cranial compartment lasts the longest time. Therefore, for more detailed study of embryogenesis and understanding of mechanisms of pathogenesis, occurrence of congenital malformations, there is a need to determine the morphometric (histometric) parameters of the cerebellum at different gestational times. The purpose of the study is to determine the morphometric parameters of the cerebellum of human embryos for 8-9 weeks of prenatal development, as well as features of cytoarchitectonics of its structures, which is inherent in the given gestation period. Anatomo-histological, immunohistochemical and morphometric examination of the cerebellum of 10 human embryos was performed. Serial sections of cerebellum preparations 8-10 microns thick were stained with hematoxylin, eosin, toluidine blue and Van Gieson, and diagnostic monoclonal antibodies of "DacoCytomation" (Denmark): Vimentin, Ki-67 and Synaptophysin were used for immunohistochemical studies. The results of measurements of the total thickness of all layers, the density of neural stem cells (NSC), as well as the area of the right and left hemispheres of the cerebellum were obtained during the study. In immunohistochemical study, we determined the direction of NSC migration and cell proliferation of all layers of the cerebellum, as well as the length of radial glia fibers. In the cerebral hemispheres of embryos of 8-9 weeks there is a clear division into ventricular, intermediate, molecular and outer granular layers. The highest density of neural stem cells was observed in the outer granular layer - 151.0±4.1 cells per 0.01 mm^2. The lowest cell density was observed in the molecular layer - 22.0±0.8 cells per 0.01 mm^2. The most intense cell proliferation was established in the ventricular layer and the outer granular layer of the cerebellum, and the least intense in the intermediate layer. Synaptophysin expression was only slightly expressed in the ventricular layer of the cerebellum. The radial glial fibers begin from the ventricular layer and penetrate all layers of the cerebellum, ending in the outer granular layer. The average length of radial glial fibers was: short - 120.8±5.7 μm, long - 195.3±9.4 μm. The exterior granular layer is represented by spherical undifferentiated cells with an average area size of 641.1±28.9 μm^2, the molecular layer - NSC with an area of 472.9±23.7 μm^2, the intermediate layer - NSC with an area of 492.2±23.1 μm^2, and the ventricular layer is represented by neuroblasts with an area of 436.1±21.8 μm^2. Thus, it is established that there is a clear division of the cerebellum layers into the ventricular layer, which is represented by neuroblasts, the intermediate layer - NSC, the molecular layer - NSC, and the outer granular layer is represented by undifferentiated cells; the densest neural stem cells are located in the outer granular layer and less densely in the molecular layer.

Key words: *cerebellum, morphometric parameters, radial glia, prenatal development.*

Introduction

Anatomic and physiological integration is evaluated as a unit of a functional system that unites in one adaptive reaction each specific case and the dynamics of nervous processes. In particular, the fetus is characterized by the acceleration and selective development of those structures of the central nervous system (CNS), as well as those functions that will be required for the newborn in order to exercise the basic types of vital activity [4, 9, 19].

The process of nerve tube formation begins from 22-23 days and ends between 25-27 days. It is known that

abnormalities in the development of the CNS result from the influence of environmental and genetic factors, but the mechanisms of pathogenesis of embryonic abnormalities of human brain development are still unknown [2, 7, 13].

Disruption of CNS formation and localization of malformation in early gestation depends on the timing and arrest of the stages of neurulation. The high incidence of anomalies of the spinal, medulla, and hindbrain is due to the fact that neurulation in the cranial compartment lasts the longest period of time. During the closure of the medullary rollers, the basis of the driving factor of morphogenesis is the intercellular interaction, which determines the formation of the brain and in violation of which irreversible abnormalities of the CNS develop [10, 14, 17, 23].

The human brain develops from tubular structures, but the morphological organization is very complex. During prenatal development, structural changes occur in the brain and the basic elements of the definitive brain are formed. At various stages of prenatal development, a detailed topographic-histological examination of the human brain will not only help in understanding the highly ordered process of its structure, but also help to identify developmental defects that are related to genetic or environmental factors [5, 8, 11, 15, 18, 22].

Thus, a detailed study of the cerebellum of the fetus and human embryos in different periods of prenatal development makes it possible to establish certain patterns of restructuring of its structure.

The purpose of the study is to determine the morphometric parameters of the cerebellum of human embryos for 8-9 weeks of prenatal development, as well as features of cytoarchitectonics of its structures, which is inherent in the given gestation period.

Materials and methods

The work is a fragment of the planned scientific work of the Department of Human Anatomy, National Pirogov Memorial Medical University, Vinnytsya "Determination of morphological changes of the central nervous system of a person during the prenatal period of ontogeny (macroscopic, histological, morphometric, immunohistochemical study)", state registration № 0118U001043.

Anatomic-histological, immunohistochemical and morphometric examination of the cerebellum of 10 human embryos was performed for 8-9 weeks. The parietal-coccygeal length was 34.0±1.7 mm, the mass was 5.0±0.7 g. The materials were obtained as a result of a late abortion at the Vinnitsa Regional Pathological Office. Defects of the CNS development in this period were absent. The fixation of the preparations of the cerebellum was performed according to own technique [20].

Subsequently, serial sections of cerebellar preparations 8-10 μm thick were made, stained with hematoxylin, eosin, toluidine blue and Van Gieson. Diagnostic monoclonal antibodies from "DacoCytomation" (Denmark) were used in immunohistochemical studies: Vimentin, Ki-67 and Synaptophysin. Ki-67 was used to evaluate the proliferative activity of neural stem cells (NSC), Vimentin - to investigate the morphology of radial glia and Synaptophysin - to evaluate the myelination of the fibers of the leading pathways and to establish their connections.

SIGETA and MBS-10 light microscope was used for morphometric examination. Magnification x4, x10, x20, x40 and x100 were used. Photographs and morphometry of the obtained sections were performed using an ETREK Ucmos camera and a ToupView computer program (computer histometry).

Statistical processing of digital data was carried out using the standard software package "Statistica 6.0" by Statsoft (license number BXXR901E246122FA).

Results

In the course of the study we obtained the following morphometric parameters of the structures of the cerebellum: the total thickness of all layers of the right cerebellum hemisphere was 1675±79 μm, the externally granular layer - 28.20±1.20 μm, the molecular layer - 20.62±1.02 μm, the intermediate layer - 1590±74 μm, ventricular layer - 36.30±1.70 μm.

In the study of the thickness of all layers of the left cerebellum hemisphere, the following data were obtained - 1643±76 μm, externally granular layer - 28.00±1.20 μm, molecular layer - 20.10±1.00 μm, intermediate layer - 1559±75 μm, ventricular layer - 36.20±1.80 μm (Fig. 1). The greatest thickness was observed in the intermediate layer, whereas the molecular layer had the lowest thickness (Fig. 2).

The density of NSCs in the ventricular layer of all structures of both hemispheres was 134.0±3.9 cells per 0.01 mm^2. In the outer granular layer (neurons and gliocytes) - 151.0±4.1 cells per 0.01 mm^2. In the intermediate layer - 74.00±3.00 cells per 0.01 mm^2. The lowest cell density was visualized in the molecular layer - 22.00±0.80 cells per 0.01 mm^2. Thus, we found that the lowest cell density was observed in the molecular layer - 22.00±0.70 cells per 0.01 mm^2, whereas the highest cell density was observed in the outer granular layer - 151.0±4.2 cells per 0.01 mm^2 (Fig. 3).

In the outer granular layer are represented by spherical undifferentiated cells with an area of 641.1±28.9 $μm^2$, the molecular layer is represented by NSC area of 472.9± 23.7 $μm^2$, the intermediate layer of NSC 492.2±23.1 $μm^2$, the ventricular layer is represented by neuroblasts with an area of 436.1±21.8 $μm^2$.

At 8-9 weeks of gestation NSC migration takes place in the radial direction and the externally granular layer tangentially.

Cell proliferation occurs more intensively in the ventricular layer, as well as in the outer granular layer of the cerebellum, less intensively in the intermediate layer (Fig. 4).

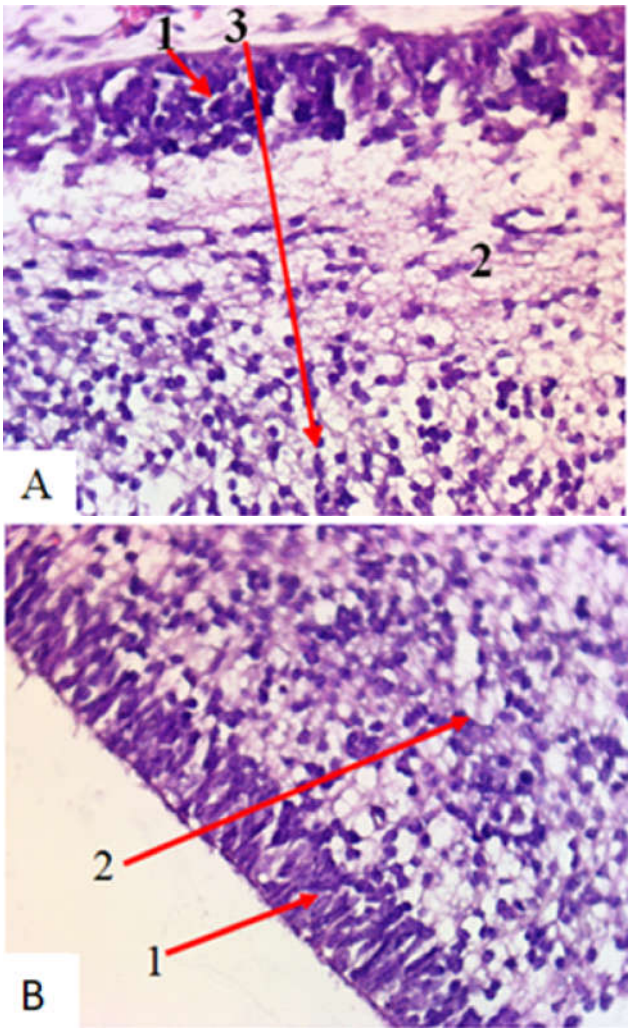

Fig. 1. Human fetal cerebellum at 8-9 weeks. A - horizontal cross-section of the cerebellum: 1 - outer granular layer, 2 - molecular layer, 3 - intermediate layer. Hematoxylin-eosin; x400. B - horizontal section of the cerebellum: 1 - ventricular layer, 2 - intermediate layer. Hematoxylin-eosin, x400.

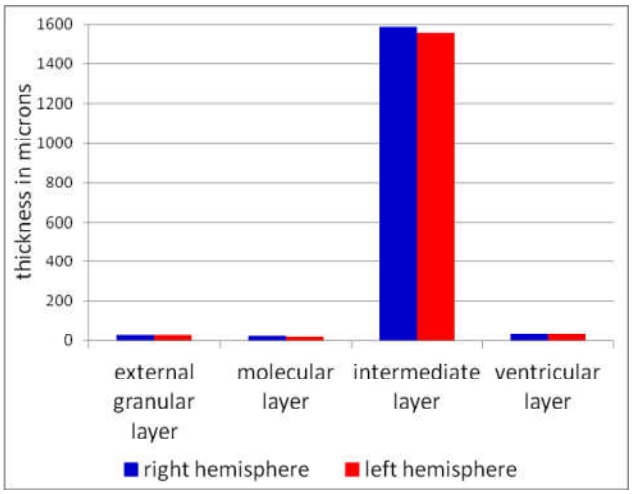

Fig. 2. The thickness of the layers of the cerebellum of an 8-9 weeks human embryo.

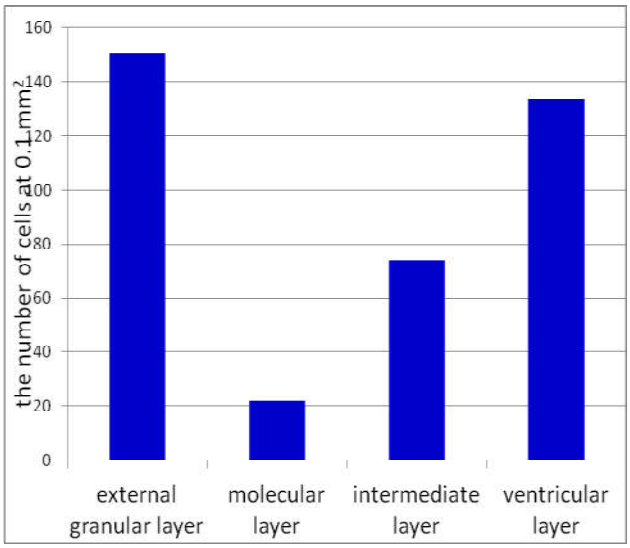

Fig. 3. The density of NSC in the layers of the cerebellum of 8-9 weeks human embryo.

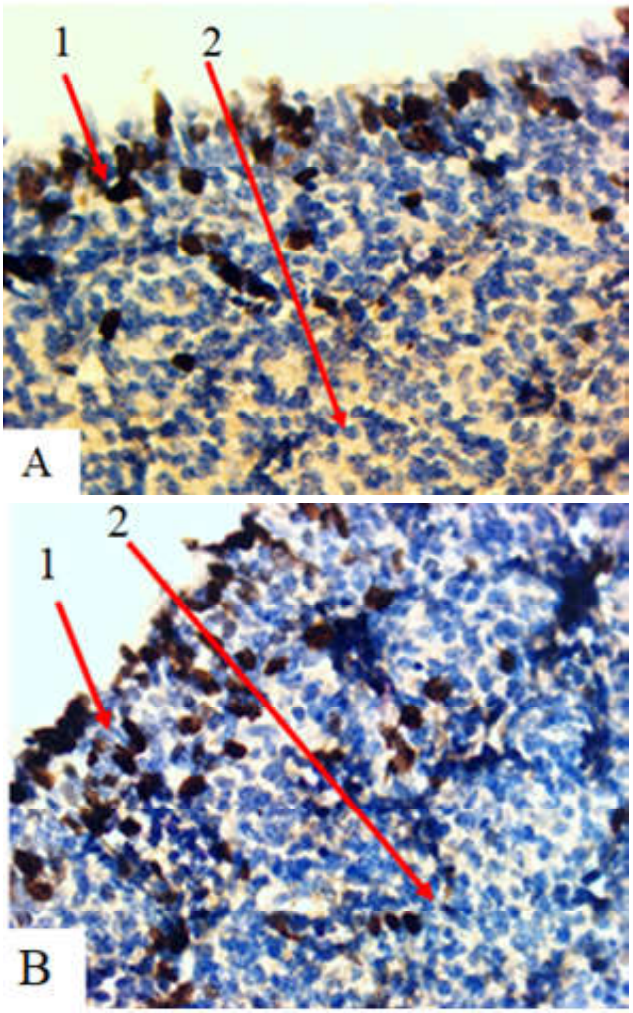

Fig. 4. Proliferation in cerebellar hemispheres at 8-9 weeks. A: 1 - ventricular layer, 2 - intermediate layer. Ki-67, x400. B: 1 - outer granular layer, 2 - intermediate layer. Ki-67, x400.

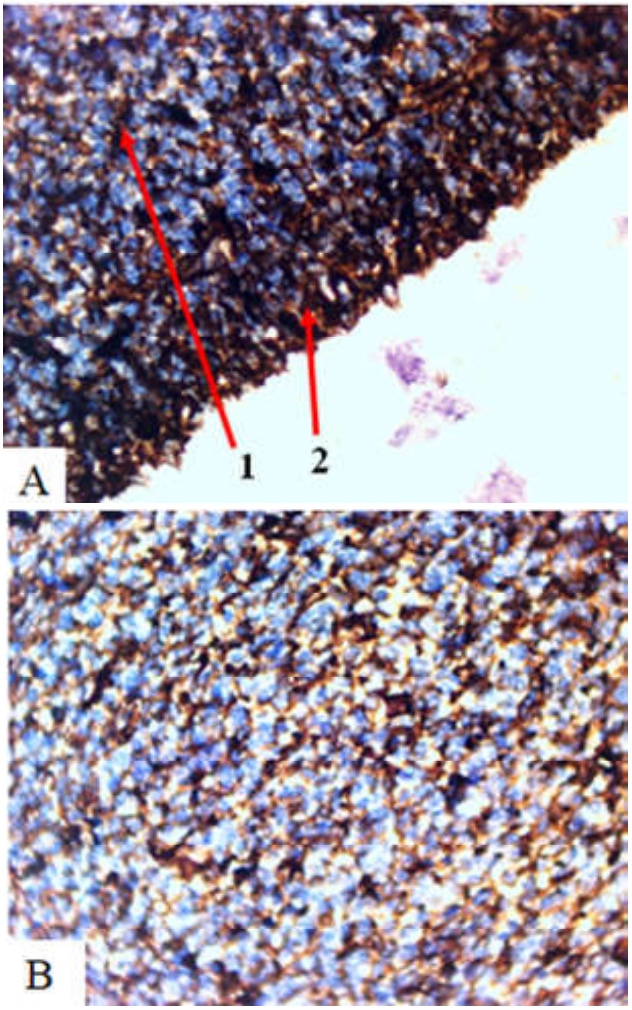

Fig. 5. Horizontal slice of the cerebellum. A: 1 - intermediate layer, 2 - ventricular layer. Vimentin; x400. B - intermediate layer. Vimentin; x400.

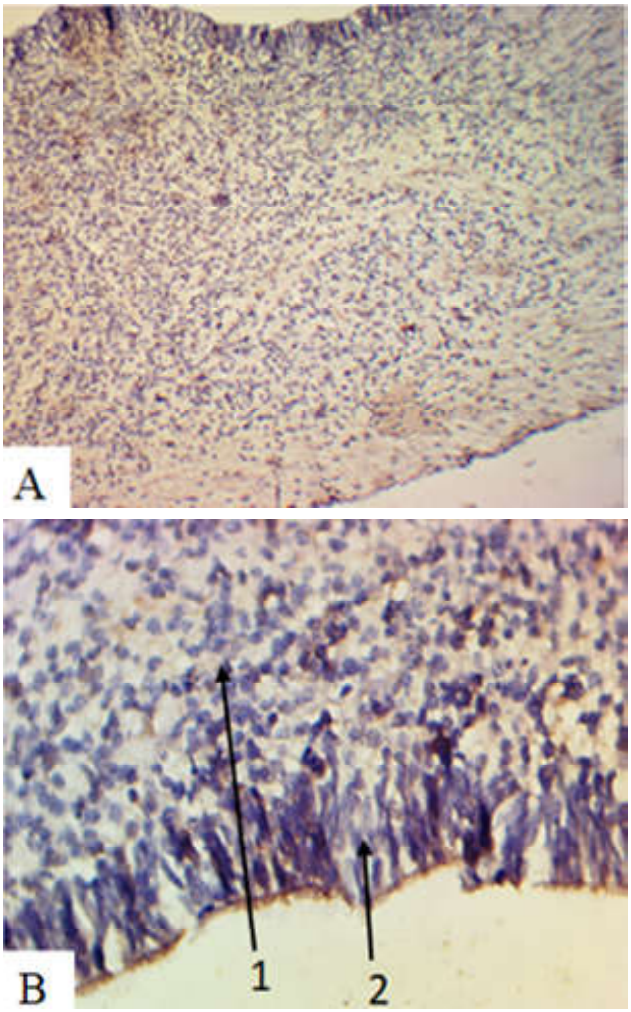

Fig. 6. Horizontal slice of cerebral hemispheres. A: Synaptophysin; x100. B: 1 - ventricular layer, 2 - intermediate layer. Synaptophysin, x400.

We have found that when using Vimentin, radial glial fibers start from the ventricular layer, penetrate all layers of the cerebellum in the radial direction and end in the externally granular layer. The expression of Vimentin in radial glial fibers was relatively moderate in the intermediate layer and relatively strong in the ventricular and externally granular layers. The average length of radial glial fibers was: short - 120.8±5.7 μm, long - 195.3±9.4 μm (Fig. 5).

The expression of Synaptophysin in this term is slightly expressed in all layers of the cerebellum (Fig. 6).

Thus, in the course of the study we established the features of cytoarchitectonics, morphometric parameters of the structures of the cerebellum of human cerebellum embryos at 8-9 weeks of prenatal development.

Discussion

Owing to the expansion of the wall of the cranial end of the nerve tube in the region of the hindbrain, the cerebellum is formed [21].

When examining histological sections, we observed that during this period from the formed hemisphere of the cerebellum over the fourth ventricle, the formation of the cerebellar worm occurs, whereas K. Cho (2011) indicates that at the end of the embryonic period and at the beginning of the fetal period, starting from 7-8 weeks, the rhombic lip and the alar plate expanded to form the cerebellar hemispheres that began to approach over the fourth ventricle. The cerebellar worm forms a little later, up to 10 weeks. The cerebellar worm forms a little later, by 10 weeks the cerebellar hemispheres have already merged along the median line, forming the cerebellar worm [3].

Thus, we found that the lowest cell density was observed in the molecular layer - 22.00±0.70 cells per 0.01 mm^2, whereas the highest cell density was observed in the outer granular layer - 151.0±4.2 cells per 0.01 mm^2. In our opinion, this phenomenon is related to the fact that NSC migrates from the outer granular layer towards the ventricular layer to form the inner granular layer, whereas J. Volpe (2009) states that the tabulation of Purkinje nuclei and cells occurs in the first weeks of development of

migration of neuroblasts in the ventricular layer. During the period of 9-10 weeks of prenatal development, neural stem cells are separated from the ependymal layer of the fourth ventricle and migrate to the surface of the cerebellum (primary migration). Thus, they form the outer germinal layer, and by the 21st week its thickness is 6-9 cell layers. Hence, cells differentiate into neuroblasts and migrate in the opposite direction. The movement of cells through the Purkinje cell layer is directed by radial glia [6, 16, 21].

At 8-9 weeks gestation NSC migration takes place in the radial direction, and the outer granular layer tangentially, as J. Volpe points out [21], NSC migration in the fetal period occurs in the radial direction, and in the embryonic period, the outward granular layer is formed where the cells go tangential direction above the surface of the cerebellum.

Cell proliferation occurs more intensely in the ventricular layer as well as in the outer granular layer of the cerebellum, however, H. Abrahám (2001) found that expression of Ki-67 in the cerebral cortex of a human fetus for 24 weeks of prenatal development more intense in the outer granular layer [1].

The expression of Synaptophysin in this term is slightly expressed in all layers of the cerebellum, whereas A. Milosevic in 1998 indicates that for 13 weeks, the expression of Synaptophysin is present in all layers of the cerebellum [12]. In our view, Synaptophysin expression is insignificantly expressed in all layers, which may be due to the fact that in this embryonic period the fetus is not as active as in 13 weeks of prenatal development.

Prospects for further development are to study the patterns of development and establishment of structures of the human cerebellum during the prenatal development, as well as the subsequent use of immuno-histochemical markers to conduct a comprehensive study and comparative analysis of similar indicators of human embryos and fetuses.

Conclusions

1. In the cerebellar hemispheres of embryos, 8-9 weeks of prenatal development, there is a clear division into ventricular, intermediate, molecular and outer granular layers. It was found that the densest NSC are located in the outer granular layer (151.0±4.1 cells per 0.01 mm^2) and less densely in the molecular layer (22.00±0.80 cells per 0.01 mm^2). The greatest thickness had an intermediate layer of the cerebellum - 1574±83 μm, the smallest - molecular layer 20.30±1.00 μm.

2. Relatively most intense cell proliferation was found in the ventricular layer and the outer granular layer of the cerebellum and the least intense in the intermediate layer. Synaptophysin expression is slightly expressed in the ventricular layer of the cerebellum.

3. It is established that the radial glial fibers start from the ventricular layer, permeate all layers of the cerebellum and end in the outer granular layer. The expression of Vimentin in radial glia fibers is relatively moderate in the intermediate layer and relatively strong in the ventricular and external granular layers. The average length of radial glial fibers was: short - 120.8±5.7 μm, long - 195.3±9.4 μm.

4. The exterior granular layer is represented by spherical undifferentiated cells with an area of 641.1±28.9 μm^2, the molecular layer is represented by NSC area 472.9± 23.7 μm^2, the intermediate layer - NSC area 492.2±23.1 μm^2, the ventricular layer is represented by neuroblasts with an area of 436.1±21.8 μm^2.

References

[1] Abrahám, H., Tornóczky, T., Kosztolányi, G., & Seress, L. (2001). Cell formation in the cortical layers of the developing human cerebellum. *Int. J. Dev. Neurosci,* 19, 53-62. doi: 10.1016/s0736-5748(00)00065-4

[2] Antipkin, Y. G., Kirilova, L. G., Avramenko, T. V., & Shevchenko, O. A. (2015). Congenital malformations of the CNS: the current state of the problem, clinical and neurological features and issues of optimization of prenatal diagnosis. *Journal of the National Academy of Medical Sciences of Ukraine*, 21(2), 201-214.

[3] Cho, K. H. (2011). Early fetal development of the human cerebellum. *Surg. Radiol. Anat.*, 33(6), 523-530. doi: 10.1007/s00276-011-0796-8.

[4] Dastjerdi, F. V., Consalez, G. G., & Hawkes, R. (2012). Pattern formation during development of the embryonic cerebellum. *Front. Neuroanat.,* 10(6). doi: 10.3389/fnana.2012.00010

[5] Fei, L., Zhonghe, Z.,Xiangtao, L., Gaojun, T., Haiwei, M., Taifei, Y. … Shuwei, L. (2011). Development of the human fetal cerebellum in the second trimester: a post mortem magnetic resonance imaging evaluation. *Anat.,* 219(5), 582-588. doi: 10.1111/j.1469-7580.2011.01418.x

[6] Hassan, M., Marc, R. D. B., Javad, A., Saeid, G., Robby, M. Z., & Mojgan, R. (2015). Cellular commitment in the developing cerebellum. *Front. Cell. Neurosci.* doi.org/10.3389/fncel.2014.00450

[7] Hibi, M., & Shimizu, T. (2012). Development of the cerebellum and cerebellar neural circuits. *Dev. Neurobiol.*, 72, 282-301. doi: 10.1002/dneu.20875

[8] Huang, H. (2010). Structure of the fetal brain: what we are learning from diffusion tensor imaging. *The Neuroscientist,* 16, 634-649. doi: 10.1177/1073858409356711

[9] Hutchins, B., Klenke, U., & Wray, S. (2013). Calcium release-dependent actin flow in the leading process mediatesaxophilic migration. *J. Neurosci.,* 33, 11361-11371. doi: 10.1523/JNEUROSCI.3758-12.2013

[10] Marklund, U., Alekseenko, Z., Andersson, E., Falci, S., Westgren, M., Perlmann, T. … Ericson, J. (2014). Detailed Expression Analysis of Regulatory Genes in the Early Developing Human Neural Tube. *Stem Cells Dev.*, 23(1), 5-15. doi: 10.1089/scd.2013.0309

[11] Martinez, S., Andreu, A., Mecklenburg, N., & Echevarria, D. (2013). *Cellular and molecular basis of cerebellar development.* Neuroanat. doi.org/10.3389/fnana.2013.00018

[12] Milosevic, A. (1998). Developmental changes in human cerebellum: Expression of intracellular calcium receptors, calcium binding proteins, and phosphorylated and nonphosphorylated neurofilament protein. *Zecevic Version of Record online,* 10(2), 442-460. doi: 10.1002/(SICI)1096-9861(19980713)396

[13] Mohammed, H. K., Abubaker, E., Deya, E. A. M., & Khalid, T.

(2015). Sonographic Evaluation of Normal Anatomy of Fetal Central Nervous System in Mid-Trimester. *Forensic Medicine and Anatomy Research.,* 3(1) 32-38. doi.org/10.4236/fmar.2015.31007

[14] Nowakowska-Kotas, M., Kedzia, A., & Dudek, K. (2014). Development of external surfaces of human cerebellar lobes in the fetal period. *Cerebellum.*, 13, 541-548. doi: 10.1007/s12311-014-0566-3

[15] Ostrem, B. E., Lui, J. H., Gertz, C. C., & Kriegstein, A. R. (2014). Control of outer radial glial stem cell mitosis in the human brain. *Cell. Rep.,* 7, 8(3), 656-664. doi: 10.1016/j.celrep.2014.06.058

[16] Rakic, P., & Sidman, L. (1970). Histogenesis of cortical layers in human cerebellum, particularly the lamina dissecans. *Comp. Neurol.,* 139(4), 473-500. doi: 10.1002/cne.901390407

[17] Saveliev, S. V. (2012). Pathology of embryonic morphogenesis of the human brain. *Bulletin of the Russian Academy of Medical Sciences,* 8, 40-46.

[18] Shiraishi, N., Katayama, A., Nakashima, T., Yamada, S., Uwabe, C., Kose, K., & Takakuwa, T. (2015). Three-dimensional morphology of the human embryonic brain. *Data Brief.,* 4, 116-118. doi: 10.1016/j.dib.2015.05.001

[19] Shkolnikov, V. S. (2015). Macro- and microstructure of the spinal cord of human fetuses with teratomas. *Reports of Morphology,* 21(1), 117-127.

[20] Shkolnikov, V. S., Zalevsky, L. L., Stelmashchuk, P. A., Tikholaz, V. O., Gryshchenko, Y. V. (2017). Patent of Ukraine № 115849 МПК A61B 17/00, A61B 17/06 (2006.01)

[21] Volpe, J. (2009). Cerebellum of the premature infant: rapidly developing, vulnerable, clinically important. *Child. Neurol.,* 24(9), 1085-1104. doi: 10.1177/0883073809338067

[22] Williams, J., Mai, C., Mulinare, J., Isenburg, J., Flood, T. J., Ethen, M. … Kirby, R. S. (2015). Updated estimates of neural tube defects prevented by mandatory folic Acid fortification - United States, 1995-2011. *MMWR Morb. Mortal. Wkly Rep.,* 64(1), 1-5.

[23] Xu, H., Yang, Y., Tang, X., Zhao, M., Liang, F., Xu, P. … Fan, X. (2013). Bergmann glia function in granule cell migration during cerebellum development. *Mol. Neurobiol,* 47, 833-844. doi: 10.1007/s12035-013-8405-y

ГІСТОСТРУКТУРНА ОРГАНІЗАЦІЯ МОЗОЧКА ЕМБРІОНІВ ЛЮДИНИ 8-9 ТИЖНІВ ВНУТРІШНЬОУТРОБНОГО РОЗВИТКУ

Залевський Л.Л., Школьніков В.С., Приходько С.О.

Висока частота розповсюдженості аномалій заднього мозку обумовлена тим, що нейруляція у краніальному відділі триває найбільший проміжок часу. Тому, для більш детального дослідження ембріогенезу, розуміння механізмів патогенезу та виникнення вроджених вад розвитку виникає необхідність у визначенні морфометричних (гістометричних) параметрів мозочка у різні терміни гестації. Мета дослідження - встановити морфометричні параметри мозочка ембріонів людини 8-9 тиж. внутрішньоутробного розвитку, а також особливості цитоархітектоніки його структур, яка притаманна для даного терміну гестації. Проведено анатомо-гістологічне, імуногістохімічне та морфометричне дослідження мозочка 10 ембріонів людини. Виготовляли серійні зрізи препаратів мозочку товщиною 8-10 мкм, які забарвлювали гематоксиліном, еозином, толуїдиновим синім та за Ван-Гізон. Для імуногістохімічного дослідження були використані діагностичні моноклональні антитіла фірми "DacoCytomation" (Данія): віментин, Кі-67 та синаптофізин. У ході дослідження отримані результати вимірів загальної товщини усіх шарів, щільність нейральних стовбурових клітин (НСК), а також площі правої та лівої півкуль мозочка. При імуногістохімічному дослідженні визначили напрямок міграції НСК та проліферацію клітин усіх шарів мозочка, а також довжину волокон радіальної глії. У півкулях мозочка ембріонів 8-9 тижня відбувається чіткий поділ на вентрикулярний, проміжний, молекулярний і зовнішній зернистий шари. Найбільшу щільність нейральних стовбурових клітин спостерігали у зовнішньому зернистому шарі - 151,0± 4,1 клітин на 0,01 мм^2. Найменшу щільність клітин спостерігали у молекулярному шарі - 22,0±0,8 клітин на 0,01 мм^2. Відносно найбільш інтенсивну проліферацію клітин встановили у вентрикулярному шарі та зовнішньому зернистому шарі мозочка, найменш інтенсивну - у проміжному шарі. Експресія синаптофізину була виражена незначно у вентрикулярному шарі мозочка. Волокна радіальної глії починаються від вентрикулярного шару та пронизують усі шари мозочка, закінчуючись у зовнішньому зернистому шарі. Середня довжина волокон радіальної глії становила: коротких - 120,8±5,7 мкм, довгих - 195,3±9,4 мкм. Зовнішньо зернистий шар представлений кулястими недиференційованими клітинами середнім розміром площі 641,1±28,9 мкм^2, молекулярний шар - НСК площею 472,9±23,7 мкм^2, проміжний шар - НСК площею 492,2±23,1 мкм^2, вентрикулярний шар представлений нейробластами площею 436,1±21,8 мкм^2. Таким чином, встановлено, що відбувається чіткий розподіл шарів мозочка на вентрикулярний шар, який представлений нейробластами, проміжний шар - НСК, молекулярний шар - НСК, а зовнішній зернистий шар представлений недиференційованими клітинами; найщільніше нейральні стовбурові клітини розташовуються у зовнішньому зернистому шарі, а менш щільно - у молекулярному шарі.

Ключові слова: *мозочок, морфометричні параметри, радіальна глія, внутрішньоутробний розвиток.*

ГИСТОСТРУКТУРНАЯ ОРГАНИЗАЦИЯ МОЗЖЕЧКА ЭМБРИОНА ЧЕЛОВЕКА 8-9 НЕДЕЛЬНОГО ВНУТРИУТРОБНОГО РАЗВИТИЯ

Залевский Л.Л., Школьников В.С., Приходько С.А.

Высокая частота распространенности аномалий заднего мозга обусловлена тем, что нейруляция в краниальном отделе продолжается длительный период времени. Поэтому, для более подробного исследования эмбриогенеза, понимания механизмов патогенеза и возникновения врожденных пороков развития возникает необходимость в определении морфометрических (гистометрических) параметров мозжечка в разные сроки гестации. Цель исследования - установить морфометрические параметры мозжечка эмбрионов человека 8-9 нед. внутриутробного развития, а также особенности цитоархитектоники его структур, которая характерна для данного срока гестации. Проведено анатомо-гистологическое, иммуногистохимическое и морфометрическое исследования мозжечка 10 эмбрионов человека. Изготавливали серийные срезы препаратов мозжечка толщиной 8-10 мкм, которые окрашивали гематоксилином, эозином, толуидиновым синим и по Ван-Гизону. Для иммуногистохимического исследования были использованы диагностические моноклональные антитела фирмы "DacoCytomation" (Дания): виментин, Ки-67 и синаптофизин. В процессе исследования нами были получены результаты измерений общей толщины всех слоев, плотность нейральных стволовых клеток (НСК), а также площадь правого и левого полушарий мозжечка. При иммуногистохимическом исследовании определили направление миграции НСК и

пролиферацию клеток всех слоев мозжечка, а также длину волокон радиальной глии. В полушариях мозжечка эмбрионов 8-9 недели происходит четкое разделение на вентрикулярный, промежуточный, молекулярный и внешний зернистый слои. Наибольшую плотность нейральных стволовых клеток наблюдали во внешнем зернистом слое - 151,0±4,1 клеток на 0,01 мм^2. Наименьшую плотность клеток наблюдали в молекулярном слое - 22,0±0,8 клеток на 0,01 мм^2. Относительно наиболее интенсивную пролиферацию клеток установили в вентрикулярном слое и внешнем зернистом слое мозжечка, а наименее интенсивную - в промежуточном слое. Экспрессия синаптофизина была незначительно выражена в вентрикулярном слое мозжечка. Волокна радиальной глии начинаются от вентрикулярного слоя и пронизывают все слои мозжечка, заканчиваясь во внешнем зернистом слое. Средняя длина волокон радиальной глии составила: коротких - 120,8±5,7 мкм, длинных - 195,3±9,4 мкм. Внешний зернистый слой представлен шаровидными недифференцироваными клетками средним размером площади 641,1±28,9 мкм^2, молекулярный слой - НСК площадью 472,9±23,7 мкм^2, промежуточный слой НСК площадью 492,2±23,1 мкм^2, вентрикулярный слой представлен нейробластами площадью 436,1±21,8 мкм^2. Таким образом, установлено, что происходит четкое разделение слоев мозжечка на вентрикулярний слой, который представлен нейробластами, промежуточный слой - НСК, молекулярный слой - НСК, а внешний зернистый слой представлен недифференцированными клетками; более плотно нейральные стволовые клетки располагаются во внешнем зернистом слое, а менее плотно - в молекулярном слое.

Ключевые слова: *мозжечок, морфометрические параметры, радиальная глия, внутриутробное развитие.*

DOI: 10.31393/morphology-journal-2019-25(3)-09 Reports of Morphology, Vol. 25, №3, Pages 52-57

ISSN 1818-1295 eISSN 2616-6194

REPORTS OF MORPHOLOGY

Official Journal of the Scientific Society of Anatomists, Histologists, Embryologists and Topographic Anatomists of Ukraine

journal homepage: https://morphology-journal.com

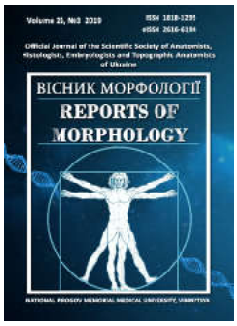

Indicators of the cell cycle in the thyroid gland in rats when using infusion of 0.9% NaCl solution on the background of thermal skin burns

Tiron O.I.
Odessa National Medical University, Odessa, Ukraine

ARTICLE INFO
Received: 10 July, 2019
Accepted: 11 August, 2019

UDC: 616.441:572.7

CORRESPONDING AUTHOR
e-mail: chekina.o@ukr.net
Tiron O.I.

Systemic damage of the organs, including the thyroid gland, is one of the key factors in the pathogenesis of burn disease due to thermal skin burns. The aim of this study was to investigate the indices of the cell cycle and DNA fragmentation of thyroid gland cells in rats with the use of infusion of 0.9% NaCl solution against the background of thermal skin burns. Experimental studies were conducted on 60 white male rats weighing 160-180 g, which was subjected to thermal burns of the skin of 2-3 degrees with a total area of 21-23% of the body surface. The first 7 days rats were infused with 0.9% NaCl solution into the inferior vena cava. Animals were removed from the experiment by decapitation (after 1, 3, 7, 14, 21, and 30 days). DNA content in the nuclei of the cells of the thyroid gland of rats was determined by flow cytometry. The statistical processing of the obtained results was carried out in the license package "STATISTICA 6.1" using nonparametric estimation methods. After 1 day after thermal skin damage and using 0.9% NaCl solution, lower ($p<0.05$) values of the S-phase index (0.234±0.094) were found compared to the control group without burn (0.652±0.134). The maximum decrease ($p<0.01$) of S-phase indicators (0.622±0.110 and 0.214±0.105, respectively) and a significant increase ($p<0.01$) of the SUB-G0G1 interval (5.288±0.840) compared to similar control group values (2.594±0.628) is observed after 3 days. The S-phase against the background of the introduction of 0.9% NaCl solution and thermal skin burn remained significantly lower than those of the similar control groups at 7 ($p<0.01$), 14 ($p<0.05$) and 21 days ($p<0.05$). At 14 days after thermal skin injury, the SUB-G0G1 interval ($p<0.05$) was lower than in the control group of rats. After 30 days, the G0G1 phase parameters were significantly lower ($p<0.01$), and the G2+M phase values were significantly ($p<0.01$) higher than those in the control group at the same time. Thus, it was found that 0.9% NaCl solution was not effective enough to correct cell division disorders during the entire observation period after skin burns.

Keywords: *thyroid gland, thermal burns of the skin, DNA cytometry, 0.9% NaCl solution.*

Introduction

The urgency of the problem of therapy of thermal burns of the skin and burn disease (BD) is caused by the increase in the number of burn injuries in modern society, the lack of efficiency of existing methods of therapy, the high frequency of development of complications of a systemic nature [14]. The inefficiency of the proposed methods of treatment is not least due to the complex pathogenesis of this damage, the numerous factors responsible for the cascade of pathological processes in thermal burns [13]. For this reason, the worldwide study of the mechanisms and pathogenetic factors of BD at the tissue, cell, subcellular and molecular levels perform, which deepens knowledge about this process and identifies potential targets of therapy [3].

One of the key factors in the pathogenesis of burn disease due to thermal burns of the skin, many researchers [6, 10, 18] are considering systemic damage to the organs of the endocrine system, which manifests itself both functionally and at the cellular and subcellular level. A special role in the pathogenesis of BD according to modern data [18] is given to the interaction of the triangle pituitary gland - adrenal cortex, pituitary gland - thyroid gland.

It is known [8] that patients with severe thermal burns of the skin have decreased plasma triiodothyronine concentrations, low thyroxine and normal range, or slightly

decreased thyrotropic hormone concentrations. This ensemble of change is collectively known as the "non-thyroid disease" syndrome [1]. The degree of manifestation of this disease is associated with the prognosis of the disease, but there is no evidence for the causality of this association. It is assumed [18] that the development of this condition is a consequence of the acute phase response to systemic irritation and microelement constraints. Thyroid injury pathogenetically is associated with the level of endogenous intoxication and the development of general inflammatory response, established a clear link between changes in thyroid hormone metabolism and activation of various proinflammatory cytokines [15].

Today, it is believed [7] that the problem of correction of thyroid gland damage remains an open question in the treatment of BD, and a problem that requires an urgent solution, given the important role of the functioning of this gland in the metabolism of the skin and other vital tissues (bone, connective tissue) that provide the restoration of homeostasis in the body. However, the most accurate method for assessing cell division is the DNA cytometry method, which is nowadays defined as a reference for the establishment of apoptosis markers, and such that allows dividing the cell phases into separate components [2]. We did not find any data on studies of thyroid cell division by DNA cytometry against the background of burn skin damage.

The aim of the study was to investigate the indices of the cell cycle and DNA fragmentation of the thyroid gland in rats using infusion of 0.9% NaCl solution against the background of thermal skin burns.

Materials and methods

Experimental studies were conducted on 60 white male rats weighing 160-180 g, conducted at the Research Laboratory of Functional Morphology and Genetics Research Center National Pirogov Memorial Medical University, Vinnytsya. The keeping and manipulation of animals was carried out in accordance with the "General Ethical Principles of Animal Experiments" (Kyiv, 2001), also guided by the recommendations of the "European Convention for the Protection of Vertebrate Animals Used for Experimental and Other Scientific Purposes" (Strasbourg, 1985), guidelines of the State Pharmacological Center of the Ministry of Health of Ukraine on "Preclinical studies of medicinal products" (2001), as well as the rules of humane treatment for experimental animals and conditions approved the Committee on Bioethics of National Pirogov Memorial Medical University, Vinnytsya (Minutes No. 1 of 14.01.2010).

Thermal burns of the skin of 2-3 degrees were carried out by applying to the pre-shaved lateral surfaces of the trunk of rats four copper plates (each with a surface area of 13.86 cm2) for 10 seconds, which were pre-heated for 6 minutes in water with a temperature of 100?C [9]. The total area of skin lesions was 21-23%. The first 7 days of rats were infused with 0.9% NaCl solution into the inferior vena cava. Animals were removed from the experiment by decapitation (after 1, 3, 7, 14, 21, and 30 days). Shaving, catheterization of veins, staging of skin burns, and decapitation of rats were performed under the conditions of intravenous propofol anesthesia (calculated at 60 mg/kg animal weight).

Within the framework of the agreement on scientific cooperation between the Research Center of National Pirogov Memorial Medical University, Vinnytsya and the Department of Histology, Cytology and Embryology of the Odessa National Medical University, DNA content in the nuclei of thyroid cells of rats was determined by flow DNA cytometry on a multifunction flow cytometer "Partec PAS" (Partec, Germany) [17]. Determined: G0G1 is the percentage of G0G1 phase cells to all cells in the cell cycle (DNA content = 2c); S is the percentage of the phase of DNA synthesis to all cells of the cell cycle (DNA content > 2c and < 4c); G2+M is the percentage ratio of the G2+M phase to all cells in the cell cycle (DNA = 4c). Determination of DNA fragmentation (SUB-G0G1, apoptosis) was performed by isolating the RN2 regions on DNA histograms before the G0G1 peak, indicating nuclei of cells with a DNA content < 2c.

The statistical processing of the obtained results was carried out in the license package "STATISTICA 6.1" using nonparametric estimation methods. The significance of the difference in values between the independent quantitative values was determined using the Mann-Whitney U test.

Results

It is established that the background of the introduction of 0.9% NaCl solution 1 day after thermal burns of the skin marked changes in the cell cycle indices of the thyroid gland - statistically significant decrease in the number of cells in phase S ($p<0.01$), which indicates insufficient restoration of the damaged cell population. Other indicators of the cell cycle have no significant or trending differences with those of the group without skin burn (Table 1). No significant or trending differences for G0G1, G2+M, and SUB-G0G1 were identified (see Table 1).

On the presented DNA-histogram (Fig. 1) of thyroid cells 1 day after skin burn on the background of the introduction of 0.9% NaCl solution, the level of DNA fragmentation in the interval SUB-G0G1 was 3.32%, and phase S - 0.19%, indicating expressed inhibition of DNA synthesis.

The maximum reduction in the percentage of thyroid cells in phase S ($p<0.01$) and, at the same time, a peak increase in the average level of SUB-G0G1 interval ($p<0.01$) was established after 3 days of observation from the start of thermal skin burn on the background of 0.9% NaCl solution introduction (see Table 1). No significant or trending differences were found for G0G1 and G2+M indicators (see Table 1).

In the presented DNA histogram (Fig. 2) of nuclear

Table 1. Indicators of the cell cycle in the cells of the thyroid gland of rats after skin burn with the use of infusion therapy 0.9% NaCl solution according to flow cytometry DNA (M±σ).

Group	Indicators of the cell cycle (%)			
	S	SUB-G0G1	G0G1	G2+M
1 day				
0.9% NaCl	0.652±0.134	2.462±0.800	91.16±2.41	8.192±2.368
Burn + 0.9% NaCl	0.234±0.094	2.732±1.141	91.90±2.65	7.868±2.678
$p_{(0.9\%\ NaCl\ -\ burn+0.9\%\ NaCl)}$	<0.01	>0.05	>0.05	>0.05
3 day				
0.9% NaCl	0.622±0.110	2.594±0.628	90.99±2.48	8.392±2.375
Burn + 0.9% NaCl	0.214±0.105	5.288±0.840	91.46±2.80	8.328±2.711
$p_{(0.9\%\ NaCl\ -\ burn+0.9\%\ NaCl)}$	<0.01	<0.01	>0.05	>0.05
7 day				
0.9% NaCl	0.650±0.139	2.632±0.724	90.90±2.17	8.448±2.113
Burn + 0.9% NaCl	0.350±0.088	3.994±1.204	88.70±3.13	10.95±3.14
$p_{(0.9\%\ NaCl\ -\ burn+0.9\%\ NaCl)}$	<0.01	=0.076	>0.05	>0.05
14 day				
0.9% NaCl	0.562±0.153	2.304±0.835	91.29±1.49	8.146±1.520
Burn + 0.9% NaCl	0.322±0.043	3.664±0.239	89.15±3.56	10.53±3.54
$p_{(0.9\%\ NaCl\ -\ burn+0.9\%\ NaCl)}$	<0.05	<0.05	>0.05	>0.05
21 day				
0.9% NaCl	0.522±0.075	2.622±0.677	90.60±2.48	8.986±2.370
Burn + 0.9% NaCl	0.364±0.092	3.250±0.755	87.98±3.30	11.66±3.27
$p_{(0.9\%\ NaCl\ -\ burn+0.9\%\ NaCl)}$	<0.05	>0.05	>0.05	>0.05
30 day				
0.9% NaCl	0.592±0.193	2.630±0.717	91.16±1.82	8.252±1.851
Burn + 0.9% NaCl	0.408±0.063	2.900±1.078	83.11±2.14	16.50±2.18
$p_{(0.9\%\ NaCl\ -\ burn+0.9\%\ NaCl)}$	=0.060	>0.05	<0.01	<0.01

suspension of cells of the thyroid gland of rats 3 days after skin burn on the background of the introduction of 0.9% NaCl solution, SUB-G0G1 (RN2, DNA fragmentation) was 5.33%, indicating the presence of a significant group of cells who are in the state of apoptosis activation.

After 7 days after thermal skin burns and 0.9% NaCl solution, a significantly lower (S<0.01) value of S-phase was observed and a slight tendency (p=0.076) to greater values of SUB-G0G1 interval compared to the group without skin burn (see Table 1). No significant or trending differences for G0G1 and G2+M indicators were detected (see Table 1).

After 14 days after thermal skin burn, significantly lower (p<0.05) values of the number of cells in the S-phase and higher (p<0.05) values of the level of the DNA fragmentation index in the interval SUB-G0G1 against the background of the introduction of the first seven days of 0.9% NaCl solution and compared to similar indicators in animals without burns (see Table 1). No significant or trending differences were found for G0G1 and G2+M.

At day 21 after thermal skin burn, significantly lower (p<0.05) cell counts in the S-phase were observed against the background of administration of the first seven days of 0.9% NaCl solution and compared with similar indices in animals without burns (see Table 1). No significant or trending differences for G0G1, G2+M, and SUB-G0G1 were identified (see Table 1).

30 days after skin burns, against the background of the introduction of the first seven days 0.9% NaCl solution tended (p=0.060) to lower values of the number of cells in the S-phase, significantly (p<0.01) less than the value of the G0G1 phase and higher (p<0.01) value of the G2+M phase

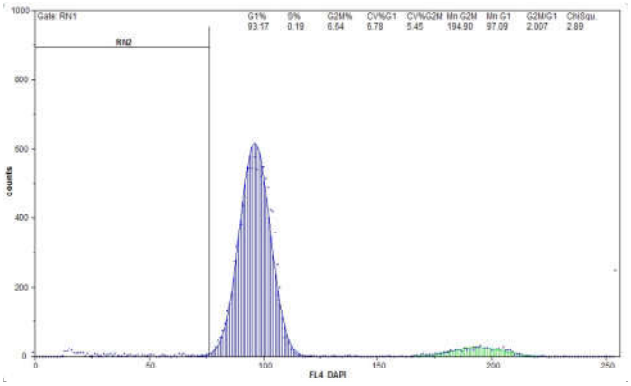

Fig. 1. DNA histogram of nuclear suspension of thyroid cells 1 day after burn injury on the background of the introduction of 0.9% NaCl solution. RN2 (SUB-G0G1, DNA fragmentation) = 3.32%.

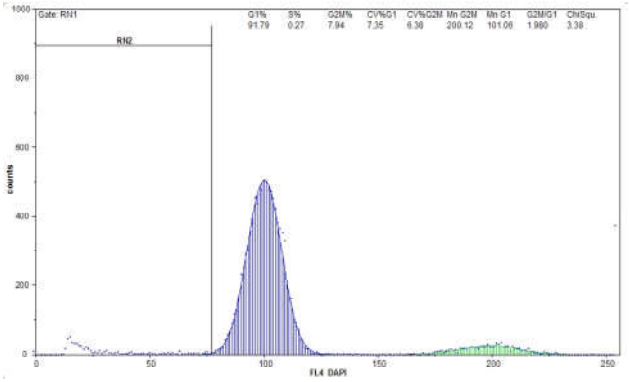

Fig. 2. DNA histogram of nuclear suspension of thyroid cells 3 days after burn injury on the background of the introduction of 0.9% NaCl solution. RN2 (SUB-G0G1, DNA fragmentation) = 5.33%.

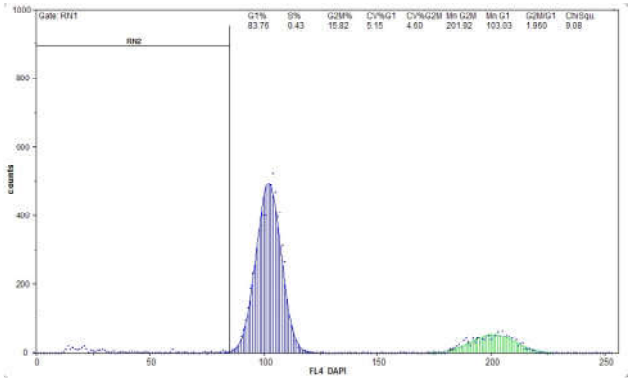

Fig. 3. DNA histogram of thyroid gland cell suspension 30 days after burn injury on the background of 0.9% NaCl solution administration. RN2 (SUB-G0G1, DNA fragmentation) = 3.60%.

compared with similar values in animals without burns (see Table 1). No significant or trending differences were observed for the SUB-G0G1 interval (see Table 1).

In the presented DNA histogram (Fig. 3) of a nuclear suspension of the cells of the thyroid gland of rats 30 days after skin burn on the background of the introduction of 0.9% solution of NaCl indicator SUB-G0G1 (RN2, DNA fragmentation) was 3.60%.

When analyzing the dynamics of changes in the cell cycle of the thyroid gland within 30 days after skin burns against the background of the introduction of 0.9% NaCl solution - G0G1 phase indicators have significantly ($p<0.05$-0.01) smaller values between 1 and 30, 3 and 21, 3 and 30, 7 and 30, 14 and 30, 21 and 30 days, as well as minor trends ($p=0.076$ in both cases) to smaller values between 1 and 21, 3 and 7 days of the experiment; phase S indicators have significantly ($p<0.05$ in all cases) greater values between 1 and 30, 3 and 21, 3 and 30, 14 and 30 days, as well as trends ($p=0.060$-0.076) to larger values between 1 and 21, 3 and 7, 3 and 14 days of experiment; G2+M phase indices have significantly ($p<0.05$-0.01) greater values between 1 and 30, 3 and 30, 7 and 30, 14 and 30, 21 and 30 days, and a slight tendency ($p=0.076$) to larger values between 1 and 21 days of the experiment; the SUB-G0G1 interval values had significantly ($p<0.01$) greater values between 1 and 3 days, and significantly ($p<0.05$-0.01) smaller values between 3 and 14, 3 and 21, 3 and 30 days of the experiment.

Discussion

Analyzing the obtained data of thyroid cell cycle indexes against the background of thermal burns of the skin and infusion of 0.9% NaCl solution and comparing the results with the data of other similar studies [12, 16] we can make some generalizations. The most pronounced cell cycle abnormalities were observed 3 days after thermal skin damage, although the first signs of these disorders in the form of a significant decrease in DNA synthesis ($p<0.01$) were observed after 1 day. However, established changes after 1 day are only the initiation of further damage to the thyroid gland, as changes at the subcellular level precede changes at the tissue and cellular levels, with subsequent disruption of the functioning of the organ. There are several factors that can be explained by the increase in the negative effect of burn injury due to increased toxicity of products, the stress of organ depletion and the potential activation of protective mechanisms, which is known to be often observed in burn skin damage [1, 11]. The thyroid gland in this case is included in the systemic damage of the organs of the endocrine system against the background of burn injury, which is manifested both functionally and at the cellular and subcellular levels and has been established in many studies [16, 18].

Perhaps the changes we recorded in the first days of observation appear due to the complex effects of burn toxins, the imbalance of hormonal regulation at the level of the hypothalamic-pituitary system, and the launch of a protective mechanism to inhibit damage, which are well-known factors of protection in critical states [5, 16]. However, our further observations in the following terms indicate insufficient protective effect and deepening of the violation of the cell cycle of the thyroid cells using 0.9% NaCl solution.

As is known [10], changes at the subcellular level precede changes at the cellular and histological levels, which corresponds to the hypofunctional state of the organ. Therefore, we can consider our indicators more sensitive marker of damage to the thyroid gland than morphological studies, which can potentially indicate the further development of deep morpho-functional damage to the gland, which is characteristic when using DNA cytometry [2, 12]. It should also be noted that these disorders were observed even in the long term of our study, which can affect the regeneration processes not only in the gland itself, but also in skin cells, the regeneration of which is controlled by the level of thyroid hormones [4, 15]. That is why damage to the thyroid gland against the background of burn injury of the skin is an important element of pathogenesis and requires effective correction [8, 14]. We can note the lack of effectiveness of using 0.9% NaCl solution to correct cell division disorders throughout the observation period.

The prospect of further research is to study the effect of other infusion solutions on thyroid cell cycle indices against the background of thermal skin burns.

Conclusions

1. 1 day after thermal skin damage and use of 0.9% NaCl solution, lower ($p<0.05$) values of the S-phase indicator were found compared to the control group of rats (0.9% NaCl solution without burn), reflecting a significant disturbance of the thyroid cell cycle.

2. The maximum decrease ($p<0.01$) of S-phase indicators and a significant increase ($p<0.01$) of the SUB-G0G1 interval compared to the same control group was observed after 3 days. The S-phase indicators against the background of the introduction of 0.9% NaCl solution and thermal skin burn remained significantly lower than those of the similar control groups at 7 ($p<0.01$), 14 ($p<0.05$) and 21 days ($p<0.05$). At 14 days after thermal skin injury, the SUB-G0G1 interval ($p<0.05$) was lower than in the control group of rats.

3. After 30 days, the G0G1 phase indicators were significantly lower ($p<0.01$) and the G2+M phase indicators were significantly ($p<0.01$) higher than those established in the control group at the same time.

References

[1] Abdullahi, A., Patsouris, D., Costford, S. R., & Jeschke, M. G. (2016). *Hypermetabolic Response to Burn Injury.* In: Preiser JC. (eds) The Stress Response of Critical Illness: Metabolic and Hormonal Aspects. Springer, Cham. https://doi.org/10.1007/978-3-319-27687-8_19

[2] Adan, A., Alizada, G., Kiraz, Y., Baran, Y., & Nalbant, A. (2017).

Flow cytometry: basic principles and applications.*Critical reviews in biotechnology,* 37(2), 163-176. doi: 10.3109/07388551.2015.1128876

[3] Auger, C., Samadi, O., & Jeschke, M. G. (2017). The biochemical alterations underlying post-burn hypermetabolism.*Biochimica et Biophysica Acta (BBA)-Molecular Basis of Disease,* 1863(10), 2633-2644. https://doi.org/10.1016/j.bbadis.2017.02.019

[4] Batista, G., & Hensch, T. K. (2019). Critical period regulation by thyroid hormones: potential mechanisms and sex-specific aspects. *Frontiers in molecular neuroscience,* 12, 77. doi: 10.3389/fnmol.2019.00077

[5] Cherkasov, V. G., Cherkasov, E. V., Kaminsky, R. F., Pastukhova, V. A., Kovalchuk, O. I., & Trofimenko, Yu. Yu. (2017). Influence of HAES-LX-5% infusion solution on the DNA content of endocrine glands cells against the background of thermal burn of skin in rats. *Worlg of Medicine and Biology,* 13(4(62)), 168-173. doi: 10.26724 / 2079-8334-2017-4-62-173-178

[6] Culnan, D., Voigt, C., Capek, K. D., Muthumalaiappan, K., & Herndon, D. (2018). *Significance of the Hormonal, Adrenal, and Sympathetic Responses to Burn Injury*. In Total Burn Care (pp. 248-258). Elsevier. https://doi.org/10.1016/B978-0-323-47661-4.00023-X

[7] D'Asta, F., Cianferotti, L., Bhandari, S., Sprini, D., Rini, G. B., & Brandi, M. L. (2014). The endocrine response to severe burn trauma. *Expert review of endocrinology & metabolism*, 9(1), 45-59. https://doi.org/10.1586/17446651.2014.868773

[8] Fliers, E., Bianco, A. C., Langouche, L., & Boelen, A. (2015). Thyroid function in critically ill patients. *The lancet. Diabetes & endocrinology,* 3(10), 816-825. doi: 10.1016/S2213-8587(15)00225-9

[9] Gunas, I., Dovgan, I., & Masur, O. (1997). *Method of thermal burn trauma correction by means of cryoinfluence. Abstracts are presented in zusammen mit der Polish Anatomical Society with the participation of the Association des Anatomistes Verhandlungen der Anatomischen Gesellschaft,* Olsztyn (p. 105). Jena - München : Der Urban & Fischer Verlag.

[10] Jeschke, M. G., Patsouris, D., Stanojcic, M., Abdullahi, A., Rehou, S., Pinto, R., ... Amini-Nik, S. (2015). Pathophysiologic response to burns in the elderly. *EBioMedicine*, 2(10), 1536-1548. doi: 10.1016/j.ebiom.2015.07.040

[11] Maiden, M. J., & Torpy, D. J. (2019). Thyroid hormones in critical illness. *Critical care clinics,* 35(2), 375-388. https://doi.org/10.1016/j.ccc.2018.11.012]

[12] Ocheretna, N. P., Guminskiy, Yu. I., & Gunas, I. V. (2018). Indicators of cell cycle and dna fragmentation of spleen cells in early terms after thermal burns of skin on the background of using "lactoprotein with sorbitol" or HAES-LX-5%. *Bulletin of scientific research,* 1, 141-146. doi: 10.11603/2415-8798.2018.1.8627

[13] Oryan, A., Alemzadeh, E., & Moshiri, A. (2017). Burn wound healing: present concepts, treatment strategies and future directions. *Journal of wound care*, 26(1), 5-19. doi: 10.12968/jowc.2017.26.1.5

[14] Rowan, M. P., Cancio, L. C., Elster, E. A., Burmeister, D. M., Rose, L. F., Natesan, S., ... & Chung, K. K. (2015). Burn wound healing and treatment: review and advancements. *Critical care,* 19(1), 243. https://doi.org/10.1186/s13054-015-0961-2

[15] Safer J. D. (2013). Thyroid hormone and wound healing. Journal of thyroid research, 2013, 124538. doi: 10.1155/2013/124538

[16] Sofianos, C., Redant, D. P., Muganza, R. A., Moore, R. L., & Ferrar, D. S. (2017). Thyroid Crisis in a Patient With Burn Injury. *Journal of Burn Care & Research*, 38(4), e776-e780. https://doi.org/10.1097/BCR.0000000000000499

[17] Tiron, O. I., Appelhans, O. L., Gunas, I. V., & Chereshniuk, I. L. (2019). Indicators of the cell cycle in the thyroid gland in rats when applying infusion of 0.9% solution of NaCl, Lactoprotein with Sorbitol or HAES-LX 5%. *Reports of Morphology,* 25(1), 62-67. doi: 10.31393/morphology-journal-2019-25(1)-09

[18] Williams, F. N., & Herndon, D. N. (2017). Metabolic and endocrine considerations after burn injury. *Clinics in plastic surgery,* 44(3), 541-553. https://doi.org/10.1016/j.cps.2017.02.013

ПОКАЗНИКИ КЛІТИННОГО ЦИКЛУ В ЩИТОПОДІБНІЙ ЗАЛОЗІ У ЩУРІВ ПРИ ЗАСТОСУВАННІ ІНФУЗІЇ 0,9% РОЗЧИНУ NACL НА ФОНІ ТЕРМІЧНОГО ОПІКУ ШКІРИ

Тірон О.І.

Одним із ключових факторів патогенезу опікової хвороби внаслідок термічного опіку шкіри є системне ушкодження органів, зокрема щитоподібної залози. Мета роботи - дослідити показники клітинного циклу та фрагментації ДНК клітин щитоподібної залози у щурів при застосуванні інфузії 0,9% розчину NaCl на фоні термічного опіку шкіри. Експериментальні дослідження проведені на 60 білих щурах-самцях масою 160-180 г, котрим було нанесено термічний опік шкіри 2-3 ступеня загальною площею 21-23% поверхні тіла. Перші 7 діб щурам проводили інфузію 0,9% розчину NaCl у нижню порожнисту вену. Тварин виводили з експерименту шляхом декапітації (через 1, 3, 7, 14, 21 та 30 діб). Вміст ДНК в ядрах клітин щитоподібної залози щурів визначали методом проточної цитометрії. Статистична обробка отриманих результатів була проведена в ліцензійному пакеті "STATISTICA 6.1" із застосуванням непараметричних методів оцінки. Через 1 добу після термічного ушкодження шкіри і використання 0,9% розчину NaCl встановлено менші (p<0,05) значення показника S-фази (0,234±0,094) порівняно з контрольною групою без опіку (0,652±0,134). Максимальне зниження (p<0,01) показників S-фази (0,622±0,110 та 0,214±0,105 відповідно) та суттєве підвищення (p<0,01) показнику інтервалу SUB-G0G1 (5,288±0,840), порівняно з аналогічними показниками контрольної групи (2,594±0,628), спостерігали через 3 доби. Показники S-фази на фоні введення 0,9% розчину NaCl і термічного опіку шкіри залишались значно меншими від аналогічних показників відповідних контрольних груп через 7 (p<0,01), 14 (p<0,05) та 21 добу (p<0,05). Через 14 діб після термічного ушкодження шкіри встановлено менші (p<0,05) значення показника інтервалу SUB-G0G1 порівняно з контрольною групою щурів. Через 30 діб показники фази G0G1 виявились суттєво меншими (p<0,01), а показники фази G2+M значно (p<0,01) більшими від показників, встановлених в аналогічний термін у групі контролю. Таким чином, встановлена недостатня ефективність використання 0,9% розчину NaCl з метою корекції порушень клітинного поділу протягом всього терміну спостереження після опіку шкіри.

Ключові слова: *щитоподібна залоза, термічний опік шкіри, ДНК-цитометрія, 0,9% розчин NaCl.*

ПОКАЗАТЕЛИ КЛЕТОЧНОГО ЦИКЛА В ЩИТОВИДНОЙ ЖЕЛЕЗЕ У КРЫС ПРИ ПРИМЕНЕНИИ ИНФУЗИИ 0,9% РАСТВОРА NACL НА ФОНЕ ТЕРМИЧЕСКОГО ОЖОГА КОЖИ

Тирон О.И.

Одним из ключевых факторов патогенеза ожоговой болезни в результате термического ожога кожи является системное

повреждение органов, в том числе щитовидной железы. Цель работы исследовать показатели клеточного цикла и фрагментации ДНК клеток щитовидной железы у крыс при применении инфузии 0,9% раствора NaCl на фоне термического ожога кожи. Экспериментальные исследования проведены на 60 белых крысах-самцах массой 160-180 г, которым был нанесен термический ожог кожи 2-3 степени общей площадью 21-23% поверхности тела. Первые 7 дней крысам проводили инфузию 0,9% раствора NaCl в нижнюю полую вену. Животных выводили из эксперимента путем декапитации (через 1, 3, 7, 14, 21 и 30 суток). Содержание ДНК в ядрах клеток щитовидной железы крыс определяли методом проточной цитометрии. Статистическая обработка полученных результатов была проведена в лицензионном пакете "STATISTICA 6.1" с применением непараметрических методов оценки результатов. Через 1 сутки после термического повреждения кожи и использования 0,9% раствора NaCl установлено достоверно меньшее ($p<0,05$) значение показателя S-фазы (0,234±0,094) по сравнению с контрольной группой без ожога (0,652±0,134). Максимальное снижение ($p<0,01$) показателей S-фазы (0,622±0,110 и 0,214±0,105 соответственно) и существенное повышение ($p<0,01$) показателя интервала SUB-G0G1 (5,288±0,840), по сравнению с аналогичными показателями контрольной группы (2,594±0,628), наблюдали через 3 суток. Показатели S-фазы на фоне введения 0,9% раствора NaCl и термического ожога кожи оставались значительно меньшими, чем аналогичные показатели соответствующих контрольных групп через 7 ($p<0,01$), 14 ($p<0,05$) и 21 день ($p<0,05$). Через 14 суток после термического повреждения кожи установлено меньшее ($p<0,05$) значение показателя интервала SUB-G0G1 по сравнению с контрольной группой крыс. Через 30 суток показатели фазы G0G1 оказались существенно меньше ($p<0,01$), а показатели фазы G2+M значительно ($p<0,01$) больше показателей, установленных в аналогичный срок в группе контроля. Таким образом, установлена недостаточная эффективность использования 0,9% раствора NaCl с целью коррекции нарушений клеточного деления в течение всего срока наблюдения после ожога кожи.

Ключевые слова: *щитовидная железа, термический ожог кожи, ДНК-цитометрия, 0,9% раствор NaCl.*

DOI: 10.31393/morphology-journal-2019-25(3)-10 Reports of Morphology, Vol. 25, №3, Pages 58-62

ISSN 1818-1295 eISSN 2616-6194

REPORTS OF MORPHOLOGY

Official Journal of the Scientific Society of Anatomists, Histologists, Embryologists and Topographic Anatomists of Ukraine

journal homepage: https://morphology-journal.com

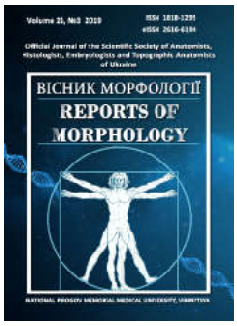

Ultrastructural organization of hemomicrocirculatory bed of the lungs affected by Doxorubicin

Zaiats L.M.[1], Yankiv O.O.[2], Gunas I.V.[2], Shapoval O.M.[2], Shypitsina O.V.[2]

[1]Ivano-Frankivsk National Medical University, Ivano-Frankivsk, Ukraine
[2]National Pirogov Memorial Medical University, Vinnytsya, Ukraine

ARTICLE INFO
Received: 9 July, 2019
Accepted: 21 August, 2019

UDC: 616.24+0616-092.9+615.33

CORRESPONDING AUTHOR
e-mail: patfisiology@ifnmu.edu.ua
Zaiats L.M.

One of the most effective anticancer drugs for breast cancer, lymphoma, soft tissue sarcoma, leukemia, some solid tumors is Doxorubicin. However, its antitumor effect directly correlates with the dose-dependent manifestation of toxicity to healthy tissues and body systems. The purpose of the study is to study the dynamics of ultrastructural changes of the hemomicrocirculatory bed under the influence of Doxorubicin. Animals were divided into 3 groups: I - intact rats (n=10); II - control (n=20); III - rats with Doxorubicin model (n=40). Doxorubicin was administered intraperitoneally at a dose of 5 mg/kg body weight once a week for 4 weeks. An animal control group was intraperitoneally injected with an equivalent volume of saline. Pulmonary tissue sampling for electron microscopic examination was performed under thiopental anesthesia 7, 14, 21, 28 days after the start of the experiment. Pieces of pulmonary tissue were fixed in 2.5% glutaraldehyde followed by fixation in 1% osmium tetroxide. After dehydration, the material was poured into araldite-epon. The sections obtained on a "Tesla BS-490" ultramicrotome were examined in an electron microscope "PEM-125K". It is established that within 7 days after the first injection of Doxorubicin in the lungs changes in the structural organization of the hemomicrocapillary bed and the disturbance of blood rheological properties are determined, as evidenced by the excessive accumulation of neutrophils in the hemocapillaries, their adhesion and aggregation. With the extension of the study period (14-28 days) there is a progressive disturbance of the submicroscopic structure of hemocapillaries of the alveolar wall and marked changes in the rheological properties of blood. In endothelial cells, swelling phenomena with organelle disorganization are determined, and in some areas there is a desquamation of endothelial cells into the lumen of the hemocapillaries with basal membrane exposures. In the lumen of the microvessels, red blood cells and leuco-platelet aggregates are noted. Thus, the introduction of Doxorubicin leads to pronounced submicroscopic changes in the hemomicrocirculatory bed. Violation of the ultrastructural organization of the hemomicrocirculatory bed of the lungs is determined after 7 days after the start of the study.

Keywords: *lungs, hemomicrocirculatory bed, Doxorubicin.*

Introduction

Today, cancer is among the most common causes of death. Cancer ranks second after cardiovascular disease in the structure of mortality in Ukraine [17].

The analysis of the literature shows that chemotherapy occupies a significant place among the methods of treatment of malignant tumors [6, 14, 18]. The use of cytostatic therapy leads to improved immediate and long-term results of treatment of patients [19-21]. Most often in the treatment of cancer, anthracycline antibiotics are used, which are included in many cancer treatment regimens. To date, it has been proven that among the anthracycline antibiotics, Doxorubicin is one of the most effective anticancer drugs for the treatment of breast cancer, lymphomas, soft tissue sarcomas, leukemia, and some solid tumors [1, 4, 7, 20]. However, the antitumor effect of Doxorubicin directly correlates with the dose-dependent manifestation of toxicity to healthy tissues and body systems, which causes its adverse reactions [15, 22]. Most of the lethal cases in cancer patients do not occur due to the disease itself, but due to the side effects of anticancer drugs [9, 16].

It is known that the use of anthracycline antibiotic Doxorubicin in the treatment of malignant tumors in patients develops heart failure, which leads to the formation of Doxorubicin cardiomyopathy [2, 6, 18].

But, in addition to cardiac injuries, there are also pronounced extra-cardiac changes of organs and systems. Pathological changes in the lungs, kidneys, liver, spleen and impaired function of the reproductive organs are most often observed [1, 3, 5, 8, 10].

The aim of this study was to study the dynamics of ultrastructural changes in the hemomicrocirculatory bed of the lungs under the influence of Doxorubicin.

Materials and methods

The experiments were performed on 70 white male rats weighing 180-220 g. Animals were divided into 3 groups: I - intact group of animals (n=10); II - control (n=20); III - animals with Doxorubicin model (n=40).

Doxorubicin was administered intraperitoneally at a dose of 5 mg/kg body weight once a week for 4 weeks. An animal control group was intraperitoneally injected with an equivalent volume of saline.

Pulmonary tissue sampling for electron microscopic examination was performed under thiopental anesthesia 7, 14, 21, 28 days after the start of the experiment. Pieces of pulmonary tissue were fixed in 2.5 % glutaraldehyde followed by fixation in 1 % osmium tetroxide. After dehydration, the material was poured into araldite-epon. The sections obtained on a "Tesla BS-490" ultramicrotome were examined in an electron microscope "PEM-125K".

Retention, manipulation and withdrawal from the experiment were carried out in accordance with the requirements of the European Convention for the Protection of Vertebrate Animals Used for Research Purposes (Strasbourg, 1986), Council of Europe Directive 86/609/EEC (1986), the provisions of the Law of Ukraine "On the protection of animals from ill-treatment" dated 15.12.2009 and orders of the Ministry of Health of Ukraine № 690 dated September 23, 2009, № 616 dated August 3, 2012.

The Commission on Bioethics of the Ivano-Frankivsk National Medical University found that scientific research did not contradict basic bioethical standards (protocol № 96/17 of 24.05.2017).

Results

Conducted submicroscopic analysis after 7 days after the first injection of Doxorubicin showed that the nuclei of individual endothelial cells with a matrix of low electron-optical density and marginal placement of chromatin granules. The nuclear envelope has tortuous contours and produces shallow invaginations. Some mitochondria are enlarged in size with single crystae. Tanks and tubules of the Golgi apparatus and granular endoplasmic reticulum are moderately expanded. The basement membrane is locally thickened. In the peripheral departments of the endothelial cells there is a large number of micropinocytotic vesicles. In the lumen of some hemocapillaries, an increased amount of leukocytes with adhesion and aggregation is determined (Fig. 1).

With the increase of the study period (14 days after the first injection of Doxorubicin), the nucleus of many endothelial cells with nucleoplasm of low electron-optical density. Chromatin granules are placed along the inner surface of the nuclear envelope. Perinuclear region is moderately expanded. Mitochondria swollen with single short crystae. The Golgi apparatus consists of expanded tanks, various sizes of bubbles and vacuoles. In individual cells, fragmentation of membranes of the granular endoplasmic reticulum with a reduced number of ribosomes on their outer surface is noted. On the luminal surface of the plasmalemma of some endothelial cells, its sail projections are observed. The basement membrane is thickened in many places. In the lumen of the hemocapillaries, the aggregation and adhesion of leukocytes and platelets are noted.

Electron microscopic data from the 21st day indicate that the severity and prevalence of edema in endothelial cells is much greater than at the previous stage of the experiment. The nuclei of many endothelial cells with enlightened nucleoplasm. Mitochondria enlarged in volume with single fragmented crystae. At the same time, mitochondria with complete lysis of the crystae are noted, but without tearing of the outer membrane. The Golgi apparatus is represented by single extended tanks and vacuoles. Tanks of granular endoplasmic reticulum are expanded and vacuolated. The number of ribosomes on their outer surface is greatly reduced. Fragmentation of the membranes of the granular endoplasmic reticulum is also observed. In some hemocapillaries, the areas of lysis of the luminal plasmalemma of the endothelial cells are determined, accompanied by the release of intracellular contents into the lumen of the microvessels. In the lumen of many hemocapillaries, erythrocyte sludge, adhesion, and platelet aggregation are noted (Fig. 2).

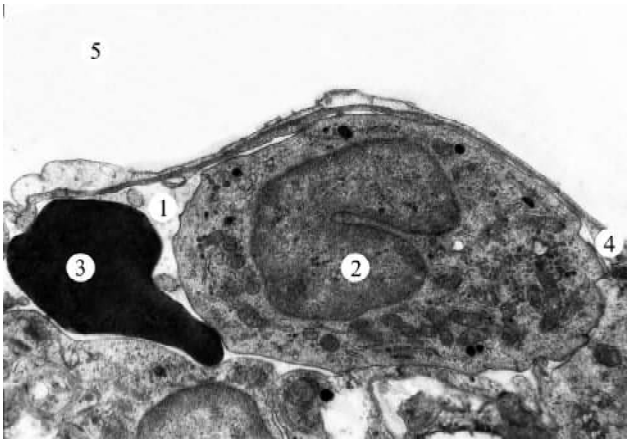

Fig. 1. Ultrastructural organization of the hemocapillaries of the alveoli wall 7 days after the start of the experiment. 1 - the lumen of the hemocapillary; 2 - leukocyte; 3 - erythrocyte; 4 - peripheral part of the endothelial cell; 5 - the lumen of the alveoli. Electronic micrograph. x6400.

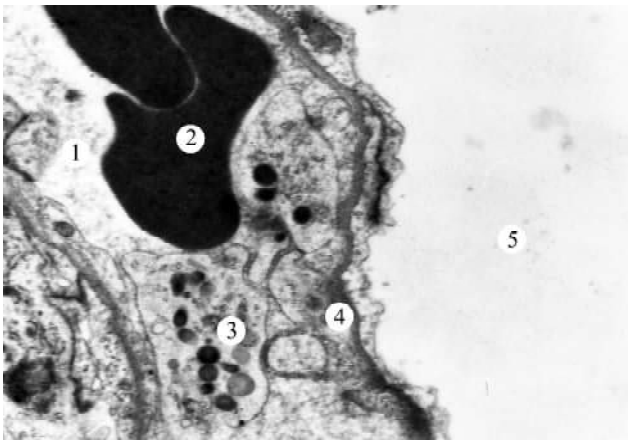

Fig. 2. Platelet adhesion and aggregation and erythrocyte sludge in the hemocapillaries of the alveolar wall 21 days after the start of the experiment. 1 - the lumen of the hemocapillary; 2 - erythrocyte; 3 - platelet; 4 - peripheral part of the endothelial cell; 5 - the lumen of the alveoli. Electronic micrograph. x9600.

The expressed disturbances of ultrastructural organization of hemocapillaries are determined after 28 days after the beginning of the experiment. Endothelial cell nuclei are enlarged in size with low electron-optical density nucleoplasm. Chromatin granules are placed along the inner surface of the nuclear membrane or grouped into separate tubercles. Perinuclear region is expanded. Mitochondria are swollen in various sizes and shapes with disoriented crystae. Focal destruction of the crystae, fragmentation and destruction of both the inner and outer membranes of the mitochondria are often noted. The components of the Golgi apparatus and the granular endoplasmic reticulum are enlarged, fragmented. In some areas, the desquamation of endothelial cells in the lumen of the hemocapillary with the basal membrane exposure is determined. Erythrocyte sludge and platelet aggregates are observed in the lumen of the hemocapillaries.

Discussion

Thus, studies have shown that within 7 days after the first injection of Doxorubicin in the lungs are determined changes in the structural organization of the hemomicrocapillary bed and impaired blood rheological properties, as evidenced by the excessive accumulation of neutrophils in the hemocapillaries, their adhesion and aggregation. With the extension of the study period (14-28 days) there is a progressive disturbance of the submicroscopic structure of hemocapillaries of the alveolar wall and marked changes in the rheological properties of blood. In endothelial cells, swelling phenomena with organ disorganization are determined, and in some areas there is a desquamation of endothelial cells into the lumen of the hemocapillaries with the basal membrane exposing. In the lumen of the microvessels, red blood cells and leuco-platelet aggregates are noted.

Changes of a similar nature in the lung tissue during the action of Doxorubicin are indicated by several other researchers [13, 15]. The authors note the pronounced plethora of vessels with signs of stasis, sludge, thrombosis. In some places, the luminescence of the alveoli is almost undetermined by edema, atelectasis, in these parts of the lung parenchyma intensively infiltrated by polymorphonuclear leukocytes.

Doxorubicin is known to be able to induce oxidative stress in cells and directly damage the cytoplasmic membrane. Disruption of the functioning of cyto- and endoplasmic membranes is accompanied by an increase in their permeability. Particularly pronounced dystrophic-destructive changes are found in the mitochondria of cardiomyocytes. When the membranes of the lysosomes are damaged, proteolytic lysosomal enzymes are released into the cytosol, their destructive effect is exacerbated against the background of macroergic deficiency. In addition, there is a vacuolation and resorption of sarcoplasm and disruption of the nucleus structure [2, 11, 12]. Similar changes in the ultrastructural organization described by us in the endothelial cells of the hemocapillaries of the alveolar wall under the action of Doxorubicin.

The prospect of further development is the correction of ultrastructural changes in the hemomicrocirculatory bed of lungs under the action of Doxorubicin.

Conclusions

1. Studies have shown that the introduction of Doxorubicin leads to pronounced submicroscopic changes in the hemomicrocirculatory bed of the lungs.

2. Violation of the ultrastructural organization of the hemomicrocirculatory bed of the lungs is determined after 7 days after the start of the study.

References

[1] Bazykov, I. A., Beier, E. V., Lukynova, V. V., & Maltsev, A. N. (2015). Comparative evaluation of the acute toxicity of Doxorubicin and its niosomal form. *Medical Bulletin of the North Caucasus,* 10(4(38)), 403-406.

[2] Chatterjee, K., Zhang, J., Honbo, N., & Karliner, J. S. (2010). Doxorubicin cardiomyopathy. *Cardiology,* 115(2), 155-162. doi: 10.1159/000265166

[3] Diamond, O. M., Turgeman, O., & Blumenfeld, Z. (2015). Minimizing the Doxorubicin-Induced gonadotoxicity by sphingosine-1-phosphate analogue FTY720. *Am. J. Clin. Exp. Obstet. Gynecol.,* 2(1), 24-33.

[4] Fernandez-Chas, M., Curtis, M. J., & Niederer, S. A. (2018). Mechanism of Doxorubicin cardiotoxicity evaluated by integrating multiple molecular effects into a biophysical model. *British Journal of Pharmacology,* 175(5), 763-781. doi: 10.1111/bph.14104

[5] Haina, Zh. M., Kosuba, R. B., & Yaremii, I. M. (2012). Corrective effect of mildronate on the performance of oxidant-antioxidant equilibrium in rats against toxic Doxorubicin. *Medical Chemistry,* 1(14), 56-59.

[6] He, H., Liu, C., Wu, Y., Zhang, X., Fan, J., & Cao, Y. (2018). A multiscale physiologically-based pharmacokinetic model for

Doxorubicin to explore its mechanisms of cytotoxicity and cardiotoxicity in human physiological contexts. *Pharmaceutical research,* 35(9), 174. doi: 10.1007/sl 1095-018-2456-8

[7] Hordiienko, Yu. A., Baklanova, Ya., Kovalenko, M. V., Stechenko, L. M., Shevtsova, A. I., & Ushakova, G. O. (2012). Changes in physiological and biochemical parameters in rats with Doxorubicin-induced cardiopathy against the use of antioxidant drugs. *Animal biology*, 14(1-2), 74-79.

[8] Hozayen, W. G., Abou Seif, H. S., & Amin, S. (2014). Protective effects of ruitn and/or hesperidin against Doxorubicin-induced hepatotoxicity. *Int. J. Clin. Nutr.,* 2(1), 11-17. doi: 10.12691/ijcn-2-1-2

[9] Kolotova, O. V., Fedorova, E. P., Ermolaeva, L. A., & Churyn, A. A. (2008). The ability to correct the toxic effects of paclitaxel. *Siberian Oncology Journal,* (1), 66-68.

[10] Kobylinska, L. I., Havrylyuk, D. Y., Mitina, N. E., Zaichenko, A. S., Lesyk, R. B., Zimenkovsky, B. S., & Stoika, R. S. (2016). Biochemical indicators of nephrotoxicity in blood serum of rats treated with novel 4-thiazolidinone derivatives or their complexes with polyethylene glycol-containing nanoscale polymeric carrier. *The Ukrainian Biochemical Journal,* 88(1), 51-60. doi: 10.15407/ubj88.01.051

[11] Linnyk, O. O., Drevytska, T. I., Tarasova, K. V., Portnichenko, G. V., Dosenko, V. E., & Mankovska, I. M. (2016). Impairment of contractile activity of cardiomyocytes under the action of Doxorubicin. *Physiological Journal,* 6(62), 65-71.

[12] Linnyk, O. O., Honchar, O. O., Nosar, V. I., Drevytska, T. I., Kovalov, O. M., & Mankovska, I. M. (2017). Effect of curcumin on mitochondrial function of cardiomyocytes in Doxorubicin-induced oxidative stress. *Physiological Journal,* 1(63), 10-16.

[13] Luu, A. Z., Chowdhury, B., Al-Omran, M., Teoh, H., Hess, D. A., & Verma, S. (2018). Role of endothelium in Doxorubicin-induced cardiomyopathy. *JACC: Basic to Translational Science*, 3(6), 861-870. doi: 10.1016/j.jacbts.2018.06.005

[14] McGowan, J. V., Chung, R., Maulik, A., Piotrowska, I., Walker, J. M., & Yellon, D. M. (2017). Anthracycline chemotherapy and cardiotoxicity. *Cardiovascular Drugs and Therapy,* 31(1), 63-75. doi: 10.1007/sl0557-016-6711-0

[15] Pakryshen, S. V., & Mokhort, M. A. (2013). Toxicodynamics of Doxorubicin (morphological study). *Modern Problems of Toxicology,* (1-2), 81-85.

[16] Ruggeri, C., Gioffré, S., Achilli, F., Colombo, G. I., & D'Alessandra, Y. (2018). Role of microRNAs in Doxorubicin-induced cardiotoxicity: an overview of preclinical models and cancer patients. *Heart Failure Reviews*, 23(1), 109-122. doi: 10.1007/s 10741 -017-9653-0

[17] Shchepotyn, I. (2013). What do we know about cancer? *Pharmacist Practitioner,* 2, 8.

[18] Shevchuk, O. O., Volska, A. S., Yaremchuk, O. Z., Kurylo, K. I., Bardakhivska, K. I., Nikolaev, V. G., & Posokhova, K. A. (2019). Prooxidant-antioxidant balance in rats against subchronic Doxorubicin toxicity and the use of enterosorption and filgrastim (literature review and results of own studies). *Medical and Clinical Chemistry,* 3(21), 13-22. doi: 10.11603/mcch.2410-681X.2019.v.i3.10555

[19] Shushanov, S. S., & Kravtsova, T. A. (2013). In vitro cytotoxic effect of Doxorubicin on human multiple myeloma cells. *Bulletin of Experimental Biology and Medicine,* 155(2), 195-200.

[20] Todor, I. M., Lukianova, N. Yu., Tymovska, Yu. O., Pivniuk, V. M., & Chekhun, V. F. (2013). Influence of Doxorubicin in liposomal form on tumors with phenotype of drug resistance. *Oncology*, 4(15), 279-285.

[21] Volkova, M., & Russell, R. (2011). Anthracycline cardiotoxicity: prevalence, pathogenesis and treatment. *Current Cardiology Reviews,* 7(4), 214-220. doi: 10.2174/157340311799960645

[22] Zupanets, I. A., Vietrova, K. V., Sakharova, T. S., & Torianik, E. L. (2013). Possibilities of correction of toxic effects of anticancer antibiotic Doxorubicin by derivatives of glucose mine and their combinations. *Ukrainian Biopharmaceutical Journal*, 4(27), 87-92.

УЛЬТРАСТРУКТУРНА ОРГАНІЗАЦІЯ ГЕМОМІКРОЦИРКУЛЯТОРНОГО РУСЛА ЛЕГЕНЬ ПІД ВПЛИВОМ ДОКСОРУБІЦИНУ

Заяць Л.М., Янків О.О., Гунас І.В., Шаповал О.М., Шипіцина О.В.

Одним із найефективніших протипухлинних препаратів, котрим лікують рак молочної залози, лімфоми, саркоми м'яких тканин, лейкемії, деякі солідні пухлини є доксорубіцин. Разом із тим, його протипухлинний ефект прямо корелює з дозозалежним проявом токсичності відносно здорових тканин і систем організму. Мета роботи - вивчити в динаміці ультраструктурні зміни гемомікроциркуляторного русла легень під впливом доксорубіцину. Тварини були розділені на 3 групи: I - інтактні щури (n=10); II - контрольна (n=20); III - щури з доксорубіциновою моделлю (n=40). Доксорубіцин вводили внутрішньоочеревинно у дозі 5 мг/кг маси тіла тварини 1 раз на тиждень впродовж 4 тижнів. Контрольній групі тварин внутрішньоочеревинно вводили еквівалентний об'єм фізіологічного розчину. Забір легеневої тканини для електронно-мікроскопічного дослідження проводили під тіопенталовим наркозом через 7, 14, 21, 28 діб після початку експерименту. Шматочки легеневої тканини фіксували у 2,5% розчині глютаральдегіду з подальшою дофіксацією в 1% розчині чотириокису осмію. Після дегідратації матеріал заливали в епон-аралдіт. Зрізи, отримані на ультрамікротомі "Tesla BS-490", вивчали в електронному мікроскопі "ПЕМ-125К". Встановлено, що вже через 7 діб після першого введення доксорубіцину в легенях визначаються зміни структурної організації гемомікрокапілярного русла і порушення реологічних властивостей крові, про що свідчить надмірна акумуляція нейтрофілів у гемокапілярах, їх адгезія та агрегація. Із продовженням терміну дослідження (14-28 діб) спостерігали прогресуюче порушення субмікроскопічної будови гемокапілярів альвеолярної стінки та виражені зміни реологічних властивостей крові. В ендотеліальних клітинах визначаються набрякові явища з дезорганізацією органел, а в окремих ділянках спостерігається десквамація ендотеліоцитів до просвіту гемокапілярів з оголенням базальної мембрани. У просвіті мікросудин відмічаються еритроцитарні сладжі й лейкотромбоцитарні агрегати. Таким чином, введення доксорубіцину призводить до виражених субмікроскопічних змін гемомікроциркуляторного русла легень. Порушення ультраструктурної організації гемомікроциркуляторного русла легень визначається вже через 7 діб після початку дослідження.

Ключові слова: *легені, гемомікроциркуляторне русло, доксорубіцин.*

УЛЬТРАСТРУКТУРНАЯ ОРГАНИЗАЦИЯ ГЕМОМИКРОЦИРКУЛЯТОРНОГО РУСЛА ЛЕГКИХ ПОД ВОЗДЕЙСТВИЕМ ДОКСОРУБИЦИНА

Заяц Л.М., Янкив Е.О., Гунас И.В., Шаповал Е.Н., Шипицина А.В.

Одним из наиболее эффективных противоопухолевых препаратов, которым лечат рак молочной железы, лимфомы, саркомы

мягких тканей, лейкемии, некоторые солидные опухоли является доксорубицин. Вместе с тем, его противоопухолевый эффект прямо коррелирует с дозозависимым проявлением токсичности относительно здоровых тканей и систем организма. Цель работы - изучить в динамике ультраструктурные изменения гемомикроциркуляторного русла легких под влиянием доксорубицина. Животные были разделены на 3 группы: I - интактные крысы (n=10); II - контрольная (n=20); III - крысы с доксорубициновой моделью (n=40). Доксорубицин вводили внутрибрюшинно в дозе 5 мг/кг массы тела животного 1 раз в неделю в течение 4 недель. Контрольной группе животных внутрибрюшинно вводили эквивалентный объем физиологического раствора. Забор легочной ткани для электронно-микроскопического исследования проводили под тиопенталовым наркозом через 7, 14, 21, 28 суток после начала эксперимента. Кусочки легочной ткани фиксировали в 2,5% растворе глютаральдегида с последующей дофиксацией в 1% растворе четырехокиси осмия. После дегидратации материал заливали в эпон-аралдит. Срезы, полученные на ультрамикротоме "Tesla BS-490" изучали в электронном микроскопе "ПЭМ-125К". Установлено, что уже через 7 суток после первого введения доксорубицина в легких определяются изменения структурной организации гемомикрокапиллярного русла и нарушение реологических свойств крови, о чем свидетельствует чрезмерная аккумуляция нейтрофилов в гемокапиллярах, их адгезия и агрегация. С продлением срока исследования (14-28 суток) наблюдали прогрессирующее нарушение субмикроскопической строения гемокапилляров альвеолярной стенки и выраженные изменения реологических свойств крови. В эндотелиальных клетках определяются отечные явления с дезорганизацией органелл, а в отдельных участках наблюдается десквамация эндотелиоцитов в просвет гемокапилляров с обнажением базальной мембраны. В просвете микрососудов отмечаются эритроцитарные сладжы и лейкотромбоцитарные агрегаты. Таким образом, введение доксорубицина приводит к выраженным субмикроскопическим изменениям гемомикроциркуляторного русла легких. Нарушение ультраструктурной организации гемомикроциркуляторного русла легких определяется уже через 7 суток после начала исследования.

Ключевые слова: *легкие, гемомикроциркуляторное русло, доксорубицин.*

REQUIREMENTS FOR ARTICLES

For publication, scientific articles are accepted only in English only with translation on Ukrainian or Russian, which contain the following necessary elements: UDC code; title of the article (in English, Ukrainian and Russian); surname, name and patronymic of the authors (in English, Ukrainian and Russian); the official name of the organization (institution) (in English, Ukrainian and Russian); city, country (in English, Ukrainian and Russian); structured annotations (in English, Ukrainian and Russian); keywords (in English, Ukrainian and Russian); introduction; purpose; materials and methods of research; research results; discussion; conclusions; bibliographic references.

The title of the article briefly reflects its contents and contains no more than 15 words.

Abstract. The volume of the annotation is 1800-2500 characters without spaces. The text of an annotation in one paragraph should not contain general phrases, display the main content of the article and be structured. The abstract should contain an introductory sentence reflecting the relevance of the study, the purpose of the study, a brief description of the methods of conducting research (2-3 sentences with the mandatory provision of the applied statistical methods), a description of the main results (50-70% of the volume of the abstract) and a concise conclusion (1 sentence). The abstract should be clear without familiarizing the main content of the article. Use the following expressions: "Detected ...", "Installed ...", "Fixed ...", "Impact assessed ...", "Characterized by regularities ...", etc. In an annotation, use an active rather than passive state.

Keywords: 4-6 words (or phrases).

"Introduction"

The introduction reflects the state of research and the relevance of the problem according to the world scientific literature (at least 15 references to English articles in international journals over the past 5 years). At the end of the entry, the purpose of the article is formulated (contains no more than 2-3 sentences, in which the problem or hypothesis is addressed, which is solved by the author).

"Materials and methods"

The section should allow other researchers to perform similar studies and check the results obtained by the author. If necessary, this section may be divided into subdivisions. Depending on the research objects, the ethical principles of the European Convention for the protection of vertebrate animals must be observed; Helsinki Declaration; informed consent of the surveyed, etc. (for more details, see "Public Ethics and its Conflict"). At the end of this section, a "statistical processing of results" section is required, which specifies the program and methods for processing the results obtained by the automobile.

"Results"

Requirements for writing this section are general, as well as for all international scientific publications. The data is presented clearly, in the form of short descriptions, and must be illustrated by color graphics (no more than 4) or drawings (no more than 8) and tables (no more than 4), the information is not duplicated.

"Discussion"

In the discussion, it is necessary to summarize and analyze the results, as possible, compare them with the data of other researchers. It is necessary to highlight the novelty and possible theoretical or practical significance of the results of the research. You should not repeat the information already listed in the "Introduction" section. At the end of the discussion, a separate paragraph should reflect the prospects for using the results obtained by the author.

"Conclusion"

5-10 sentences that summarize the work done (in the form of paragraphs or solid text).

"Acknowlegements"

Submitted after conclusion before bibliographic references.

"References"

References in the text are indicated by Arabic numerals in square brackets according to the numerology in the list of references. The list of references (made without abbreviations) sorted by alphabet, in accordance with the requirements of APA Style (American Psychological Association Style): with the obligatory referencing of all authors, work titles, journal names, or books (with obligatory publication by the publishing house, and editors when they are available), therefore, numbers or releases and pages. In the Cyrillic alphabets references, give the author's surnames and initials in English (Cyrillic alphabet in brackets), the title of the article or book, and the name of the magazine or the publisher first to be submitted in the original language of the article, and then in square brackets in English. If available, doi indexes must be provided on www.crossref.org (at least 80% of the bibliographic references must have their own doi indexes). Links to online publications, abstracts and dissertations are not welcome.

After the list of references, it is necessary to provide information about all authors (in English, Ukrainian and Russian): last name, first name and patronymic of the author, degree, place of work and position, **ORCID number** (each of the authors of the ORCID personal number if absence - free creation on the official website http://www.orcid.org) to facilitate the readers of this article to refer to your publications in other scientific publications.

The last page of the text should include the surname, name and patronymic of the author, degree, postal address, telephone number and e-mail of the author, with which the editors will maintain contact.

Concluding remarks

The manuscript should be executed in such a way that the number of refinements and revisions during the editorial of the article was minimal.

When submitting the article, please observe the following requirements. The volume of the article - not less than 15 and not more than 25 pages, Times New Roman, 14 pt, line spacing - one and a half, fields - 2 cm, sheet A4. Text materials should be prepared in the MS Word editor (* .docx), without indentations. Math formulas and equations to prepare in the embedded editor; graphics - in MS Excel. Use the units of the International Measurement System. Tables and drawings must contain the name, be numbered, and references to them in the text should be presented as follows: (fig. 1), or (table 1). The drawings should be in the format "jpg" or "tif"; when scanned, the resolution should be at least 800 dpi; when scanning half-tone and color images, the resolution should be at least 300 dpi. All figures must be represented in the CMYK palette. The statistical and other details are given below the table in the notes. Table materials and drawings place at the end of the text of the manuscript. All elements of the text in images (charts, diagrams, diagrams) must have the Times New Roman headset.

Articles are sent to the editorial board only in electronic form (one file) at the e-mail address nila@vnmu.edu.ua

Responsible editor - Gunas Igor Valeryovich (phone number: + 38-067-121-00-05; e-mail: gunas.red@gmail.com).

Signed for print 04.09.2019
Format 60x84/8. Printing offset. Order № 2008. Circulation 100.
Vinnytsia. Printing house “Tvory”, Keleckaya St., 51a
PO Box 8825, 600-Richchya Str., 21, Vinnytsya, 21007
Phone: +38 (0432) 603 000
+38 (096) 97-30-934, +38 (093) 89-13-852
e-mail: tvory2009@gmai.com
http://www.tvoru.com.ua